# Engineering Applications of Surface Plasmon Resonance: Protein–Protein and Protein–Molecule Interactions

by

Nicholas Ignagni

A thesis

presented to the University of Waterloo

in fulfilment of the

thesis requirement for the degree of

Master of Applied Science

in

Chemical Engineering

Waterloo, Ontario, Canada, 2011

I hereby declare that I am the sole author of this thesis. This is a true copy of the thesis, including any required final revisions, as accepted by my examiners.

I understand that my thesis may be made electronically available to the public.

# Abstract

Protein-protein and protein-molecule interactions are complicated phenomena due to the tendency of proteins to change shape and function in response to their environment. Protein aggregation whether onto surfaces or in solution, can pose numerous problems in industry. Surface plasmon resonance (SPR) devices and quartz crystal microbalances (QCM) are two real-time, label free methods that can be used to detect the interactions between molecules on surfaces. These devices often employ self-assembled monolayers (SAMs) to produce specific surfaces for studying protein-protein interactions. The objective of this work was to develop methodologies utilizing SPR to better understand protein-protein and protein-molecule interactions with possible applications in the food and separation industrial sectors.

A very well characterized whey protein, β-lactoglobulin (BLG), is used in numerous applications in the food industry. BLG can undergo different types of self-aggregation due changes in external environment factors such as buffer strength, pH or temperature. In this work, a hydrophilic SAM was developed and used to study the interaction and non-specific adsorption of BLG and palmitic acid (PA), a molecule which is known to bind to BLG. It was found that PA tended to reduce BLG conformational changes once on the surface, resulting in a decrease in its surface adhesion. Fluorescent excitation emission matrices (EEM's) using a novel fluorescence probe technique were utilized to detect protein on the surface as well as conformational changes on the surface of the sensor, although the extent these changes could not be quantified.

Another whey protein, α-lactoglobulin (AL), was utilized as a surrogate protein to study the adsorption of colloidal/particulate and protein matter (CPP) extracted from filtration studies of river water. A large fraction of natural organic matter (NOM), the major foulant in membrane based water filtration, is CPP and protein. Understanding the interactions between these components is essential in abating NOM membrane fouling. Several SPR methods were investigated in order to verify the interactions. A mixture of AL and CPP particles in solution prevented the non-specific adsorption of AL to the SAM surface. This change in association was then detected through SPR. Fluorescent EEM's of the sensor surface verified that CPP and AL bound to the surface. This finding has fundamental significance in the interpretation of NOM-based membrane fouling.

To better understand the mechanisms behind non-specific adsorption, a mechanistic mathematical model was developed to describe the adsorption of BLGs onto the hydrophilic SAM. The resulting model performed well in terms of predicting adsorption based on SPR data. The model incorporated the monomer-dimer equilibrium of BLG in solution, highlighting the impact of protein aggregation on non-specific adsorption mechanisms.

For future studies, improvement in fluorescent FOP surface scan methodology would help identify different protein/molecules and conformations on the surface.

## Acknowledgements

I would like to thank Professor Legge for taking me on as a graduate student and all the help and advice he has given me. Dr. Legge was an excellent supervisor and even better as a mentor and friend.

I would like to acknowledge the work done by Dr. R.H. Peiris, which included the collection of CPP, PCA work, and helping me with fluorescence spectroscopy. I would like to thank him for all the discussions and data interpretations.

I thank my lab mates for their friendship and all the discussions we had in the lab.

I thank my family for always being there to help me out.

# Table of Contents

# List of Tables

# List of Figures

# List of Abbreviations

| | |
|---|---|
| 11-MUA | 11- mercaptoundecanoic acid |
| AL | α-lactoglobulin |
| BLG | β-lactoglobulin |
| BSA | bovine serum albumin |
| CPP | colloidal/particulate and protein matter |
| DDT | dichlorodiphenyltrichloroethane |
| DOC | dissolved organic content |
| EDC | 1-ethyl-3-(3-dimethylaminopropyl) carbodiimide |
| EEM | emission-excitation matrix |
| EtOH | ethanol |
| FOP | fibre optic probe |
| GRW | Grand River Water |
| LS | light scattering |
| MWCO | molecular weight cut-off |
| NHS | *N*-Hydroxysuccinimide |
| NMR | nuclear magnetic resonance |
| PA | Palmitic acid |
| PCA | principle component analysis |
| PD | penetration depth |
| QCM | Quartz Crystal Microbalance |
| RET | radationless energy transfer |
| RI | refractive index |
| RSA | random sequential adsorption of particles |
| RU | response unit |
| $RU_{max}$ | Calculated Maximum Association |
| SAM | Self-assembled monolayers |
| SE | sedimentation equilibrium |
| SP | surface plasmon polaritron |
| SPR | Surface Plasmon Resonance |
| TCDD | 2,3,7,8-tetra-chlorodibenzo-*p*-dioxin |
| TEG | Triethylene glycol monoamine |
| TNT | tri-nitro-toluene |
| UF | Ultrafiltration |
| θ | incidence angle |

# Chapter 1. Introduction

## 1.1. Research Motivation

Protein-molecule interactions are a well-researched topic in the food, pharmaceutical and water purification industries. Small changes in the local environment around the protein, such as interactions with surfaces, can have a drastic effect on the protein structure (Rabe *et al.* 2011). The resulting change in protein structure can lead to new interactions with adjacent molecules or proteins, creating a complex and dynamic system (Rabe *et al.* 2007). These interactions can interfere with industrial processes such as in the fouling during membrane-based water filtration or heat exchange surfaces in the food industry (Peiris *et al.* 2010a, Hanemaaijer *et al.* 1989). In the pharmaceutical industry, the controlled interaction between nanoparticles and therapeutic proteins are desired to help design new drugs (Almeida & Souto 2007). The measurement and understanding of fundamental mechanisms that govern these interactions are paramount to developing strategies for greater process control.

Surface Plasmon Resonance (SPR) is a phenomenon that can be utilized to measure the direct interaction between proteins (Homola 2008). SPR first saw applications in studying antibody-antigen interactions (Homola 2008). The number of applications based on SPR is quickly expanding, such as research on nanoparticle interactions, the development of advanced molecule sensors, and industrial applications such as a quality control agent for therapeutic proteins and drugs (Myszka & Rich 2000).

One important process in the food industry is the extraction and concentration of the protein β-lactoglobulin (BLG) (Dickinson & Galazka 1991, Capron *et al.* 1999). BLG is the primary component of whey, a by-product from the concentration of milk for cheese production. The milk concentration process produces a large amount of liquid whey which can then be ultrafiltered to produce whey protein concentrates (Bhattacharjee *et al.* 2006). BLG can then be isolated from the whey protein concentrates through a two stage ultrafiltration process followed by ion exchange membrane chromatography (Bhattacharjee *et al.* 2006). BLG sees use as an emulsifier and stabilizer for various food products (Capron *et al.* 1999). As such, BLG is one of the principal foulants in both membrane and heat exchange surfaces, thus it has been studied at

various ionic strengths, buffers and pHs (Lalande & Tissier 1985, Lee & Merson 1975, Gottschalk *et al.* 2003).

Although the function of BLG is not fully understood it shares similarities with a class of proteins known as retinol-binding proteins (Kontopidis *et al.* 2004). Along with retinol, BLG binds numerous fatty acids, with the highest affinity towards palmitic acid (PA) (Narayan & Berliner 1998). Studies have shown that interactions with fatty acid-contaminated BLG have affected its solution properties at the air water interface (Cornec & Narsimhan 1998). BLG also has the tendency to aggregate forming dimers above pH 4 with higher order aggregates existing between pHs 4.5 and 5.2 (Gottschalk *et al.* 2003). This wealth of documentation and its use in the food industry make it an ideal candidate as a model protein for SPR experiments that focus on better understanding the fundamentals of protein aggregation and protein-molecule interactions.

Fouling is also prevalent in membrane-based water purification. The flux decline associated with membrane fouling greatly increases the energy cost of microfiltration and ultrafiltration processes (Palecek & Zydney 1994). Research is being done in order to predict optimal treatment strategies for high fouling environments (Peiris *et al.* 2010a, Elshereef *et al.* 2010, Peiris *et al.* 2010b). This research requires the classification of the foulants which if better understood, could contribute to approaches for minimizing or preventing fouling before it occurs. The non-humic foulants in this case are primarily composed of colloidal/particulate and protein which accumulate on the membrane surface from the fresh water filtration (Peiris *et al.* 2010b). It is believed that the interactions between protein and the colloidal particles play a pivotal role in membrane fouling (Peiris *et al.* 2011).

Since these fouling events are prevalent in all forms of industry that deal with protein and protein separations, there may be similar connecting themes which cause protein build-up on surfaces. This nonspecific adsorption of protein is a generally an unwanted phenomenon that occurs on many other surfaces, such as on biosensors and biomedical tools/implants (Masson *et al.* 2006, Shen & Lin 2011) . There are many studies which have focused on understanding protein adsorption, sometimes with the goal of controlling protein loading and orientation and other times to completely prevent the adsorption from occurring (Rabe *et al.* 2011). All this requires a

detailed understanding of protein interactions and the mechanisms that govern how proteins adsorb onto surfaces.

### 1.1.1. Research Objectives

1. Develop SPR as a methodology for following protein-protein interactions or protein aggregation.

2. Develop an appropriate SPR sensor surface to study protein-protein interactions.

3. Develop BLG as a model experimental system for validating SPR as a methodology for following protein-protein interactions and protein aggregation behaviour.

4. Determine the role of PA in BLG aggregation.

5. Utilize SPR to measure protein interactions with colloidal material isolated from natural water.

6. Develop a mechanistic model to describe BLG protein aggregation behaviour based on SPR data.

### 1.1.2. Thesis Organization:

Chapter 2 begins with the explanation of the theoretical fundamentals and methodologies of surface plasmon resonance (SPR). Principles for constructing biosensor surfaces utilizing self-assembled monolayers (SAMs) are also outlined, along with applications. Chapter 3 explains the methodologies utilized to conduct the experiments in the following chapters. Chapter 4 presents a statistical analysis of SPR data to determine the change in adsorption strength observed when BLG interacts with PA. Chapter 5 explains the method development used to determine if interactions occur between the model protein α-lactalbumin (AL) and colloidal particles extracted from Grand River water. Chapter 6 is the development of a mechanistic model for BLG adsorption onto SAMs.

# Chapter 2. Literature Review

## 2.1. β-Lactoglobulin Characteristics and Aggregation Properties

β-Lactoglobulin (BLG) is a globular protein and one of the main components of whey (Schokker *et al.* 1999), a by-product of cheese manufacturing. Other whey components include α-lactalbumin, bovine serum albumin, and immunoglobulin along with various nutrients and fats. BLG is often concentrated and extracted from whey protein, and utilized as an additive in other food products due to its effect on the foods texture and stability (Euston *et al.* 2000).

BLG is an 18.3 kDa protein with 162 amino acid residues. It has two genetic variants, A and B, which differ by two amino acids which accounts for only a 70 Da (Mackie *et al.* 1999) difference between the two proteins. BLG is part of the lipocalin family, and has an internal hydrophobic cavity which allows it to bind to fatty acids and other non-polar molecules such as retinol (Frapin *et al.* 1993, Ragona *et al.* 2000). The biological function of BLG is debated, some consider it to be a nutritional protein, and others believe that the ligand binding properties seen in ruminant BLG suggest a transport role for digestion (Wu *et al.* 1999).

BLG exists as a dimer at neutral pH and low ionic strength, but forms higher order aggregates at pH 4.8 (Elshereef *et al.* 2010), despite the isoelectric point of BLG being 5.2. The higher order aggregates appear to have an "open ended" aggregation at pH 4.8 and low ionic strength (Majhi *et al.* 2006). The open ended aggregates have an average size equivalent to a BLG octamer (Townend & Timasheff 1960, Timasheff & Townend 1961). It is suggested that electronic interactions play a large role in reversible BLG aggregation and dimerization (Majhi *et al.* 2006). The ionic strength of solution has different effects on aggregation depending if BLG is above or below its isoelectric point. At pH 2.0 BLG exists as a monomer at low ion concentrations, and as the ionic strength is increased BLG begins to form dimers (Aymard *et al.* 1996). At pH 6.9, BLG is in equilibrium with its dimer (Elshereef *et al.* 2010). As the BLG concentration increases, the amount of dimeric protein increases as well (Wahlgren & Elofsson 1997). BLG has also been known to form amyloid fibrils in the presence of co-solvents such as urea (Hamada & Dobson 2002).

BLG is often isolated through membrane extraction processes, but this process is plagued by decreases in flux due to membrane fouling (Bhattacharjee *et al.* 2006, Zydney 1998). Part of membrane fouling is due to the nonspecific adsorption of BLG to the filtration membranes (Mulvihill & Donovan 1987). Once nonspecific adsorption occurs there is a tendency for proteins to unfold and undergo conformational changes (Norde 2008). In the unfolded state proteins may then aggregate with other proteins in the media (Mulvihill & Donovan 1987). Although membrane filtration is important in BLG separation processes, heat treatment is also utilized to separate whey proteins. Despite the alternative methods, BLG fouling still occurs on the heat exchange surfaces (Lalande & Tissier 1985). Although the aggregation and fouling mechanism might not be precisely the same as in membrane fouling, many proteins still undergo nonspecific adsorption before fouling begins (Chan & Chen 2004). Heat induced aggregation is also influenced by pH, and is thought to involve partial denaturation of BLG monomers after the dimers have undergone dissociation, which is then followed by aggregation (Gezimati *et al.* 1997, Qi *et al.* 1997). As a result of the denaturation/aggregation, there is a loss of BLG functionality during this heat processing.

The fundamental driving forces for many of the above undesired phenomenon are due to the complex interactions of proteins. As such there are numerous methods that have been developed to probe these interactions to identify mechanisms, binding constants, and other important factors.

### 2.1.1. Measuring Protein-Protein Interactions

Several techniques such as sedimentation equilibrium (SE), light scattering (LS) and nuclear magnetic resonance (NMR) measure protein interactions directly in solution (Phizicky & Fields 1995). Other methods such as quartz crystal microbalance (QCM), SPR and certain light scattering techniques (Phizicky & Fields 1995) require the immobilization of one of the proteins involved in the interaction onto a sensor surface, and detecting mass accumulation due to interactions between the target molecule in the bulk solution and immobilized protein. Solution and surface based techniques are often utilized to verify one another, although some small discrepancies between the two techniques have been found (McWhirter *et al.* 2008). The following is not meant to be a complete list of measurement methods for protein-protein

interaction and the reader is directed to the review by Phizicky and Fields (1995) (Phizicky & Fields 1995) for more information.

SE is a method which utilizes an analytical centrifuge to produce a concentration gradient in solution which is monitored through optical methods. This concentration gradient is a balance between the flux of molecules sedimenting and their diffusional fluxes, which are then utilized to calculate the hydrodynamic radius of the molecules (Ghirlando 2011). SE is often utilized to confirm kinetic constants extracted from other protein-interaction methods such as SPR or LS (Dall'Acqua *et al.* 1996). For example, this method was utilized to determine kinetic aggregation constants for BLG at neutral pH (Zimmerman *et al.* 1970).

Static and dynamic LS have been utilized by researchers to predict "weak" intermolecular interactions between proteins from measurements of translation diffusion coefficients and hydrodynamic radii (Fernández & Minton 2009, Hanlon *et al.* 2010). There are numerous methods and interpretations that can be utilized for LS analysis which is beyond the scope of this thesis. A more detailed theoretical discussion can be found in Schurr *et al.*(1977) (Schurr & Bloomfield 1977). On most accounts, LS is utilized to determine protein self-aggregation at high concentrations (Fernández & Minton 2009). LS is not only restricted to solution experiments but can also be utilized to study surface aggregation as well. A study by Bee *et al.* (2010) utilized LS to determine size distribution of steel- monoclonal antibodies aggregates for preventing adverse reactions in patients during needle based drug delivery (Bee *et al.* 2010).

NMR utilizes interactions between atomic dipoles and electromagnetic pulses to determine structural relationships between adjacent molecules. With enough data these relationships can be translated to an atom resolution three dimensional diagram of a protein (Takeuchi & Wagner 2006). In recent years, NMR techniques have expanded allowing for mapping of protein-protein (Heise 2008) and protein-small molecule binding sites (Ragona *et al.* 2000).

Of the methods outlined above, SPR and QCM are the most similar in that they produce real time, kinetic data of surface interactions. They differ in that QCM measurements are a function of density, viscosity and stiffness (material parameters), while the SPR sensorgram is dependent on the solution's dielectric constant (Köβlinger *et al.* 1995). QCM utilizes an external electrode potential applied to piezoelectric quartz, which produces mechanical stress and with the proper

geometry, induces a resonant oscillation. Deposition of mass onto the QCM induces changes in the resonant frequency (O'Sullivan & Guilbault 1999). QCM has been utilized as a DNA biosensor, immunosensor and for drug analysis (O'Sullivan & Guilbault 1999). Recently QCM with dissipation monitoring, which allows for simultaneous measurement of other viscoelastic properties of the deposition layer, is seeing use in biological applications (Dixon 2008).

### 2.1.2. Protein-Colloidal Interactions

In order to produce drinking water, surface and ground water must undergo various pre/post-treatment processes to remove natural organic matter (NOM) and pathogenic organisms (Fiksdal & Leiknes 2006). A common pre-treatment for the removal of NOM is the ultrafiltration (UF) of water. Unfortunately, NOM is considered to be major membrane foulant which results in a decreased efficiency in UF systems (Saravia *et al.* 2006, Jermann *et al.* 2007). The non-humic components of NOM, protein/amino acid residues as well as colloidal particulate matter bind synergistically to increase membrane fouling (Jermann *et al.* 2008, Amy 2008, Lee *et al.* 2006, Susanto *et al.* 2008). Studying the components of NOM through fluorescent emission excitation matrices (EEMs) is a relatively quick and label free approach, which has been shown to be suitable for identifying high fouling events. The intrinsic fluorescence of the amino acids tryptophan and tyrosine are easily detected and representative of the protein component of NOM (Peiris *et al.* 2010a). Tryptophan is present in many proteins, such as the components of whey BLG and α-lacalbumin (AL). AL differs from BLG in that it has a high tryptophan content and does not self-associate as readily as BLG (Bhattacharjee *et al.* 2006). The ability to measure the interaction between AL and colloidal matter would help improve the understanding of the high fouling events and would be beneficial to many industries.

## 2.2. Surface Plasmon Resonance Introduction

Surface plasmon resonance (SPR) has attracted the interest of many researchers and has been gaining momentum ever since its discovery in 1968 (Phillips & Cheng 2008). There are several recently published review articles that cover a range of applications of SPR through different industries; from waveguides (Barnes *et al.* 2003) to nanoparticles and fluorescent interactions (Eustis & El-Sayed 2006) to detection of binding constants of biological species (Homola 2008). The sensitivity of the surface plasmon, also known as a surface plasmon polaritron (SP) (Barnes

1998), to changes in a layer close to the conductor surface as well as its label free nature has led to numerous applications in both biological and chemical detection.

### 2.2.1. Theory

SPR is an optical phenomenon involving the excitement of SP by p-polarized light (Barnes *et al.* 2003). SPs are a consequence of the interaction of light with the free electrons present in conductors such as metals. The coupling of a light beam to the metal's electrons traps the wave to the surface, essentially creating an evanescent wave (Barnes *et al.* 2003). This evanescent wave penetrates into both the metal and adjacent dielectric layer and thus the resonance conditions depend strongly on the thickness and dielectric constant of the layer close to the conductor surface (de Bruijn *et al.* 1991). The sensitivity of these changes in refractive index (RI) is so minute that they are directly correlated to a surface concentration within the penetration depth of the SPR machine. The penetration depth distance is equivalent to 37% of the evanescent wave's field strength at the dielectric/metal interface (Stenberg *et al.* 1991). Another important implication of measuring the RI is that the analyte in question does not need to be labelled. The signal can be varied such that measurements can be made in real-time, every 0.1-1 second for the instrument used in this research. The real-time measurement interval was changed based on the speed and equilibration time of the adsorption kinetics. This extreme sensitivity makes SPR ideal for measuring kinetic interactions (e.g. protein-protein interactions, immunoassays).

The current methods utilized to excite SPs are through a prism coupler, a waveguide coupler and a grating coupler (Homola 2008). Depending on the configuration each has its advantages and disadvantages with prism couplers in the Kretschmann configuration most typically used (Homola 2008). In this mode a light beam passes through a triangular prism on one side, interacting with the thin metallic layer on the other, and finally reflecting and passing out of the prism on the opposite side (Figure 2.1) (Kretschmann & Raether 1968). The type of detection method used will determine the wavelength of light beam required or whether the beam is monochromatic or polychromatic. Different methods are based on either changes in coupling angle, coupling wavelength, intensity or phase of the reflecting light (Homola 2008). For example, in the case of a coupling angle detection format, a monochromatic light beam is shown at an angle such that the beam is totally internally reflected within the prism. The angle of

incidence is then changed and a dip in intensity is observed when the light beam has coupled to the surface plasmon, which is measured as the output (Matsubara *et al.* 1988). This allows for real-time measurement of binding events that occur near the sensor surface (Figure 2.2).

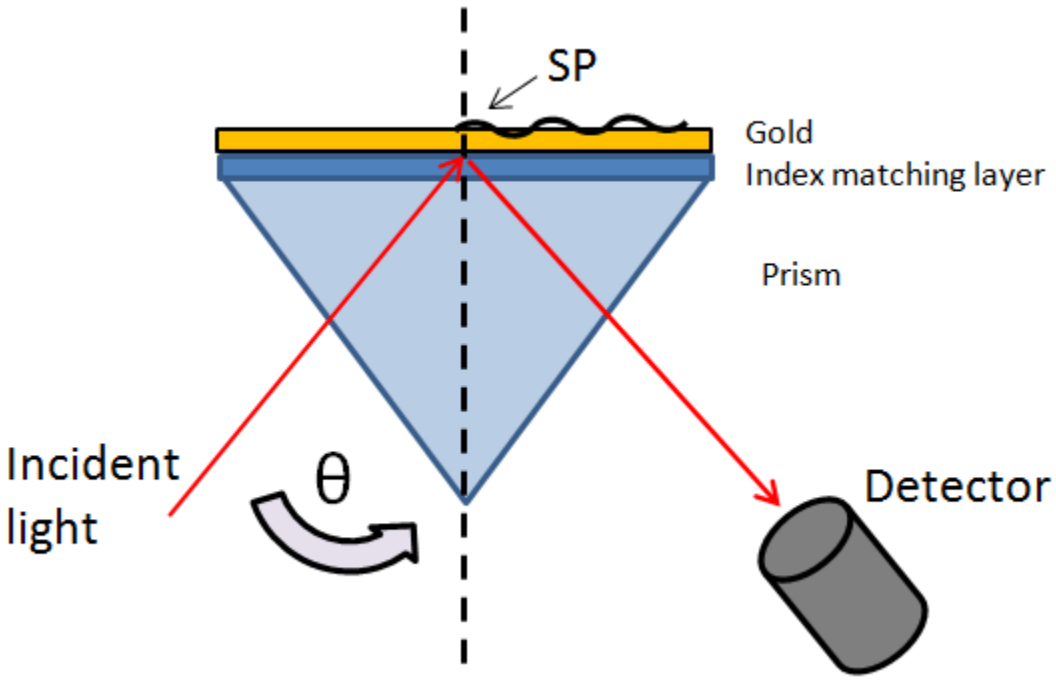


**Figure 2.1: The Kretschmann configuration for SP excitement using the coupling angle detection format.**

**A monochromatic light beam is shown through the prism and totally internally reflected to the other side. As the incident angle (θ) is varied, conditions at which SPR occur are detected as a minimum of intensity**

In 1991 researchers utilized radio-labelled proteins in conjunction with an SPR device to prove that within a certain thickness above the metal interface the SPR signal is directly proportional to the mass per unit area accumulated at that layer (Stenberg *et al.* 1991). Thus, the SPR signal can be converted to a surface concentration, and with a known excitation area, can directly be converted to accumulated mass. The wavelength of the laser employed controls the penetration depth of the evanescent wave and thus limits the size of the molecules that can be accurately detectable by the instrument. Also depending on the configuration, extremely fast reactions may not be accurately measured. The signal to mass conversion in this situation can be utilized for qualitative rather than quantitative results.

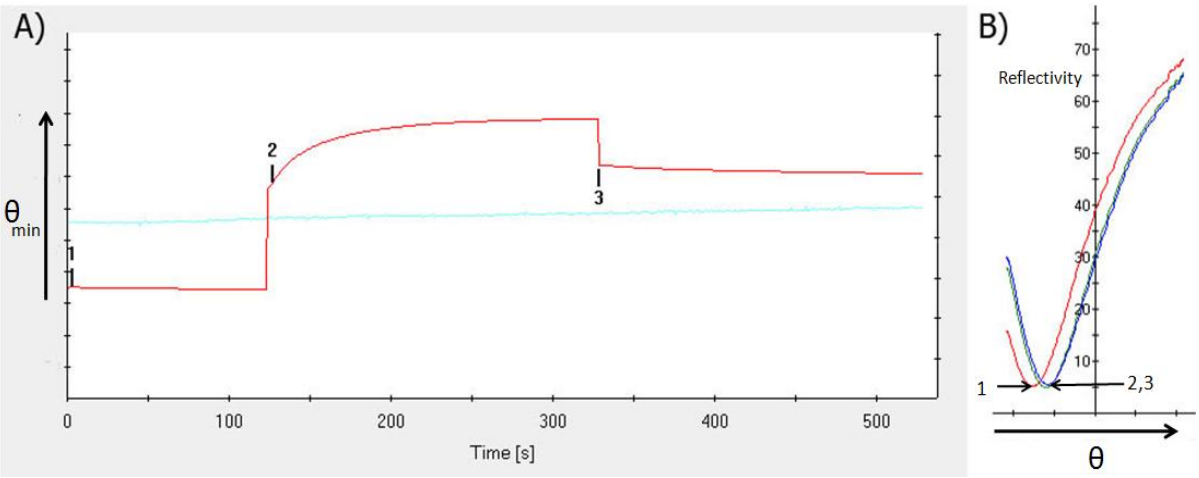


**Figure 2.2: A sample experiment taken from Autolab SPRINGLE.**

**Point 1 indicates the start of the experiment as running buffer is injected over the surface. At point 2 the analyte is injected (in this case BLG) and there is a jump due to RI mismatching. Point 3 is when the running buffer is used to wash the surface and begin the dissociation step. B) The reflectivity vs. θ (incident angle) for points 1, 2 and 3 are shown. As θ is varied, the minimum reflectivity is the point at which maximum SPR is occurring and is taken as the signal seen in part A.**

In a typical system, the analyte is injected into the sample chamber, after a baseline has been established with running buffer (Figure 2.2A). Some systems utilize a micro fluidic flow system, in which the running buffer is used to establish a baseline, and the inlet feed is switched to an analyte solution (Day & Myszka 2003). The different setup of each system means that they both require different kinetic interpretations of the data. Regardless of injection method, in order to properly interpret the data obtained by an SPR kinetic curve, care must be taken to control the experimental conditions such as analyte concentration, temperature and analyte/running buffer refractive index (RI) matching (Persson *et al.* 1997, Melendez *et al.* 1996, Meléndez *et al.* 1997). The SPR itself is very sensitive to temperature changes between the buffer solution and the analyte. This can cause a significant baseline shift upon injection into the system. The first few seconds of the signal curve can be convoluted as the solution equilibrates with the operating temperature simultaneously as mass accumulates on the surface. Matrix effects occur if there is a mismatch between the analyte and running buffer RI due to analyte concentration/salt concentration/pH (Figure 2.2A). This affects the layer properties and thus can affect the SPR signal (Autolab 2006). For example if the analyte dimerizes post injection, this will change the bulk RI of the solution and thus have an effect on the SPR sensorgram. Finally, since SPR detects the mass accumulating on the sensor surface, it cannot distinguish between the target

analyte and any contaminating protein or molecule that may be attracted to the surface, typically referred to as nonspecific adsorption. All of the above mentioned effects, temperature, bulk solution matching, and nonspecific adsorption can generate false signals. In a dual channel configuration these signals can be subtracted out, leaving only the desired binding events and thus increasing sensitivity (O'Brien II *et al.* 1999). If this approach is unavailable, control experiments are conducted so that the signals can be subtracted for short-term measurements (Sigal *et al.* 1997).

### 2.2.2. Applications

Smaller molecules are difficult to detect using SPR, with molecular weights <1000 Da requiring a significant increase in analyte concentration (Beccati *et al.* 2005). Another method to overcome this is by careful experimental design. Competitive or inhibitive assays are often utilized which are indirect sensing methods. An inhibitive assay was used for the continuous detection of dichlorodiphenyltrichloroethane (DDT) in mountain water, with detection limits well below the government safety requirements (Mauriz *et al.* 2007). In this experiment, monoclonal DDT antibodies were used as the analyte, which were attracted to a layer of bovine serum albumin (BSA) or ovalbumin conjugated with DDT. As the DDT in the analyte solution increases, it binds with the monoclonal antibody preventing it from interacting with the surface. In this way the signal is inversely proportional to the amount of DDT in the analyte solution. A competitive methodology has also be utilized to detect low molecule substituent such as 2,3,7,8-tetra-chlorodibenzo-*p*-dioxin (TCDD), a toxic chemical to humans (Shimomura *et al.* 2001). TCDD was as the analyte and TCDD -horseradish peridoxase conjugates (TCDD-HRP) were used as the competitor. The SPR instrument cannot detect TCDD due to its small size and thus only detects the molecules conjugated with HRP. A second step in the competitive assay was to use an HRP antibody to determine the amount of TCDD-HRP that was bound to the surface. In this way the researchers were able to detect TCDD at levels of about 0.1 ng/ml.

SPR is also seeing an increase in use for biomedical and pharmaceutical applications. The detection of cortisol in saliva (Stevens *et al.* 2008) and the classification of drug's primary binding site to albumin (Day & Myszka 2003) are both examples of how SPR is being used effectively in this field. Saliva is an extremely complex matrix and in a typical SPR experiment one would expect large amounts of nonspecific adsorption. Stevens *et al.* (2008) used filtering

techniques in conjunction with SPR to negate the effects on nonspecific adsorption while still being able to measure cortisol. The latter experiment involving the classification of a drug's primary binding site shows how SPR can be used in pharmaceutical applications, particularly in drug design and testing. Another recent study has demonstrated the use of SPR to measure nanoparticles conjugated with different drugs and how this affected their association kinetics with a model layer (Tassa *et al.* 2010). The ability to measure nanoparticle-drug enhancement is a vital tool especially since nanotechnology is in its infancy and there are few inexpensive and quick techniques to measure these nanoparticle interactions. In another SPR application researchers developed an on-line sensor to detect recombinant protein produced in a bioreactor (Jacquemart *et al.* 2008). They plan to be able to modify their SPR sensor to be able to simultaneously assess the activity of the recombinant protein on-line. This would provide a greater control over bioreactors thus theoretically allow for higher throughput and reduced costs.

SPR has also found use in industries outside of biotechnology, for example, to image electrochemical reactions (Shan *et al.* 2010). In this experiment the researchers created a fingerprint on a glass slide; this meant that any proteins or contaminants on the fingerprint ridges will block the gold from being electrochemically reduced. SPR was able to not only create an inverse image of the finger print, but also detect tri-nitro-toluene (TNT) and wax residues which were handled by the researchers prior to the experiment. All these papers show that with proper preparation and experimental design SPR can be a powerful tool.

## 2.3. Self-assembled Monolayers

As proteins approach a flat planar surface they undergo a structural re-arrangement due to their polyamphilic nature to balance the oppositely charged and non-polar amino acids with surface forces (Norde 2008). The protein will change its structure in order to reach a thermodynamically favourable state (Rabe *et al.* 2011). In some cases a complete re-orientation of the protein layer, resulting in a change in affinity between the surface protein layer and proteins from solution, is required in order to reach equilibrium (Rabe *et al.* 2007). To analyse interactions between proteins at surfaces, special care must be taken beforehand to properly construct an adequate model surface for experimentation.

Self-assembled monolayers (SAMs) are easy to form and produce stable surfaces. They are able to undergo chemical reactions for the purpose of creating specialized functions, often for measuring interactions with different molecules and proteins (Zhang 2003). As the name suggests, when provided with the right environment SAMs can spontaneously form over a surface, i.e. at STP and with the correct substrate and solvent, creating a layer of molecules not unlike a cell's membrane phospholipid bilayer (Figure 2.3). The ease of construction and robustness of functionalization make SAMs the target of current research for biosensor surfaces.

### 2.3.1. SAM Substrates

The supporting substrate is one of the most important controls when forming stable monolayers. The most common substrate is gold and silane (Schreiber 2004), although monolayers have been formed with other materials (Schreiber 2000). Gold easily forms covalent bonds with sulphur at room temperature, which acts as a backbone for the self-assembly reaction. Unfortunately, gold is also easily contaminated in air due to oxidation and its extreme preference to bind organic molecules (Ron *et al.* 1998). A contaminated layer has an increased likelihood of forming gaps in the monolayer leading to rapid instability and difficult reproducibility (Ishida *et al.* 1999, Ron *et al.* 1998). The ability for gold to conduct SPs means that any adsorption on these surfaces can be investigated using SPR.

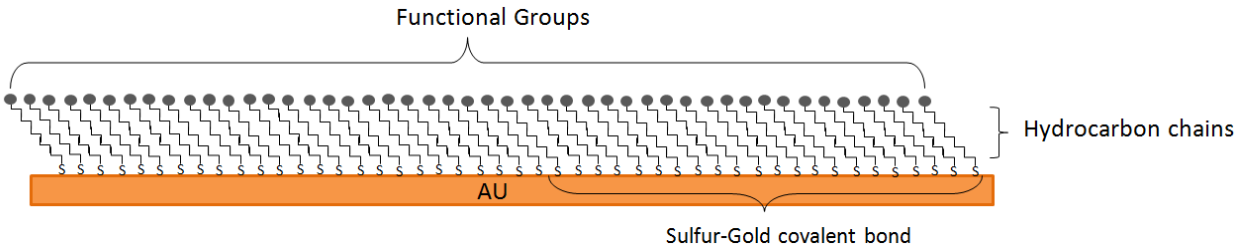


**Figure 2.3: Depiction of a typical SAM formed utilizing an alkanethiol adsorbed onto a gold layer**

**The alkanethiol is 11-mercaptoundecanoic acid (11-MUA). The head groups are –COOH. The sulphur groups bind to the gold surface, while the hydrocarbon chain stabilizes the head groups. Depending on the molecule used for SAM formation the head groups exposed to the surface can include -COOH, $-CH_3$, -OH, $-NH_2$ or poly-ethylene glycol depending on the desired function.**

### 2.3.2. Monolayer Structure and Protein Adsorption

A simple SAM would be comprised of only one type of molecule, containing a thiol end group which covalently binds to the gold. Alkanethiols, a thiol covalently linked to a longer hydrocarbon chain, are the most common SAM molecules. The hydrocarbon chain is covalently

bound to a functional group, which is oriented toward the solution. The most common solvent utilized to dissolve the SAM molecule for contact with the gold layer is an alcohol, such as ethanol or methanol. Most assembly takes less than 24 hours (Schoenfisch & Pemberton 1998). Functional groups can be selected prior to adsorption or changed post adsorption with different chemical reactions. The functional groups lead to different surface properties such as hydrophobic, hydrophilic, positively charged, negatively charged and protein inert monolayers (Ulman 1996). Different layers attract proteins through a variety of mechanisms depending on the protein being analysed (Norde 2008). The length of the hydrocarbon chain can have different effects on protein adhesion properties (Patel *et al.* 1997). There are many reviews available that cover the further physical aspects of SAMs (Schreiber 2000, Schreiber 2004).

### 2.3.3. SAM Characterization

Once the layer is formed there exists a variety of methods for SAM characterization and detection. A relatively quick SAM stability test is to conduct cyclic voltammetry on the layer in the presence of a ferrocyanide solution. The ferrocyanide will oxidized the gold at specific voltages, unless the SAM layer is present and blocks the electrons for the electrochemical reaction (Ganesh *et al.* 2006). Other methods for SAM characterization include impendence measurements and Nyquist plots (Dijksma *et al.* 2000).

### 2.3.4. SAM Fouling and Degradation

The fouling of SAMs occurs in a similar way to the fouling of gold since the thiol groups of SAMs exposed to air can easily be oxidized (Schoenfisch & Pemberton 1998). As oxidation occurs the layer becomes disordered, resulting in pocket formation, gold degradation/oxidation and SAM conformational changes (Willey *et al.* 2005). Often complete removal is required to re-use the gold surface. SAMs can be removed through surface plasma cleaning (Raiber *et al.* 2005), immersion in piranha solution, or electrochemical cleaning; the effectiveness of each depends on the nature of the SAMs (Guo *et al.* 1994). Some cleaning methods, such as plasma cleaning, can damage the gold surface thus making electrochemical methods preferred for single chips SAMs (Canaria *et al.* 2006). There have been other reports of the thermal self-healing of SAMs (Bucher *et al.* 1994).

### 2.3.5. Protein Immobilization

In order to conduct most SPR kinetic analyses, the proteins should be immobilized to the sensor surface, i.e. covalently linked to the SAM layer without significant conformational changes. The most common method is through 1-ethyl-3-(3-dimethylaminopropyl) carbodiimide (EDC)/*N*-Hydroxysuccinimide (NHS) chemistries (see Section 3.2.3) for amine coupling (Samanta & Sarkar 2011). Most often this method results in the protein being immobilized in a random orientation. This may have adverse effects on the kinetic constant determination. For example, antibody orientation has a significant effect on the strength of binding of the target analyte and in some cases specificity of the surface (Kausaite-Minkstimiene *et al.* 2010). If a more oriented surface is desired, DNA directed immobilization, or peptide and biotin linker immobilizations are just some of the popular methods (Samanta & Sarkar 2011). Recently, creating a three-dimensional dextran layer on top of SAMs has become popular due to dextran's ability to resist nonspecific adsorption as well as increasing packing density of adsorbed protein (Masson *et al.* 2006).

### 2.3.6. SAM Applications

The surfaces produced by SAMs have diverse applications. Some SAMs are utilized to form highly oriented antibody surfaces to create microarrays for high throughput parallel diagnostics of unknown analytes and in drug discovery experiments (Hodneland *et al.* 2002). In other cases protein resistant SAMS are utilized to study the mechanism of protein resistant surfaces to help create effective artificial biomedical implants (Shen & Lin 2011). Other protein association mechanisms studied are for early disease detection, predicting amyloid fibril propagation and the associated growth mechanism for early detection and defence to Alzheimer's disease (Aguilar & Small 2005). These mechanistic studies will help in drug design and in the future be utilized as a quality control for drug applications (Cooper 2002).

# Chapter 3. Materials and Methods

## 3.1. Chemical Reagents and Solutions

β-Lactoglobulin (BLG) and α-lactalbumin (AL) were used in their powdered form and were donated by Davisco Foods International (LeSueur). The BLG and AL were of 95% purity. Bovine serum albumin (BSA- 95% purity) was purchased from Sigma Aldrich International. Triethylene glycol monoamine (TEG) was purchased from Molecular Biosciences (Boulder, Colorado, USA). To form TEG blocking solution 1M of TEG was mixed with water (Frederix *et al.* 2004). Ethanolamine blocking solution was made in accordance to the SPR user manual (Autolab 2006). All other chemicals used were of analytical grade and obtained from Sigma Chemical (St. Louis, MO). Running buffer was comprised of Milli-Q water (18.2 MΩ cm) and 20 μM phosphate buffer at either a pH of 6.2 or 7.2. Coupling buffer was the same as running buffer unless otherwise stated. Phosphoric acid was utilized to decrease the pH of the buffer. For experiments involving AL (Chapter 5) running buffer was 100 μM phosphate buffer at pH 7.4, unless otherwise stated. Self assembled monolayer (SAM) solutions were created using a mixture of ethanol (EtOH) and 1 mM 11-mercaptoundecanoic acid (11-MUA) (Autolab 2006). For immobilization solutions, equal volumes of 0.5 M of 1-ethyl-3-(3-dimethylaminopropyl) carbodiimide (EDC) and 0.1 M of N-hydroxy succinimide (NHS) were mixed and immediately injected (Autolab 2006) over the sensor surface.

## 3.2. Basic SPR Experiments

All SPR experiments were performed at 25 $^{o}$C using a cuvette-based AutoLab SPRINGLE (Echo Chemie BV, The Netherlands) analyzer. This device utilizes surface plasmon resonance (SPR) phenomena generated on the surface of Au coated $SiO_2$ disks to measure the mass accumulating on the sensor surface.

### 3.2.1. SPR Disk Preparation and SAM Formation

New Au-$SiO_2$ SPR disks (Metrohm USA, Inc.) were first washed with 95% EtOH and Milli-Q water and then dried under a nitrogen stream. Once dry, the disks were immediately immersed in SAM forming solution for 12 hours to generate stable SAM layers (Autolab 2006). The disks were then washed with 95% EtOH followed by Milli-Q water, dried under a nitrogen stream and placed into the SPR SPRINGLE for analysis. All SPR experiments utilized a 11-MUA SAM.

### 3.2.2. Typical Protein-SAM SPR Experiment

All of the experiments for protein-SAM association were adapted from a sequence that was provided in the SPRINGLE software "Curve-SA-a full kinetic plot" (Autolab 2006). The analyte utilized in the following example is BLG. In this sequence, the sample delivery lines were flushed and replaced with running buffer. The experiment was initiated with an injection of 50 µl of running buffer to establish a baseline for 120 seconds (Figure 3.1A). The next step was the association phase in which 50 µl of BLG solution was injected into the cuvette for 3600 seconds (Figure 3.1B). The association time depends on the type of analyte being used as well as the functionalization of the sensor surface. The SPR response units (RU) are directly proportional to a surface concentration (Autolab 2006). Following the association step, the surface was washed with 500 µl of running buffer to remove any weakly bound BLG from the surface. The dissociation phase began immediately after a 50 µl injection of running buffer into the cuvette. The change in concentration gradient from the bulk solution to the BLG-rich surface caused some of the BLG to diffuse into the bulk phase, which is seen as a loss of mass on the SPR sensorgram (Figure 3.1C). If the same spot is used for subsequent experiments a regeneration sequence may need to be performed. The regeneration phase consisted of an injection of 250 µl of the desired regeneration solution into the cuvette (Figure 3.1 utilized 0.1 M HCL). 200 µl of the regeneration solution is used to flush the cuvette followed by a 50 µl injection which is kept on the surface for approximately 10-15 minutes to allow any further protein desorption. Running buffer was again used to wash the surface and a baseline check was performed before the system went into maintenance mode to preserve the quality of the gold disk. For a more rigorous cleaning procedure see Section 3.5.3.

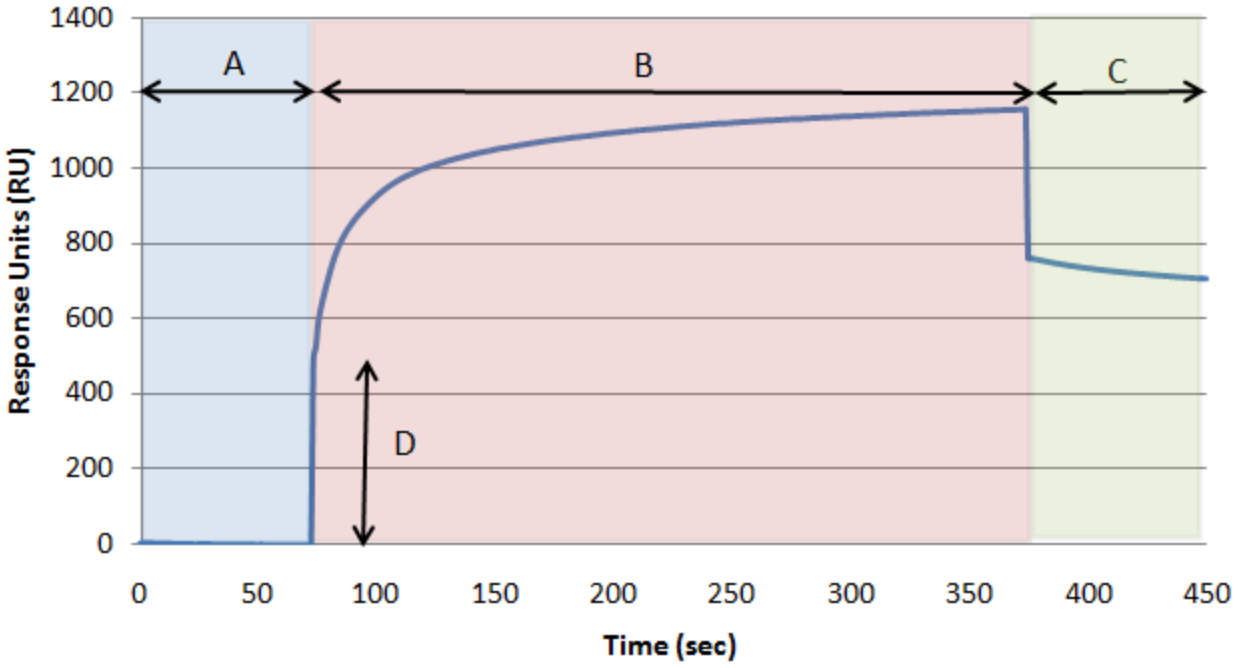


**Figure 3.1: SPR sensorgram of BLG-SAM interactions.**

**BLG concentration is 1.4 mg/ml in 100 mM phosphate buffer - pH 4.7. A) baseline phase; B) association phase; C) dissociation phase; D) Change of refractive index (RI) due to mismatch between running buffer and association buffer.**

### 3.2.3. Typical Protein-SAM Immobilization

Before a protein association experiment, the surface of the SPR disk may need to be functionalized to take advantage of specific analyte-ligand interactions. The method for immobilizations was adapted from the "AutoLab SPR getting started" manual and a sequence that came with the SPRINGLE software "Immobilization" (Autolab 2006). In this sequence a coupling buffer was used to wash and fill the lines, followed by a baseline step. Immobilization solution was injected over the surface for 5 minutes (Figure 3.2A). After the surface had been rinsed with a small amount of running buffer, 50 µl of the desired surface-bound protein was injected into the cuvette for 15 minutes (Figure 3.2B).

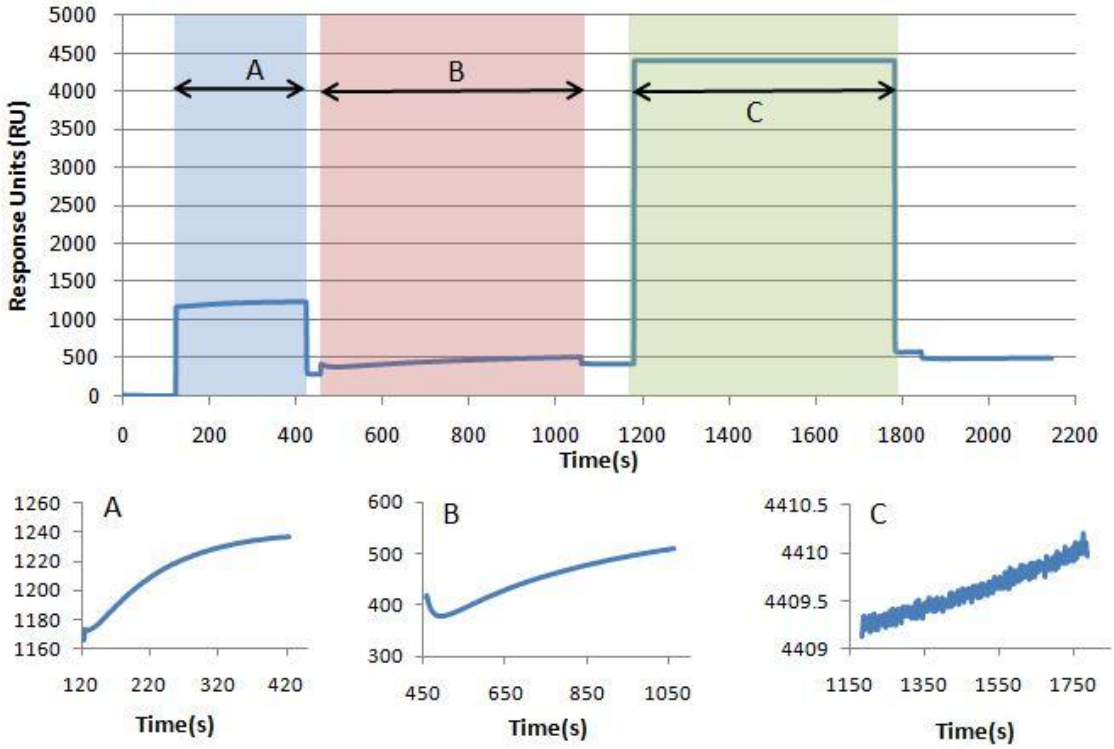


**Figure 3.2: Immobilization of AL to 11-MUA SAM.**

**Inset figures A,B and C represent the steps of the immobilization as shown in the top panel. A) NHS/EDC activation step. B) AL (1mg/ml in 100 mM phosphate buffer - pH 7.4,) injection and association/immobilization. C) Blocking of surface with TEG. Wash steps (using 100mM phosphate coupling buffer (pH 7.4)) were conducted between the immobilization runs prior to injection of a new chemical substance.**

Deactivation of the surface was required before any association step to prevent non-specific protein interactions. Ethanolalmine or TEG was utilized as deactivating/blocking agents with TEG being the stronger of the two (see Section 3.2.4) (Frederix *et al.* 2004). The surface was then cleaned with coupling buffer and 0.1 M HCl.

### 3.2.4. SAM Blocking

Used for control experiments, the SAM blocking method is adapted from a typical immobilization experiment. In this sequence no protein was immobilized to the surface. SAM surfaces were first activated using a 50 µl mixture of immobilization solution. The mixture was allowed to interact with the layer for five minutes before a wash with Milli-Q water. This was then followed with TEG (1 M in Milli-Q water) injected into the cuvette for 40 minutes. The layer was washed again with 500 µl Milli-Q water, cleaned for 5 minutes with 0.1 M HCl, followed with a 500 µl Milli-Q water wash.

### 3.2.5. SPR Data Analysis

Data was exported to Excel 2007 for analysis. All data was zeroed to the point just after the bulk RI increased (Figure 3.1D) which followed the post injection unless otherwise stated. The dissociation curves were normalized by dividing by their respective maximum association signal, and then zeroed to the first point just after the bulk RI change.

### 3.2.6. Surface Fluorescence Analysis Using a Fibre Optic Probe

After a dissociation event had been performed, a Varian Cary Remote Read Fibre Optic Probe (Palo Alto, CA) coupled to an Eclipse Fibre Optic Coupler was used to scan the gold disk. The signal was measured using a fluorescence spectrofluorometer with a pulsed xenon flash lamp as the light source (Varian Cary Eclipse, Mississauga, ON, Canada). This would generate an emission-excitation matrix (EEM) of the area on the disk. After the desired SPR experiment had occurred, all liquid was drained from the cuvette and the disk removed from the SPR. The disk was then air dried and placed on a black surface so that the probe could be positioned. The probe was placed such that its contact points were flush with the gold surface and care was taken so that the bound material was not disturbed. The angle at which the data was collected was fixed at $45^{o}$ (Figure 3.3). The EEMs were obtained with a PMT voltage = 700 V and excitation and emission slit widths = 20 nm each. To eliminate any significant background noise, an EEM of a bare SAM layer was subtracted from the data collected for the sample analysis. The final data matrix consisted of 300 x14 intensity readings. 300 emission points were examined per run with emission wavelengths ranging between 300–600 nm. With each emission point 14 excitation wavelengths was sampled, varying by 10 nm increments from 250-380 nm. This procedure was carried out under constant humidity conditions. The fluorescence EEM analysis procedure that was used for the fluorescence signal correction and the selection of the spectrofluorometer parameter settings to obtain reproducible fluorescence signals were as previously described (Peiris *et al.* 2008, Peiris *et al.* 2009). The EEM data was exported to MATLAB (MathWorks, Natick, MA) for statistical analysis and averaging.

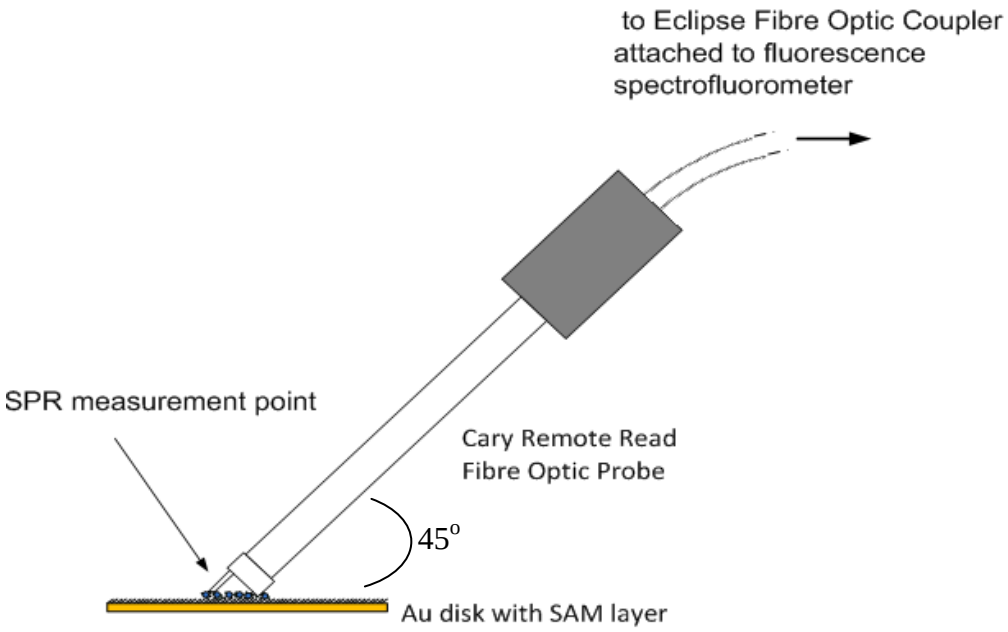


**Figure 3.3: Set-up for the FOP.**

**An illustration of how the fibre optic probe was positioned on the surface of the SPR sensor disk to capture EEMs after association events had occurred and had been measured in the SPR. Figure reprinted with permission from R.H. Peiris.**

### 3.2.7. Effect of BLG on Buffer pH

Since BLG also have an effect on the pH of the final solution, BLG and phosphate buffer were mixed at different pHs, and monitored daily for one week. The mixtures were left covered at 4°C in the fridge.

## 3.3. β-Lactoglobulin Interactions with Palmitic Acid

The following describes the methods utilized in Chapter 4 to assess the PA and BLG interactions. The molecules must be combined in the same solution to allow time to associate (Wang & Swaisgood 1993). Two approaches were utilized.

### 3.3.1. PA in Ethanol/Buffer

A stock solution of BLG (4 mg/ml in 100 mM phosphate buffer - pH 6.2) was mixed with PA in EtOH. The molar ratio of the BLG to PA was typically 20:1. The concentration of PA in EtOH was calculated such that the final solution to be injected into the SPR cuvette only contained 15% EtOH, which ensured no conformational change of the BLG (Mousavi *et al.* 2008). The mixtures were left to interact for a minimum of 4 hours before the solution was injected over the

11-MUA SAM sensor surface (see Section 3.2.2). The running buffer used in this experiment was 100 mM phosphate buffer (pH 6.2). The SPR association method was adapted from a normal association approach (see Section 3.2.2), where only the association and dissociation times were changed to 250 seconds and 120 seconds, respectively. The surface was regenerated with 0.3 M HCl for 125 seconds.

### 3.3.2. PA in Buffer

A 0.15 M solution of PA was prepared in chloroform and dispensed into glass test tubes. The chloroform was evaporated under a nitrogen stream to leave the PA (Figure 3.4). A solution of BLG solubilised in running buffer was placed into the tubes containing the remaining PA, sonicated at 22$^{o}$C for 40 minutes, and allowed to associate overnight at 25$^{o}$C. The controls were also sonicated under the same conditions. To vary the ratio of BLG and PA, volumes of the PA/chloroform solution were adjusted such that the BLG dimer and PA ratio ranged between 2:1 and 1:20. The solutions were then injected into the SPR cuvette. The SPR method and running buffer was the same as that utilized in the PA/BLG in EtOH/phosphate buffer experiment.

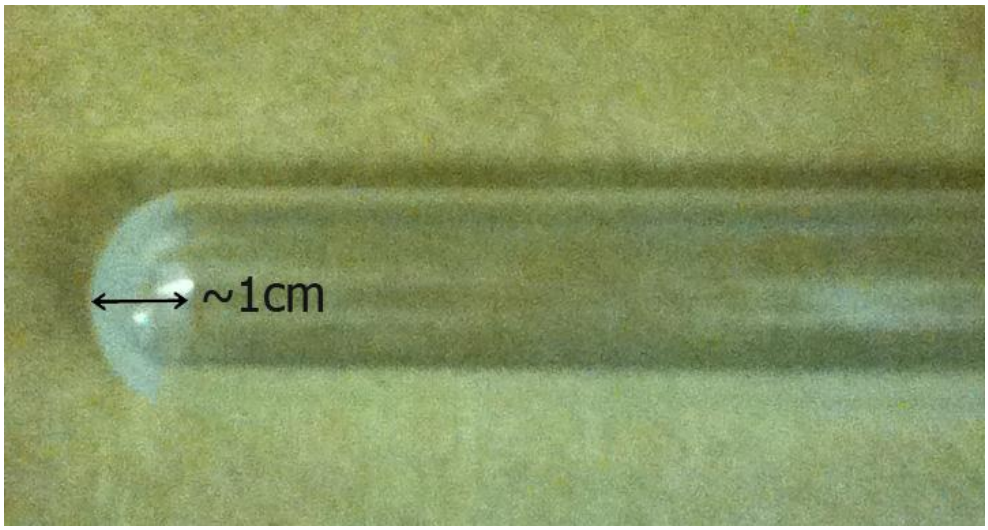


**Figure 3.4: PA deposited in test tube after all chloroform has been evaporated.**

### 3.3.3. EEMS of PA/BLG

The determination of the EEM was identical to that described in Section 3.2.6.

## 3.4. Method Development for BLG and Colloidal/Particulate Matter Interactions

### 3.4.1. Extraction of Natural Colloidal/Particulate Matter

Mixtures of colloidal/particulate and protein-like (CPP) matter were extracted from Grand River Water (GRW) (Southwestern Ontario, Canada) based on a previously described procedure that involves microfiltration and ultrafiltration (UF) stages (Peiris *et al.* 2009). For a complete methodology please see Peiris *et al.*, 2010a (Peiris *et al.* 2010a). The UF of the GRW utilized flat sheet UF membranes with a molecular weight cut-off (MWCO) of 20 kDa (Polysulfone - YMEWSP3001; GE Osmonics) and 60 kDa (Polyethersulfone - YMPWSP3001; GE Osmonics) from Sterlitech Corp. A layer of CPP from the UF was extracted and dissolved in 20 ml Milli-Q water using a vortex mixer. During the experimental period, the dissolved organic content (DOC) of the membrane feed ranged from 3.9 – 6.5 mg/L and turbidity values of 1.2 – 3.8 NTU. The pH of the membrane feed varied between 7.8 and 8.4. The pH of the extracted CPP solutions ranged between 7.1 and 8.3. The water collected from the Grand River was stored at 4 °C before the experiments and used within 48 hours of the collection time.

### 3.4.2. SPR Analysis

AL was used as a surrogate protein for assessing the interactions between colloidal and protein-like matter. Three different methods were utilized to probe the interactions between CPP and the AL.

### 3.4.3. Al Immobilization and CPP Association

A typical immobilization experiment was conducted in order to immobilize AL to the sensor surface (Figure 3.2). EDC/NHS mixture was injected to activate the layer for 5 minutes; AL (1 mg/ml, 30 μM phosphate buffer) was then injected into the cuvette to be immobilized onto the sensor surface. The layer was then blocked using ethanolamine followed by a wash with running buffer. This was followed by a cleaning step (0.1 M HCl) to remove any weakly bound protein and a final wash with coupling buffer. The association step with CPP was then conducted on the immobilized protein surface. 50 μl of CPP (~0.11 mg/ml Milli-Q water, calculated based on a dry weight basis) was injected to study its association with the surface. The SPR association method was adapted from a typical SPR experiment (see Section 3.2.2).

### 3.4.4. Multiple Injections

AL and CPP were sequentially injected into the SPR cuvette and allowed to associate for 400 seconds. For example, the Ax1Cx3 run, 50 µl AL (0.5 mg/ml) was injected into the cuvette and allowed to associate. After 400 seconds, the cuvette was drained which was followed by an injection of 50 µl CPP (~0.11 mg/ml Milli-Q water). This was followed by 2 more drain/injection cycles of CPP. Dissociation and regeneration (0.1 M HCl) proceeded as normal (see Section 3.2.). The method was repeated for different sequences of CPP and AL. The experiments were replicated twice.

### 3.4.5. Mixture of AL-CPP Experiments

Association experiments were adapted from previous experiments (see Section 3.2.2). Injections onto the SAM layer consisted of three separate solutions (50 µl) of (i) AL (0.5 mg/ml, running buffer), (ii) CPP (~ 0.11 mg/ml; Milli-Q water) and (iii) a mixture of AL and CPP, containing the same individual AL and CPP concentrations as in (i) and (ii). To ensure the homogeneity of the CPP solution during the SPR analysis, only soluble CPP was used. This was achieved by allowing the solutions to gravity settle for approximately 12 hours, or until visible particulates could be seen at the bottom of the cuvettes. The pH of the CPP solution was ~7.0. After each association step, the SAM layer was rinsed with 500 µl of running buffer and a dissociation step was performed. The resulting SPR kinetic curves were zeroed one second after injection to eliminate bulk solution effects. SPR analyses were performed in triplicate.

### 3.4.6. Fluorescence EEM analysis

See Section 3.2.6.

## 3.5. Modeling BLG Adsorption

### 3.5.1. SAM-BLG SPR Experiment

BLG and SAM association runs were conducted exactly as in a "typical Protein-SAM SPR experiment" (see Section 3.2.2). The data represented an average of a minimum of two runs. In some cases three or more runs were available and were utilized for that particular experiment.

### 3.5.2. Calculations and Model fitting

The SPR data (RU) is directly proportional to mass accumulation on the sensor surface. For presentation purposes, each SPR data point was normalized by dividing by 500 RU. This new

data points are referred to as normalised RU (NRU). Data was exported to Excel for formatting and then imported into MATLAB for analysis. A total of 10 unknown model parameters were estimated by utilizing the genetic algorithm (ga) from the nonlinear optimization toolbox and presented in table 6.1. The objective function ga optimized the least squares difference between the NRU data and model data. The model data was the summation of the integrated rate equations for the three monomers. The rate equations (Equations 3-7, see Section 6.2.2.) were solved numerically using the ODE15s function. Initial parameters to start the search were the variables reported by Rabe *et al.* (2007) (Rabe *et al.* 2007), and Wahlgren and Eloffson (1997) (Wahlgren & Elofsson 1997). All seven concentrations from both batches were simultaneously utilised to optimize the fit (See Appendix C). Afterwards, a 15% deviation was allowed for each parameter, and the parameters were individually optimized at each concentration.

### 3.5.3. Electrochemical Cleaning of SAM layer

To conduct multiple association runs on the SAM surface, an electrochemical cleaning method was utilized from a method developed by Liu *et al.*, 2008 using the nucleation of nanobubbles to remove protein from the surface (Liu *et al.* 2008). All electrochemistry was conducted within the SPR cuvette. A cleaning cycle started with an application of a positive voltage (3.2 V) for 10 seconds, followed by a 5 second open circuit voltage all in running buffer. The cuvette was then flushed and the running buffer was replaced. The voltage and cuvette flushing were applied 4 more times. The potentiostat used to conduct the electrochemical investigations was an Ametek VERSASTAT 3 from London Scientific (London, Ontario).

# Chapter 4. Surface Plasmon Resonance and Fluorescence Emission Excitation Matrices Measurements of β-Lactoglobulin Adsorbed onto Carboxylic Acid-Terminated Self Assembled Monolayers: Assessing Interactions with Palmitic Acid and Protein Conformational Changes

## 4.1. Introduction

The nonspecific adsorption of proteins to surfaces is a complex phenomenon. Proteins interact with the surface through a combination of forces such as van der Waals, electrostatic and hydrophobic/hydrophilic interactions. Once a protein is in close contact with a surface it is exposed to a vastly different environment than seen in the bulk solution. This may result in changes to protein conformation which subsequently leads to changes in the protein's interaction with other molecules present in solution (Murray & Cros 1998). The changes in structure and affinity are of paramount importance such as when designing surfaces with high protein resistance for drug delivery devices, using detergents for cleaning proteins from surfaces, and utilizing surfactants for biomaterials and biofilms (Chapman *et al.* 2000, Rippner Blomqvist *et al.* 2004).

BLG, the primary component of whey, is utilized in the food industry as an emulsifier and texturizer (Floris *et al.* 2008). BLG is often isolated through membrane extraction processes, but this process exhibits large significant decreases in flux due to membrane fouling. Part of membrane fouling is due to the nonspecific adsorption of BLG to the filtration membranes (Marshall *et al.* 1997). Although there are a number of methods to reduce fouling such as introducing surfactants to clean the membranes (Raiber *et al.* 2005), these surfactants can also interact with the proteins. In particular, BLG has been known to bind a number of surfactants through its hydrophobic cavity (Konuma *et al.* 2007). This cavity can also bind a number of fatty acids, the highest affinity being towards palmitic acid (PA) (Ragona *et al.* 2000). Depending on the method used to extract BLG, PA may still be associated with the protein once purified, and this may have an effect on BLG binding and its solution properties at interfaces (Cornec & Narsimhan 1998). To study the effects PA had on BLG's surface aggregation, a model surface was created using self-assembled monolayers (SAMs). Surface plasmon resonance (SPR) was utilized to study the adsorption changes of BLG and BLG-PA.

## 4.2. Statistical Design and Factors

A full factorial, two level design was used to analyze results of association and dissociation changes of BLG-PA with a 11-MUA SAM. The final surface concentration values were taken after each experiment and used for the statistical analysis. Four factors were studied, outlined below.

### 4.2.1. Factor A – SPR Association Time

As protein concentration increases on a surface, its tendency to undergo irreversible conformational changes increases (Snopok & Kostyukevich 2006). These changes involve a balance of electrostatic and hydrophobic/hydrophilic forces, and usually promote a stronger adhesion to the surface (Roach *et al.* 2005). An increase in association time of typical SPR experiments results in an increase in BLG surface concentration. This higher concentration of surface BLG, along with an increase in exposure time of adsorbed BLG with the surface, would promote more irreversible conformational changes. Two association times where utilized in this study: a short association time of 120 seconds and a long association time of 300 seconds.

### 4.2.2. Factor B – Association Solvent

Two methods were employed to dissolve PA into buffer solution for studying the interaction with BLG. One method involved mixing PA in a 15% ethanol (EtOH)/buffer solution. This concentration of EtOH solvent should slightly increase the β-sheet content of BLG but also allow for PA to dissolve into the buffer (Dufour & Haertlé 1990). Above 30% EtOH, the secondary structure of BLG is significantly affected, changing from a β-sheet to α-helical (Mousavi *et al.* 2008, Reddy *et al.* 2006, Lee *et al.* 2006). For the second approach, PA was deposited on the surface of a glass substrate and then PA micelles were generated by the addition of buffer followed by sonication.

### 4.2.3. Factor C – Palmitic Acid

BLG was either exposed to a high concentration (20:1, BLG: PA ratio) of PA or no PA.

### 4.2.4. Factor D – Running Buffer/Dissociation Solvent

The dissociation buffer contained either 15% EtOH as in factor B or was pure running buffer. The change in dissociation solvent is expected to change the local environment for the adsorbed

BLG on the SAM. A summary of the factors and the associated coded values are presented in Table 4.1. For statistical analysis see Appendix A.

**Table 4.1: Factors and coded values for factorial experiment.**

| Factor | Loading | Notes |
|---|---|---|
| A – Association Time | + | 300 second association time |
| | - | 120 second association time |
| B – Association Solvent | + | EtOH/buffer |
| | - | Buffer |
| C – Palmitic Acid | + | 20:1 – PA:BLG ratio |
| | - | No PA |
| D – Running Buffer/ Dissociation solvent | + | EtOH/buffer |
| | - | Buffer |

## 4.3. SPR Sensorgram Analysis

SPR sensorgrams are presented in the next section to allow comparison of the curves. Some important information might otherwise be missed if only the final SPR values for the model were presented.

### 4.3.1. Association Experiments

BLG was injected over the SAM layer in a typical SPR experiment. The four curves shown in Figure 4.1 are distinguished based on factor B (solvent type) and factor C (presence of PA). Since the mass of the PA is too small to be detected by SPR, the observed signal can be attributed largely to BLG binding.

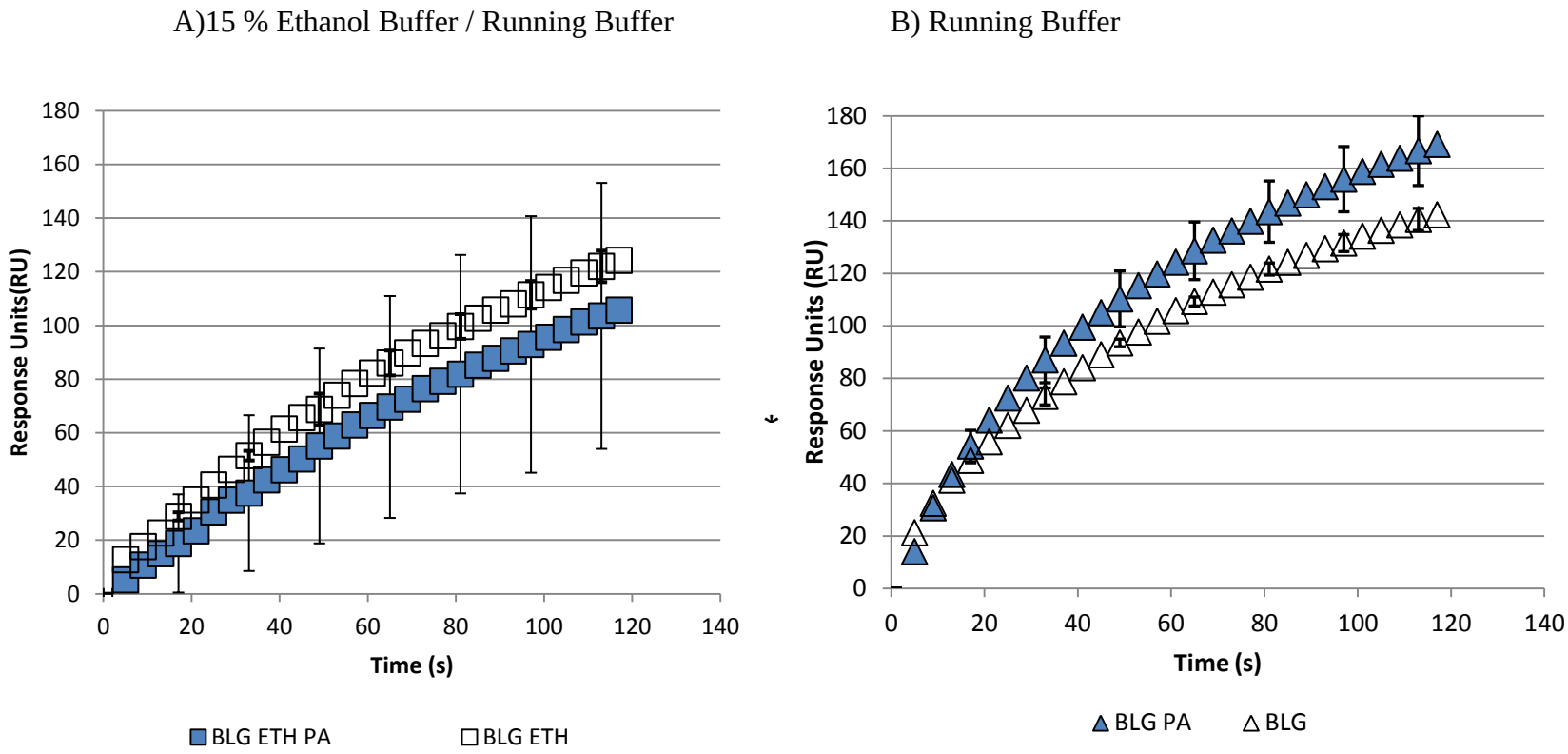


**Figure 4.1: Effect of PA on BLG adsorption.**

**A) The association of BLG and BLG-PA complex with the SAM in a 15% EtOH/buffer solvent. B) The association of the BLG and BLG-PA complex with the SAM in running buffer. Error bars represent standard error (n = 3) calculated from individual points at times shown.**

### 4.3.2. EtOH-Solvent Effects

The presence of EtOH in the buffer reduced the binding of BLG to the SAM layer by about 20 response units (RU) (Figure 4.1). The decrease in binding can be attributed to the hydrophobic surface of the protein being less prone to interact with the hydrophilic SAM. The protein becomes more hydrophobic as the EtOH content of the buffer is increased (Dufour & Haertlé 1990, Mousavi *et al.* 2008, Reddy *et al.* 2006). This is because the change in structure of the protein exposes more hydrophobic amino acids residues to the solution (Reddy *et al.* 2006). Since the EtOH content was kept below 20%, it is expected that drastic denaturation of BLG did not occur, although a slight increase in β-sheet content is expected based on work by Dufour & Haertlé,(1990) (Dufour & Haertlé 1990).

### 4.3.3. PA Association in the Absence of EtOH

Previous experiments with BLG showed that by increasing the buffer concentration at pH 6.2 there was a decrease in its association with the SAM. This was due to the charge shielding effect of the buffer which reduced BLG surface polarity (Majhi *et al.* 2006, Hartvig *et al.* 2011, Silva *et al.* 2010). It would appear then that the primary means for BLG to interact with the hydrophilic SAM is through electrostatic/polar interactions. In the presence of PA, 20% higher adsorption onto the SAM was observed when compared to BLG alone (Figure 4.1B). This increase in adsorption may be due to an increase in the polar properties of BLG as a result of the carboxylic group provided by the PA molecule. The carboxylic group of PA in BLG's hydrophobic cavity is known to be exposed to solution and not sterically hindered within the protein (Ragona *et al.* 2000).

### 4.3.4. PA Association in the Presence of EtOH

In the presence of EtOH the standard error associated with the SPR curve increased substantially such that there was no statistical difference between the BLG-PA and BLG association events. It was believed that this error was due to a leak in the cuvette, or instability of the SAM when exposed to the EtOH. In the presence of the EtOH, more hydrophobic groups are being exposed by the BLG which reduced its affinity toward the hydrophilic SAM and counteracted the effect of PA. More experiments are required to fully interpret the effect of PA on association events, as the error was substantially large in these experiments. Nonetheless, it appears that there is a

significant change in association due to a conformational change of BLG, and the presence of PA. To further provide evidence for the conformational changes, the dissociation of BLG was analysed. The error in the dissociation events was comparably less, and as a result, data could be transformed and utilized for statistical analysis.

### 4.3.5. Dissociation Effects – Normalization

The results of the dissociation event are presented unaltered in Figure 4.2A and as normalized curves in Figure 4.2B. The final values after dissociation where used to generate the model (see Appendix A).

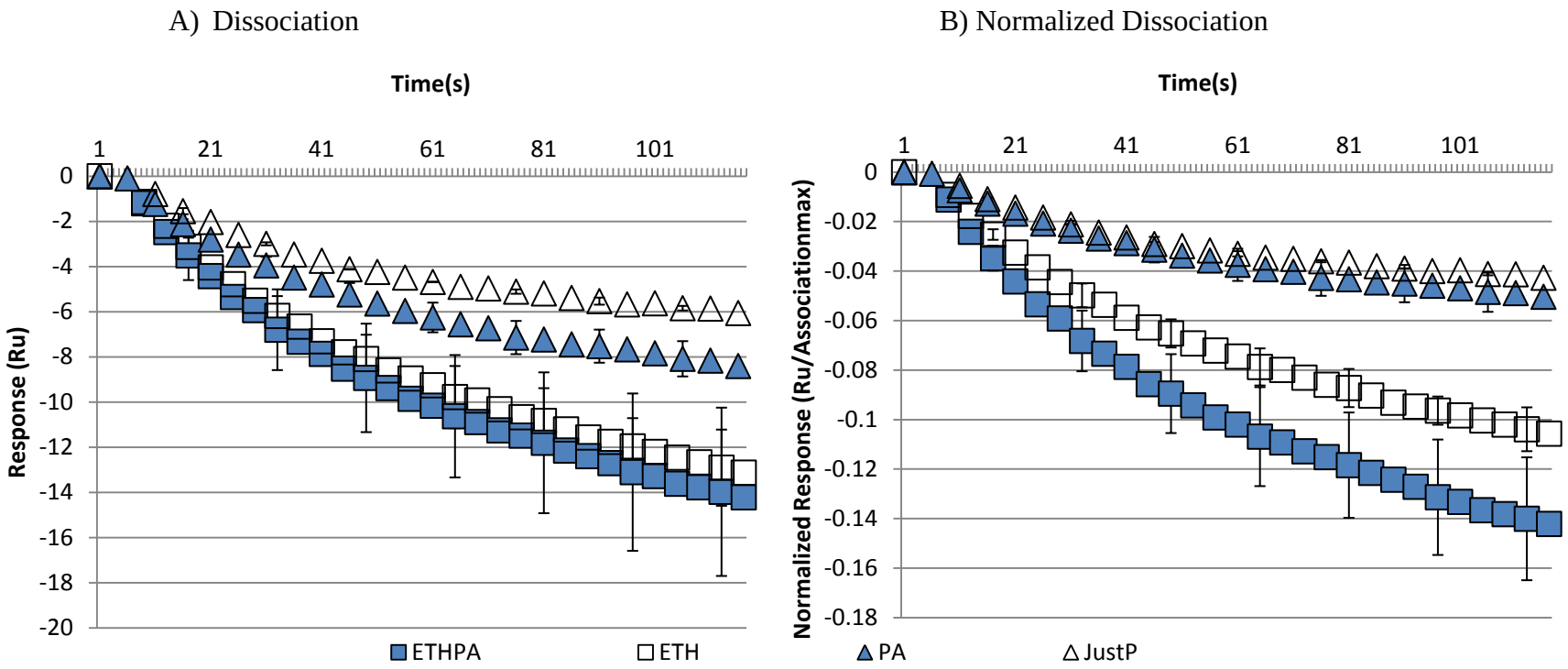


**Figure 4.2: Effect of PA on BLG desorption.**

**A) BLG dissociation. B) BLG dissociation normalized with respect to the maximum concentration of the association experiment conducted in Figure 4.1. Error bars represent standard error (n = 3) calculated from individual points at times shown.**

In the presence of EtOH, the final value of for the dissociation had a confidence interval equivalent to 30% of the mean response (Figure 4.2A), which is believed to be due to the large confidence interval for the corresponding association steps which were 55% of mean (Figure 4.1A). The large observed confidence intervals for the association events would affect the initial conditions which govern the rest of the dissociation (Rabe *et al.* 2007). To minimize the effect of the variations in the association behaviour the dissociation curves were normalized by dividing by the maximum concentration (final association value) of the previous association step. This method reduced the confidence interval for all curves to approximately 11% of the mean. The experiments with EtOH and PA experienced no change the confidence interval (Figure 4.2B), although their mean values are substantially different. The method of normalization of dissociation data is favourable for the purpose of comparing two conformational states which are time dependant (Nakatani *et al.* 2004).

After normalization there are no significant differences between the SPR signal of the BLG-PA and BLG in running buffer. Qualitatively, if both experiments had equal amounts of protein bound to the surface they would not display different amounts of dissociation (Figure 4.2A). The interaction of BLG and PA in EtOH resulted in a 40% greater dissociation (Figure 4.2B) which is believed to be due to BLG-PA's ability to resist denaturation on the surface. This is discussed in Section 4.3.6.

### 4.3.6. Dissociation Analysis

The BLG-PA complex is reported to have increased resistance to denaturation when exposed to urea, thermal degradation, and hydrolysis due to increased stability of the secondary and tertiary structures (Creamer 1995). If the urea concentration is increased, denaturation of BLG was possible (Creamer 1995). The BLG-PA complex also seems to have increased stability when adsorbed to a surface as it is more likely to dissociate. This indicates that there is a resistance to unfolding and conformational changes which normally would increase its adhesion. Current surface modeling theories suggest protein undergo conformational change in proportion to the protein surface concentration and time spent on the surface (Rabe *et al.* 2007, Snopok & Kostyukevich 2006, Tie *et al.* 2003). At higher concentrations the lateral protein-protein interactions result in the protein being more likely to undergo orientation or slight

conformational changes rather than a significant conformational change such as spreading (Norde 2008). Thus by increasing the association time, factor A, a significant effect on the dissociation strength would occur. Consequently, factor A was also involved in multiple three factor interactions, with buffer composition (factor B and D) and with PA concentration (factor C) (Figure 4.3).

A) Short Association time

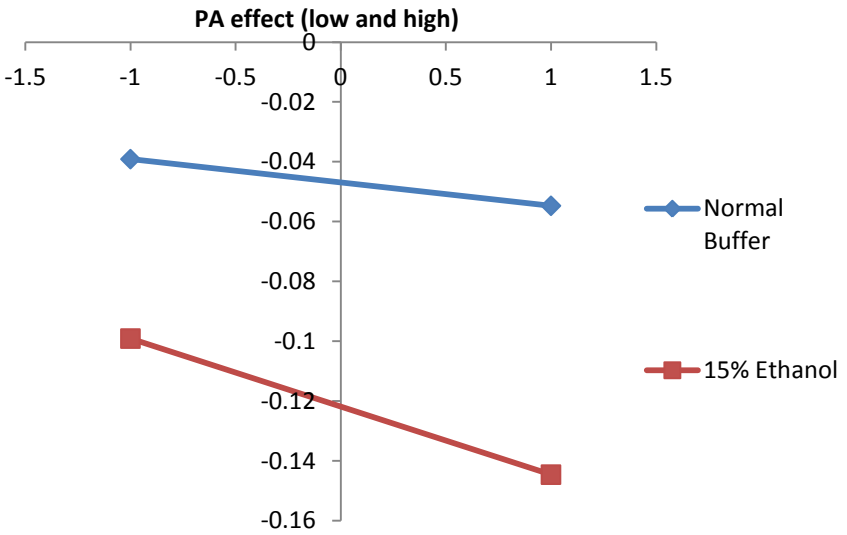


B) Long association time

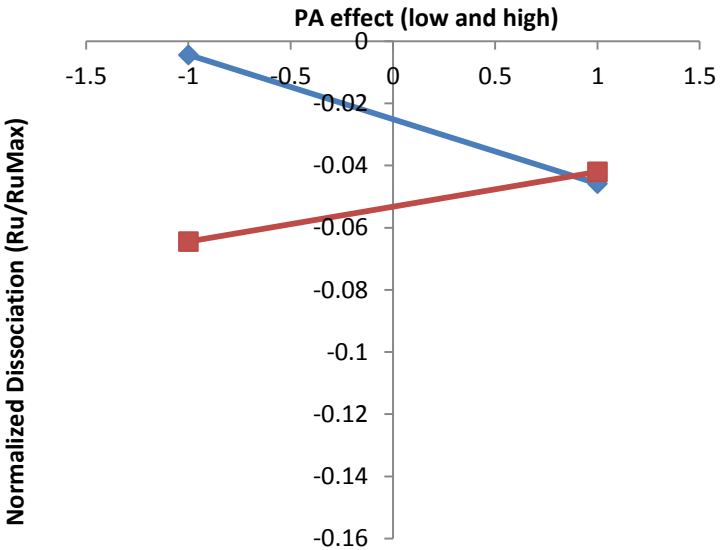


**Figure 4.3: Model dissociation concentrations in different buffers for long and short association times.**

**A) Short association time; B) Long association time. The y-axis presents the effect of PA at no (-1) and high (+1) concentrations. The equation for the model can be seen in Appendix B, Equation 1B.**

The largest change that occurred was a 50% increase in overall protein adhesion when going from a short association time (Figure 4.3A) to long association time (Figure 4.3B). The addition of PA in running buffer at longer association times increased the dissociation from the surface on average by 0.02 $RU/RU_{max}$ (Figure 4.3A & B). PA-BLG in EtOH at longer association times showed increased stability on the surface and thus had a stronger adhesion, and a decrease in dissociation of 0.02 $RU/RU_{max}$. In running buffer, PA reduced BLG's ability to change conformation as seen by the greater dissociation from the surface once PA was added. In EtOH the kinetics of denaturation increased since BLG's conformation was already modified (Reddy *et al.* 2006). The BLG is thus thought to undergo two conformational changes in the EtOH/buffer mixture. One conformation to compensate for the EtOH as an additional solvent and another once bound to the surface.

To determine the effect that the solvent had on the protein conformation, an experiment was conducted in which the protein was adsorbed onto the surface with running buffer, but the dissociation buffer was switched and contained 15% v/v EtOH. These effects along with both long and short associations are shown in Figure 4.5.

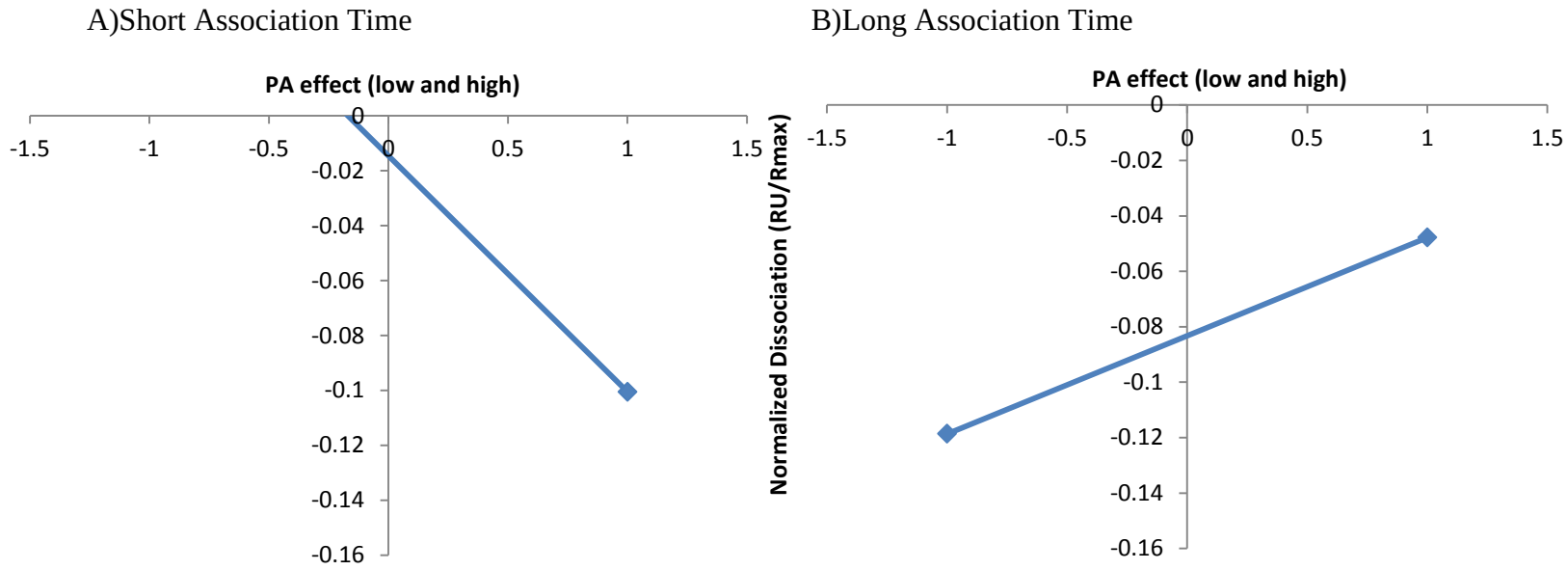


**Figure 4.4: Model dissociation concentrations for long and short association times utilizing dissociation buffer change.**

**A) Short association time; B) Long association time. The y-axis presents the effect of PA at no (-1) and high (+1) concentrations. The equation for the model can be seen in Appendix B, Equation 1B. The experiments utilized the running buffer in the association portion of the experiment but the running/dissociation buffer was changed to contain 15% ETH/buffer. (*note: the value for the off chart point was 0.07 ($RU/RU_{max}$).**

For short association times and low PA concentrations, a positive dissociation was observed (i.e.: it appeared that mass was accumulating on the surface rather than being removed). This was represented as a positive data point in Figure 4.4A. The positive change can be attributed to a significant modification of BLG's secondary and tertiary structure due to the proteins exposure to EtOH. The protein conformational change would shift its effective RI, generating a false positive signal (Johnsson *et al.* 2002). For short association times with PA a significant conformational change did not occur and dissociation proceeded as normal. For longer association times (Figure 4.4B), PA resulted in increased binding strength of the BLG to the surface. This can be attributed to the increased concentration of BLG on the surface and thus an increase in protein lateral interactions which would prevent significant conformational changes (Norde 2008). At the longer association times studied, BLG and BLG-PA would have likely already undergone some sort of conformational change, which would result in an increase in adhesion to the layer. It appears that at these longer association times, BLG-PA has a much stronger adhesion to the layer than BLG. The interpretation of these results is difficult as the exact nature of the surface induced denaturation is unknown.

## 4.4. Fluorescent EEM Surface Analysis

Fluorescent EEMs of BLG-PA on the sensor surface were collected following a typical SPR experiment to determine the conformational changes which occurred on the SAM. Protein intrinsic fluorescence has been used to detect conformational changes in BLG and many other proteins (Lee *et al.* 2004,O'Neill & Kinsella 1987). Multivariate analysis of fluorescent EEM has been used to predict/determine aggregation behaviour by analysing tryptophan fluorescence and scattering data of BLG (Elshereef *et al.* 2006). Tryptophan fluorescence has also been utilized to monitor BLG binding to PA in the presence of fluorescent quenchers, while other researchers have monitored the nature of quenching of BLG once bound to fatty acids (Muresan *et al.* 2001, Busti *et al.* 1998).

### 4.4.1. Fluorescent EEM analysis – FOP Surface Scans

A Fibre optic probe (FOP) was used to conduct scans of BLG adsorbed onto SAM layers. Surface scans were conducted after the dissociation step following a typical SPR experiment in which either BLG or BLG-PA had adsorbed. The resulting EEMs were averaged and analysed (Figure 4.5 & 4.6).

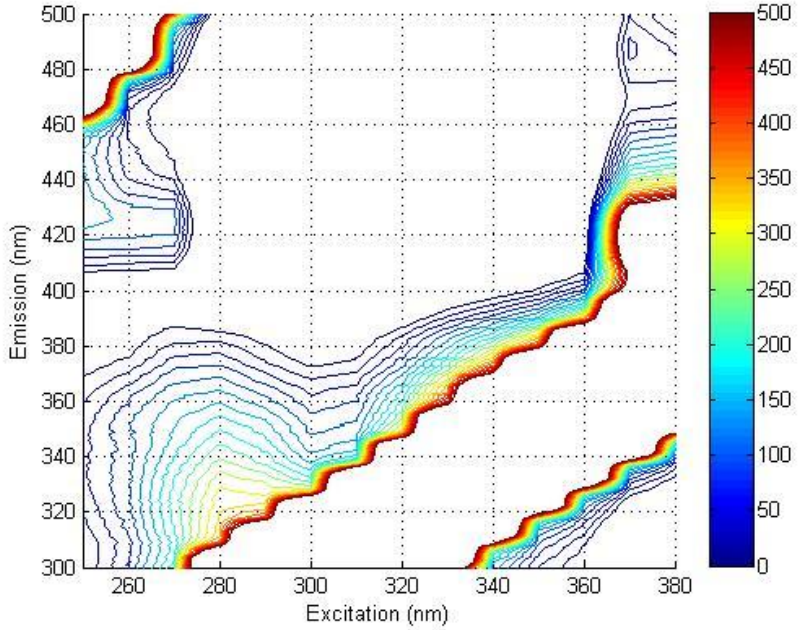


**Figure 4.5: Surface EEM's for BLG-PA.**

**Averaged (n = 4)**

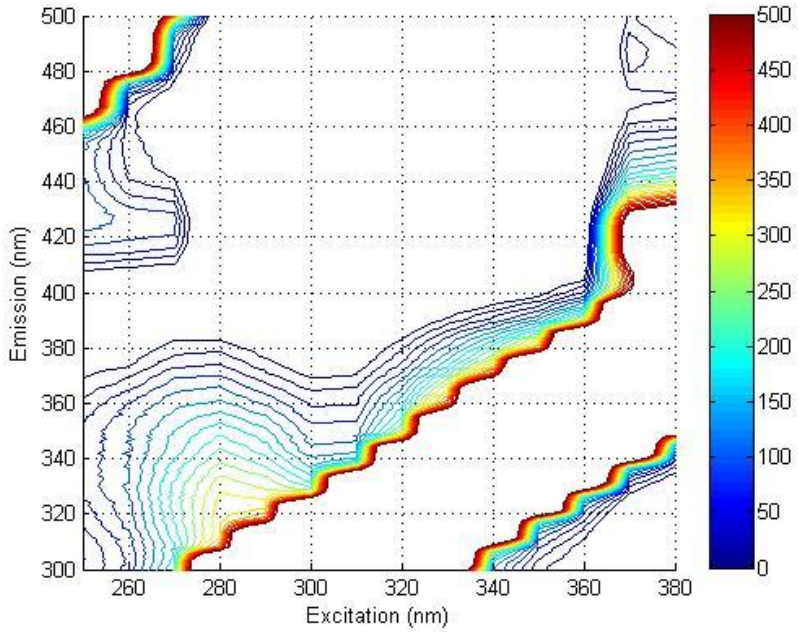


**Figure 4.6: Surface EEM of BLG.**

**Averaged (n=4)**

Tryptophan fluorescence is expected to occur at an excitation of 300 nm and emission 334 nm in solution (Lee *et al.* 2004). For surface scan EEMs, the excitation peak shifted from 300 to 280 nm (a 20 nm blue shift). Peaks for both BLG-PA and BLG tryptophan fluorescence also showed a blue shift from 334 nm to ~310 nm, although it is difficult to determine the exact location of the peak due to scattering interference. The blue shift is attributed to tryptophan being exposed to a more hydrophobic environment upon adsorption (Naujok *et al.* 1993, Clark *et al.* 1994), a phenomenon that has been seen for tryptophan for BLG and other proteins (Mills & Creamer 1975, Meynier *et al.* 2004). This hydrophobic environment could be due to a closer proximity of the tryptophan molecule and hydrophobic amino acids. To determine if there were any differences between the EEMs in Figures 4.5 and 4.6, they were subtracted and results are presented in Figure 4.7.

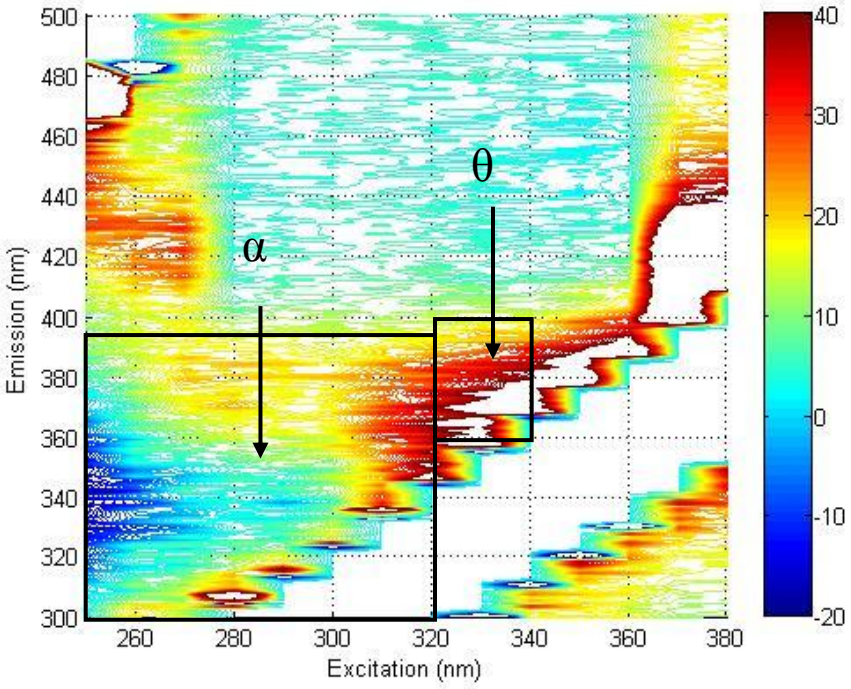


**Figure 4.7: Results from subtracting the BLG EEM from the BLG-PA EEM.**

**Table 4.2: Significance test for difference in the area under the curve between BLG and BLG/PA peaks in θ region.**
**$\sigma^2$ represents the variance (n = 3). The ±90% represents the 99% confidence interval for the difference between BLG and BLG/PA peaks.**

| BLG (area) | BLG/PA (area) | Δ |
|---|---|---|
| 14940<br>$\sigma^2$=1.76 x$10^6$ | 18863<br>$\sigma^2$=2.0 x$10^6$ | -3923 ± 90% |

The α area was defined as emissions from 300 - 390 nm and excitations from 250 - 320 nm. This area is the region representative of tryptophan fluorescence (Peiris *et al.* 2008, Peiris *et al.* 2010b). The α area shows an increased fluorescence at higher emission/excitation wavelengths and a negative peak at lower emission/excitation wavelengths. A decrease in fluorescence/quenching has been found to be associated with denaturation and conformational changes of BLG (Lee *et al.* 2006, Lee *et al.* 2004). The presence of a shoulder at an excitation of 250 nm and emission of 340 nm indicates that BLG without PA has undergone more denaturation due to the lack of radiation-less energy transfer from tyrosine to tryptophan (Creamer 1995). Unfortunately, there were no significant differences in the α area due to large signal noise and attenuation. The θ area was defined as emission of 350 - 400 nm and excitation 320 - 340 nm. It was selected since it was the most consistent (statistically) difference between the two peaks. This θ area does display a significant difference between BLG-PA and BLG peaks (Figure 4.7), although the exact value can not accurately be determined (Table 4.2). The difference between the BLG and BLG-PA scattering would relate to a difference in quaternary structure of adsorbed BLG molecules, with an increase in scattering correlating to closely packed aggregates (Vetri & Militello 2005), suggesting conformational changes between BLG and BLG-PA molecules.

## 4.5. Conclusions

The BLG-PA complex showed increased stability once bound to the SAM but given enough time to undergo conformational changes, displayed a much stronger adhesion to the layer. When EtOH was part of the solvent these conformational changes resulted in increased adhesion due to the conformational changes and hydrophobic forces. The conformational changes were confirmed by using the intrinsic fluorescence of tryptophan of the BLG. Detection of conformational changes of BLG using surface scans of the sensor discs following the binding

studies is possible, although significant error was present in the tryptophan peak due to instrument/methodology limitations. Scattering data was significant enough to reveal closely packed, more aggregate-like BLG when bound to the fatty acid PA. Future improvements should focus on refinement of FOP reproducibility, specifically collecting data for the tryptophan fluorescence. Further studies in which the BLG-PA and BLG complexes are removed from solution of PA would reinforce the evidence of conformational changes.

# Chapter 5. Surface Plasmon Resonance Method Development for Measuring Interactions between Components of Natural Organic Matter: A System Utilizing α-Lactalbulmin and Colloidal Substances from River Water.

## 5.1. Introduction

The intrinsic fluorescence of natural water systems allows for a relatively quick and label free method for characterizing and identifying constituents in natural organic matter (NOM) and has been used to understand and predict high-fouling events in water-membrane based filtration processes (Peiris *et al.* 2010a, Peiris *et al.* 2010b). Intrinsic fluorescence can be measured using an array of emission and excitation wavelengths to produce an emission-excitation matrix (EEM). An EEM of the water sample can then be used to identify different components contained within the sample using multivariate statistical approaches such as principle component analysis (PCA). PCA has been used to identify three components of the natural water: humic substances, colloidal protein/particulate substances (CPP) and protein substances (Peiris *et al.* 2010b). In these studies, the peak associated with the protein substances was found to have a strong interaction with the CPP such that the addition of an interaction term between the two in the PCA model significantly improved the prediction of peak intensity (unpublished data). This interaction term is hypothesized to be a result of physical interactions between the protein in question and CPP matter, rather than an interference pattern between the two components. In order to verify this claim, SPR was utilized in several experiments to confirm the presence of physical interactions between CPP and protein matter. In this study the interactions were tested between CPP filtered from river water and surrogate model protein α-lactalbumin (AL).

### 5.1.1. Definitions

Chapter 5 utilizes the following definitions for description of SPR adsorption events.

When not referring specifically to an SPR association step, association refers to the interactions between two molecules.

The dissociation is defined as the physical process that occurs during the breakage of a molecule-molecule or molecule surface bond.

For the purpose of this thesis, the adhesion strength of the components on the surface was defined as the difference in signal from the initial point of the dissociation curve to end of the dissociation curve. A stronger adhesion would mean a smaller difference at the end of the dissociation step.

Adsorption refers to a molecules binding to a planar surface or monolayer.

## 5.2. Interactions of CPP with Immobilized AL

SPR is a technique commonly used for following various types of biological interactions. Typically interactions are measured using a covalent protein-ligand immobilization approach (see Section 3.2.3). Antibodies are classically chosen as the ligand to be immobilized onto the sensor surface due to their specific binding properties towards the target analyte. In this case however, the interest was in determining the nonspecific association between AL and the extracted CPP. For covalent immobilization, surface exposed amine groups on the protein are covalently linked to self-assembled monolayers (SAMs) (Patel *et al.* 1997). The CPP most likely contains a low percentage of protein, and other components of the CPP would likely not immobilize to the SAM. This ruled CPP out as a possible immobilization candidate. AL was thus chosen to be immobilized. To test the immobilization approach, AL would need to be able to absorb to the SAM layer.

### 5.2.1. AL-SAM Association

Typical river water samples were estimated to have a protein concentration ranging from 1 mg to 1 g per litre (Peiris *et al.* 2010b). This range was used as a starting point to assess AL and SAM association. Ideally, the loading of AL on the surface would mimic the real protein to CPP ratio found in river water samples. Normally a large number of immobilizations and thus gold sensor disks would be required to optimize the signal. Only one optimization was conducted, with the goal of loading the surface with a single monolayer of AL (see Appendix B) to test CPP interaction.

Several “typical SPR experiments” (see Section 3.2.2.) were conducted on different sensor locations of a 11-MUA SAM coated sensor disk at various AL concentrations. All CPP-AL interaction experiments were conducted utilizing pH 7.4 buffer which was the same pH of the Grand River water from which the CPP was extracted. The buffer concentration was kept low (~

30 μM) as this has been reported to have a negative effect on protein adsorption and electrostatic interactions (Zhang *et al.* 2007, Majhi & Ganta 2006).

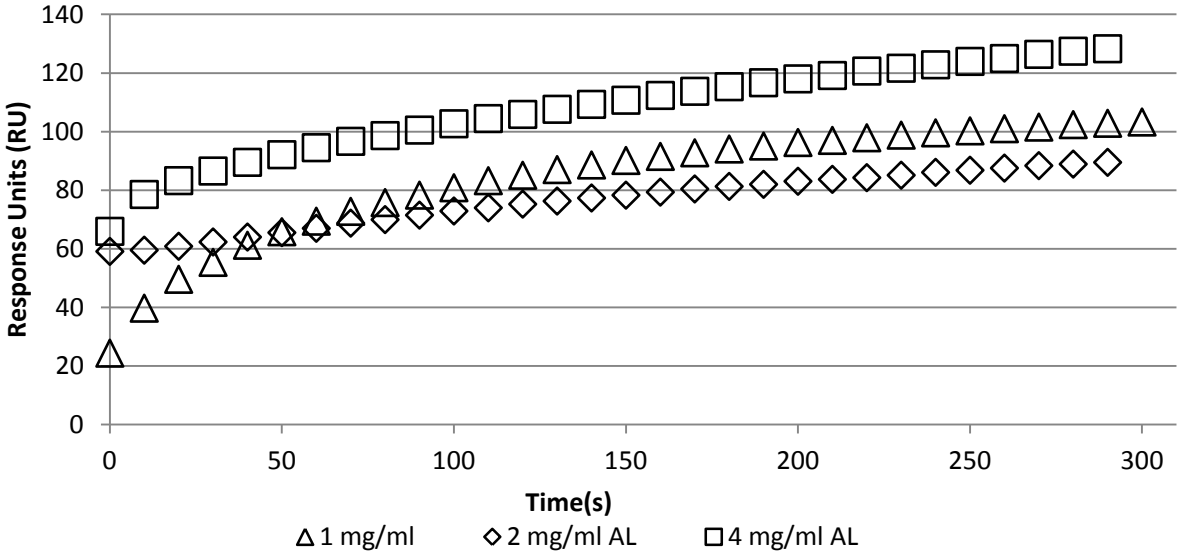


**Figure 5.1: Association of AL with the SAM layer at different concentrations.**

**AL concentrations were: 1, 2 and 4 mg/ml. Average standard error = 1.7 RU (n=2) estimated from experiments conducted at 2 mg/ml.**

The 4 mg/ml AL concentration had the highest interaction with the surface, followed by 1 then 2 mg/ml. The 1 mg/ml had a greater interaction than the 2 mg/ml, which was attributed to small variations in the total number of functional groups between different sensor disk surfaces. Comparing the rate at which 1 mg/ml and 2 mg/ml approached their maximum signal, it appeared that 1mg/ml was much slower than 2 mg/ml, which is as expected. The maximum signal generated after the allotted time was approximately 130 RU at 4 mg/ml, which closely corresponds to what would be expected for full monolayer coverage (Table 5.1). The protein should be loaded onto the surface as fast as possible such that steric hindrance between adjacent proteins occur and prevents significant spreading and denaturation of the protein (Norde 2008).

### 5.2.2. AL Immobilization

Calculations based on the hydrodynamic radius of AL predicted a maximum signal of 145 RU assuming full monolayer coverage (Table 5.1). See Section 3.2.3 for the immobilization SPR sensorgram (Figure 3.2).

**Table 5.1: Assumptions used for determining monolayer coverage and the maximum possible response for AL-SAM association.**

| Hydrodynamic Radius of AL (Branco *et al.* 2010) | Area Assuming circular footprint | Surface Area of Disk | MW of AL molecule (Branco *et al.* 2010) | RU-Max assuming full monolayer coverage |
|---|---|---|---|---|
| 2.48 nm | 19.32 $nm^2$ | 2 $mm^2$ | 14.2 kDa | 145 RU |

### 5.2.3. CPP-SAM Association

If the CPP molecules are too large (above 200 nm), the molecules will exceed the penetration depth of the SPR instrument and the mass to signal ratio will fall into a non-linear regime (Stenberg *et al.* 1991, Autolab 2006). If the CPP molecules are too small (300 Da), there will be no significant change to the refractive index and thus no signal will be detected (Autolab 2006). To determine if the SPR signal could detect CPP-SAM adsorption several association steps were conducted at varying CPP concentrations. CPP was extracted, mixed in Milli-Q water (0.11 mg/ml) for use with the SPR (see Section 3.4.1). The concentrations of CPP examined were: no dilution, 1:2 dilution (0.06 mg/ml) and 1:4 dilution (0.03 mg/ml).

A) B)

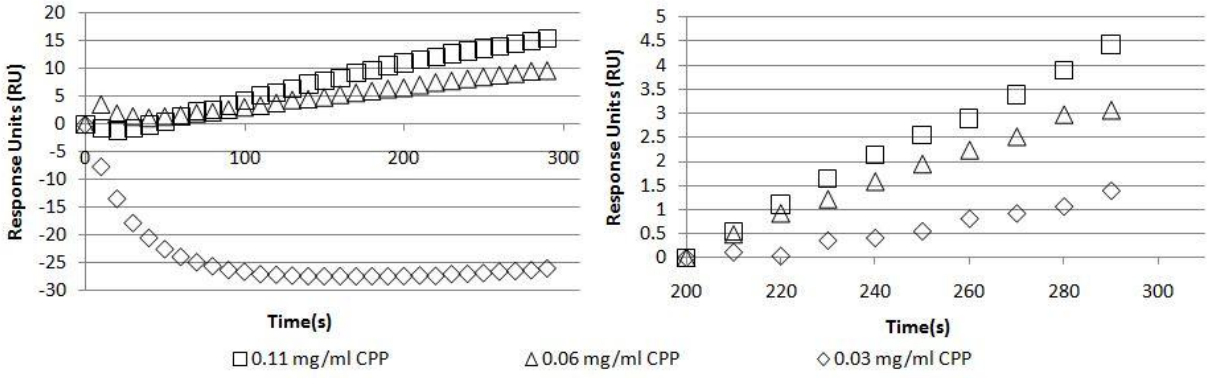


**Figure 5.2: Association of CPP with the SAM layer at different concentrations.**

**A) Figure zeroed at the start of the experiment; B) zeroed 200 seconds into the experiment.**

The SPR sensorgrams showed that the CPP interacted with the SAM layer with appropriate concentration-related kinetics (Figure 5.2). At 0.03 mg/ml there appeared to be a large dissociation from the surface. In this case, the dissociation was interpreted as a false negative

error in the SPR signal. The error is attributed to temperature differences between the injection solution and instrument. Small temperature differences have been observed to cause signal changes of up to 30 RU (Autolab 2006). It was hypothesized that the temperature difference between the CPP solution (~25 $^{o}$C) and the instrument (~27 $^{o}$C) resulted in these changes. As the temperature equilibrated in the SPR cuvette, the SPR signal dropped slowly, resulting in the changes seen in Figure 5.2A. When the signal was re-zeroed after sufficient time to allow for establishment of temperature equilibrium (Figure 5.2B), the expected concentration-dependent profile for adsorption kinetics was observed. Overall, CPP shows minimal association with the SAM layer when compared to AL.

### 5.2.4. The Effect of CPP Settling on CPP-SAM Association

When samples of CPP were allowed to sit at 4°C for approximately 12 hours, particulate matter accumulated in the bottom of the cuvette. Once gently mixed, the solids would re-suspend into solution. An SPR experiment was conducted to determine if the settled vs. mixed CPP mixture displayed different adsorption behaviour. In one instance the CPP was stirred to eliminate any settled particulates along the sides of the cuvette whereas, in another run, the solution was not stirred and the bulk CPP was sampled. A typical SPR experiment was performed utilizing the same running buffer and 11-MUA SAM layer as in previous CPP experiments.

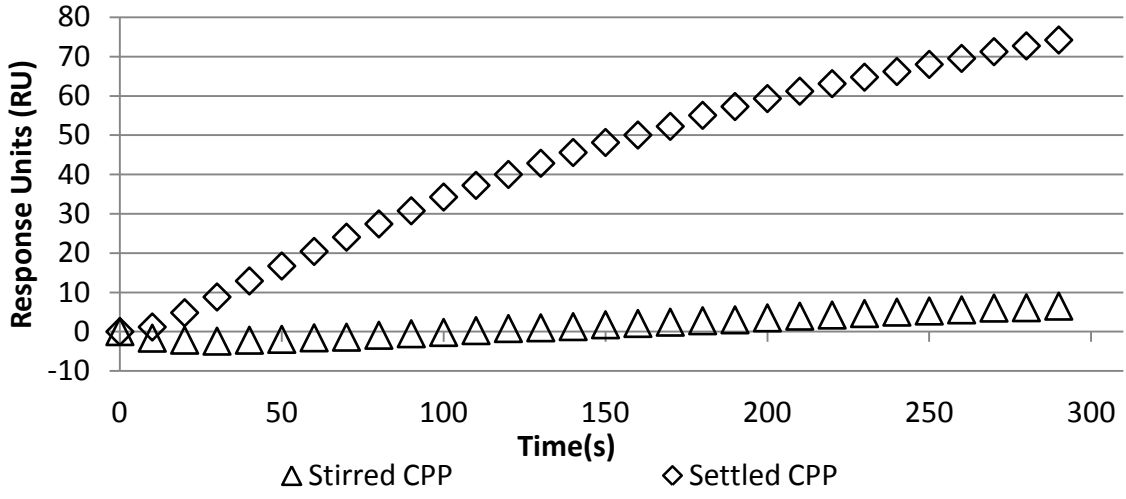


**Figure 5.3: CPP association with the SAM layer with different CPP preparation.**

**When the stock solution was stirred prior to sampling (△) versus sampling of the solution above the settled particulate matter (◇).**

The stirred CPP did not adsorb as much to the SAM layer in comparison to the settled CPP mixture. Although the exact differences between the settled and mixed CPP were not investigated, it is hypothesized that the settled CPP solution consisted largely of hydrophilic molecules that could then interact with the SAM layer through hydrogen bonding and electrostatic interactions (Frederix *et al.* 2004, Silin *et al.* 1997). Due to the enhanced binding displayed in Figure 5.3, settled CPPs were utilized in further experiments.

### 5.2.5. CPP Association with AL

Following AL immobilization, CPP at the highest concentration possible (0.11 mg/ml) was injected into the SPR cuvette and the association kinetics were monitored. Sensorgrams of this association are presented in Figure 5.4.

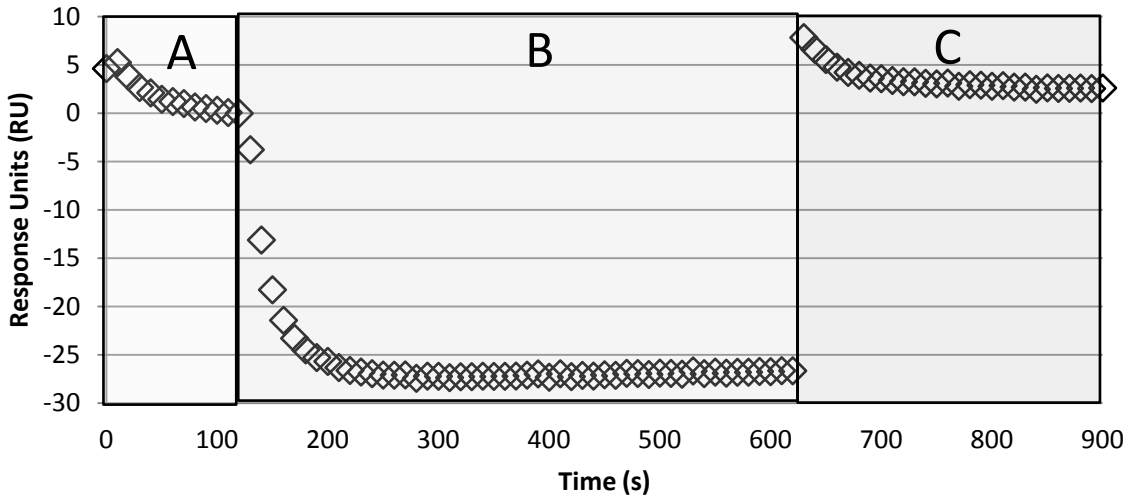


**Figure 5.4: Sensorgram of CPP interaction with the immobilized AL surface.**

**A) The baseline measurement (t = 0-100 seconds); B) association behaviour following injection of CPP into the cuvette (t = 100-610 seconds) and C) wash step followed by the dissociation step (t = 610-920 seconds)**

Following the injection of CPP (Figure 5.4B) a rapid decrease in the SPR signal occurred. The decrease in signal is attributed to the change in temperature resulting from the addition of the CPP and running buffer solution. After association the sensorgram levels out (t>250 seconds) and a slight linear increase in signal is observed on the surface from t = 250-600 seconds. Post dissociation, a small amount of CPP appears attached to the surface (about 5 response units (RU)). This is represented by the difference between SPR baseline and very last signal point at t

= 900 seconds. Overall the change in SPR signal during the association step and the accumulation of mass on the surface indicate relatively small amount of interaction between CPP and AL. Since the amount of binding is so small, reducing the concentration of CPP in order to produce a concentration series would not provide detectable levels of binding with the current configuration.

A disadvantage of preparing a surface using the covalent-immobilization method was that the adsorption orientation of the AL onto the SAM layer is random (Mateo *et al.* 2000). This means that AL is not optimally oriented to interact with the CPP. This heterogeneous surface may result in an underestimation of the kinetic constants due to a reduced theoretical binding capacity (Hodneland *et al.* 2002). Other complications arise if the immobilization density is too high such that normal AL-CPP sites may be covered or sterically hindered by adjacent protein (Bonanno & DeLouise 2007). With so many proteins located in such a small area, the forces that normally govern the CPP-AL interaction would be significantly different than in solution.

## 5.3. AL-CPP using Multiple Injection Method

The multiple injection method involved the initial adsorption of either AL or CPP onto the sensor surface. Multiple association steps are then conducted on surface (see Section 3.4.4.). As AL/CPP were not covalently attached to the surface, they would be free to re-orient themselves or desorb into solution.

### 5.3.1. Association Analysis

For each experiment a baseline was first established followed by a total of four injections over the surface each with an association phase lasting 400 seconds. No washes were conducted before or after the injections until the fourth injection at which time a wash occurred and the dissociation phase began. This was then followed by a regeneration step using 0.1 M HCL. Four different experiments were conducted (Table 5.2).

**Table 5.2: Description of experiment codes.**

| Experiment Code | Type of Injection |
|---|---|
| Cx4 | 4 sequential injections of CPP |
| Ax4 | 4 sequential injections of AL |
| Ax1-Cx3 | 1$^{st}$ injection - AL, followed by 3 sequential injections of CPP |
| Cx1-Ax3 | 1$^{st}$ injection - CPP followed by 3 sequential injections of AL |

The individual sensorgrams were zeroed at the baseline and overlaid for analysis.

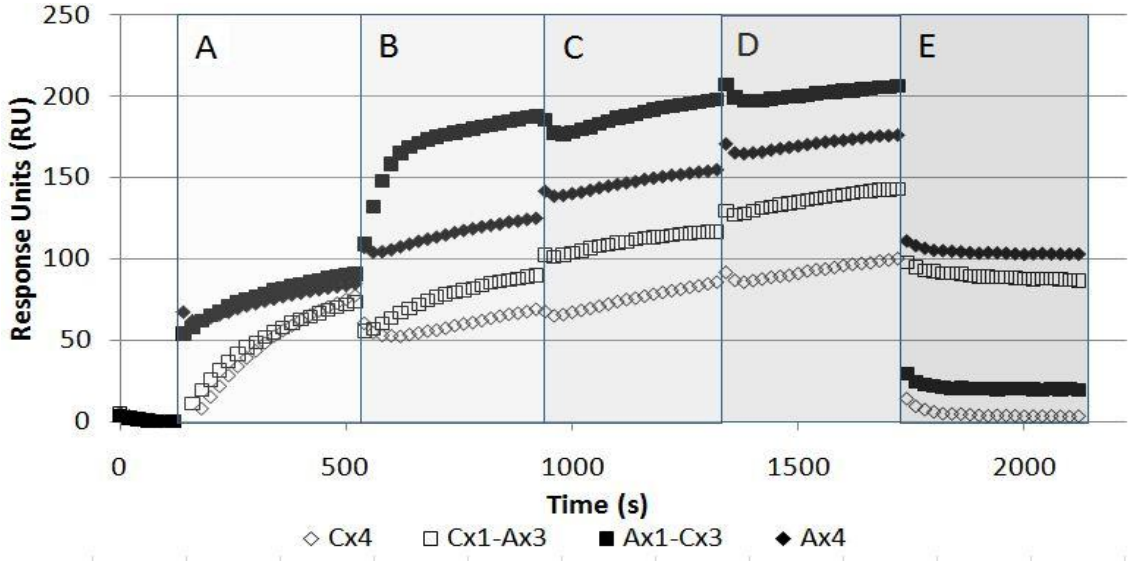


**Figure 5.5: Multiple injection SPR plot.**

**All plots were zeroed at the baseline. (A-D) Sequential injections of either CPP or AL. Experimental name coding is provided in Table 5.2. E). Dissociation step during which the surface was washed with running buffer then followed by a 50 µl injection of running buffer. The average standard deviation was 10.5 RU (n=2-3) calculated by averaging the standard deviation for every point of the plot.**

Figure 5.5 depicts the sensorgrams zeroed at the baseline and was used to compare the different loadings on the surface for the different experiments. The results are further summarized in Table 5.3.

**Table 5.3: Summary of results for the multiple injection experiments.**
**Final loadings were taken at the end of the dissociation step from a baseline of zero. To calculate the approximate percent colloidal (%) and percent dissociation see Appendix B. Standard error (n=2) was 10.5 RU.**

| Experiment Code | Maximum Association (RU) | After buffer Wash (RU) | Approximate Percent Colloidal (%) | Percent Dissociation (%) |
|---|---|---|---|---|
| Cx4 | 100 | 3 | 100 | 97 |
| Ax4 | 176 | 103 | 0 | 42 |
| Ax1-Cx3 | 206 | 20 | 78 | 91 |
| Cx1-Ax3 | 143 | 87 | 63 | 39 |

Examining the 1$^{st}$ association in the series of four, it appears AL has the highest initial adsorption. It is difficult to determine if this is entirely protein, due to the bulk shift at the

beginning of the experiment (Figure 5.5A). Transitioning from the 1st to 2nd sensorgrams Ax1-Cx3 (Figure 5.5A & B) shows the largest adsorption/association, in which CPP was injected over a surface which contained adsorbed AL. The initial phase of the association displayed a much faster adsorption/association for the first 60 seconds, and then levelled off to a rate of adsorption similar to the other sensorgrams. The presence of AL on the surface improved the binding of CPP to the SAM supporting the notion of interactions between CPP and AL.

For the Cx1-Ax3 sensorgram, AL was injected over a surface that was first exposed to CPP. It displayed similar kinetics to the AL curves in Figure 5.5A, suggesting that CPP loading does not have a significant effect on AL's interaction with the layer. This conclusion seems to conflict with the results from Ax1-Cx3 sensorgram. It is possible that although CPP is bound to the layer, it does not affect the electrostatic attraction between AL in the bulk and the SAM. This effect is also observed during dissociation analysis (see Sec 5.2.3).

As the experiment continued, the available surface sites for binding would be expected to decrease, and the system would approach saturation with a reduction in the rate of association, as observed in the 3rd and 4th sensorgrams (Figure 5.5C & D). The sensorgrams began to display an almost linear, rather than exponential increase in surface concentration.

Table 5.3 provides a numerical summary of the data from the dissociation in Figure 5.5E. The surface with the highest final loading was Ax4, which had the longest exposure to AL. Next were Cx1-Ax3, Ax1-Cx3, and finally Cx4, in decreasing order of association. The large decrease in RU that occurred between the end of Figure 5.5D and the start of Figure 5.5E was mostly due to loosely bound material being washed from the surface. It was then observed that although CPP did accumulate on the surface, it did not adhere very strongly after a buffer wash since 97% of CPP dissociated (Figure 5.5E, Table 5.3). This is a large amount of dissociation when compared to the Ax4 experiment, in which 42% of AL dissociated (Table 5.3). To determine exactly what was dissociating from the surface in the mixed scenarios (Cx1-Ax3 and Ax1-Cx3), the dissociation curves were analysed.

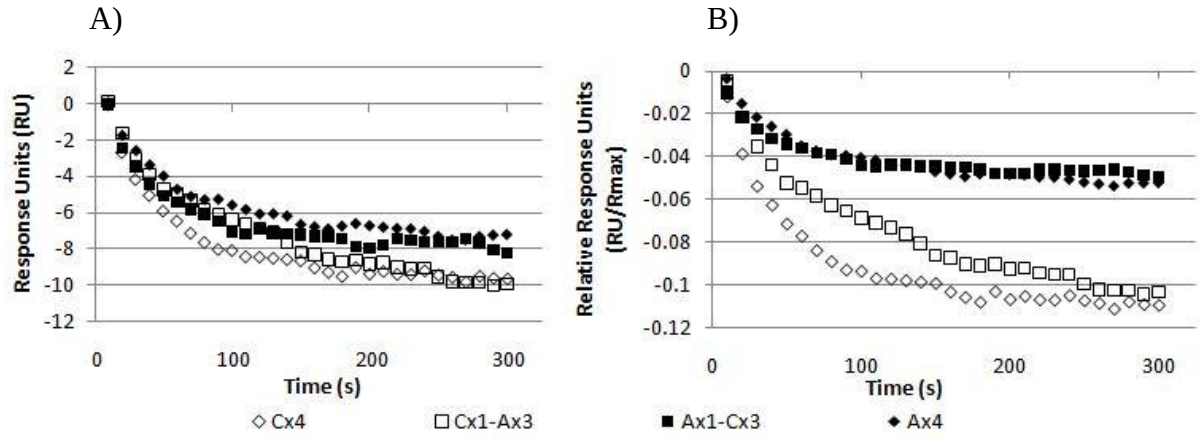


**Figure 5.6: Dissociation after multiple injection experiment, zeroed from start of dissociation. A) Zeroed at start of dissociation; B) RU normalized to "maximum association" from Table 5.3.**

### 5.3.2. Dissociation Analysis

Analysis of the dissociation sensorgrams can provide clues as to the composition of the surfaces (Rabe *et al.* 2007). There was very little difference between the dissociation curves in Figure 5.6A. Near the end of the dissociation, a difference was observed between surfaces with CPP initially adsorbed versus those with AL initially adsorbed (t > 200 seconds). The curves were normalized by dividing by the respective maximum association presented in Table 5.3. This normalization allows for a comparison between the relative strength of binding between the components on the SAM (Chapters. 3 & 5). After normalization, the dissociation curves appeared to be separated into two groups (Figure 5.6B), those with AL first loaded on the surface and those with CPP first loaded on the surface. AL has a stronger adsorption to the SAM as well as a stronger adhesion, since it does not dissociate as readily as CPP (Figure 5.6B). Another curve with high adhesion to the SAM layer was Alx1-Cx3. The Ax1-Cx3 surface contains CPP particles not present on Ax4 surface, but both had the same dissociation characteristics. The biggest similarity between these two runs was they both have AL as a base layer. The opposite was true for the surfaces that had first been loaded with CPP. In particular, Cx1-Ax3 which was approximately 37% protein had the same adhesion to the surface as the Cx4, 100% CPP solution (Figure 5.6B). A possible explanation is that the CPP particles shield AL from binding strongly to the SAM layer and the AL instead bind to CPP. This, along with association data from Figure 5.5 suggest that the CPP on the SAM does not disrupt the adsorption of AL, but instead affects the adhesion of AL to the SAM. When the bulk solution characteristics are changed to induce dissociation, the CPP-SAM bond dissociates but the CPP-AL interaction remains and the CPP-

AL complex diffuse into the bulk solution. This interpretation required an interaction between CPP and AL molecules.

Based on AL's strong adhesion to the SAM, it was hypothesized that AL would adhere to the first surface it is exposed too, either a SAM or CPP. If AL and CPP were to interact in solution before exposure to the surface, it would have an effect on the subsequent association of AL with the SAM layer.

## 5.4. Mixed Injection Method

The mixed injection method was used to test the consequence of mixing AL and CPP in solution, before being exposed to the surface. Three solutions were injected over the SAM layer: AL, CPP and a mixture of AL-CPP (Figure 5.7).

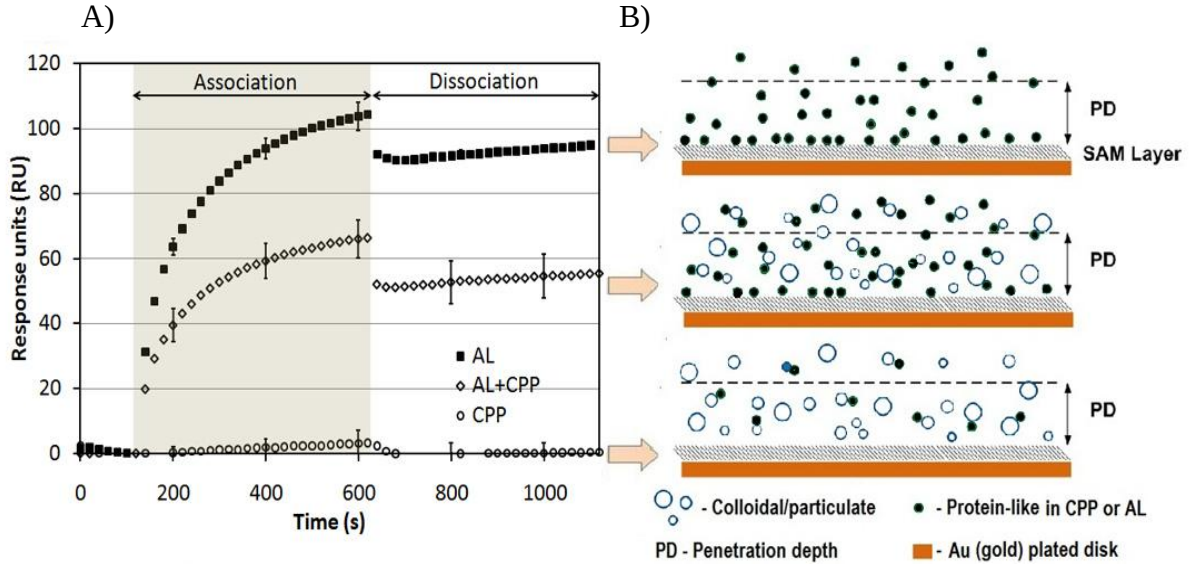


**Figure 5.7: SPR data of the association and disassociation behaviour of CPP, AL and CPP/AL mixture.**

**(A), AL and a mixture of CPP and AL (each with comparable loadings) on the SAM layer of the SPR sensor disk. The error bars represent the standard error (n = 3) at randomly selected measurement points. (B) A schematic representation of the association between colloidal/particulate and protein-like matter for the three SPR response curves in A. When protein-like matter interacts with colloidal/particles, the resulting "soluble" protein-colloidal/particle aggregates can be expected to remain in the bulk solution and those positioned above the SPR signal penetration depth (PD) = 400 nm for the SPR analyzer used in this study) do not generally contribute to responses related to interactions with the SAM layer due to degradation of the evanescent wave.**

To modify the AL: CPP ratio, different concentrations of the two components were mixed together, which resulted in a significantly diluted CPP mixture showing almost no adhesion to the sensor surface (Figure 5.7A). In contrast, the sensorgram for AL exhibits a medium interaction with the SAM layer as would be expected based on previous experiments. When a solution containing both AL and CPP with similar concentrations to those for the individual AL and CPP solutions was injected over the surface, an intermediate level of interaction between CPP and AL association was observed (Figure 5.7A).

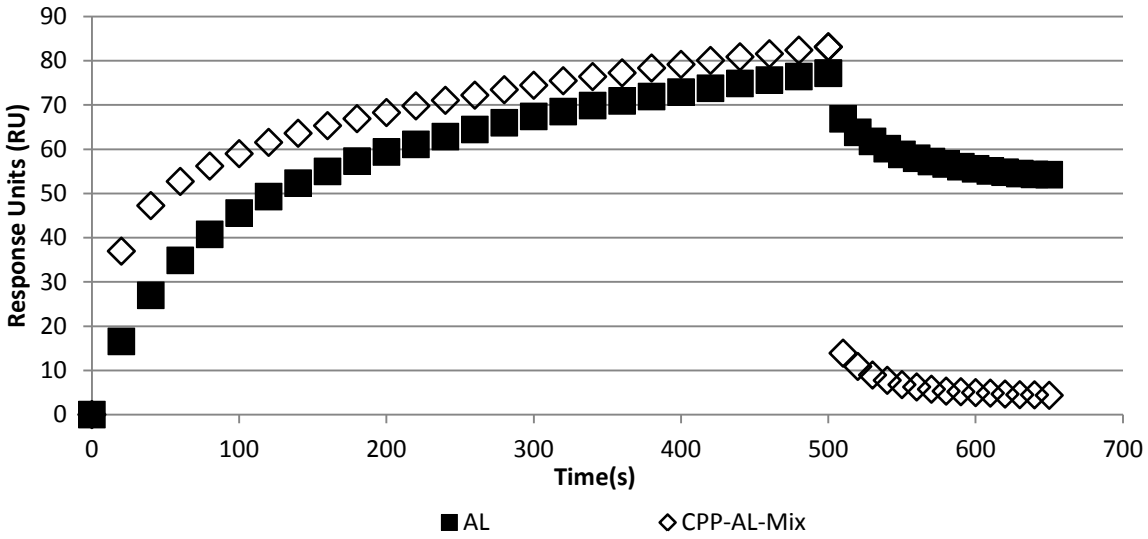


**Figure 5.8: Averaged sensorgram for a mixed injection experiment with AL and CPP/AL mixture.**

**Concentrations for AL were 0.2 mg/ml. For CPP (0.09 mg/ml)/AL mixture the ratio was 2.2:1, AL: CPP. Association occurred for 500 seconds, followed by a 150 second dissociation. Standard error = 11.5 RU (n=2). Standard error was calculated for each point for each curve, and the worst standard deviation was taken**

As the amount of AL in solution increased, the mixed CPP-AL solution shifted towards the AL response curve resulting in very little difference seen between the AL and AL/CPP mixture sensorgrams (Figure 5.8). These results indicate that the CCP extract contributed to reducing the interaction between the AL and the SAM layer. This can be attributed to inter-molecular or inter-particle physical interactions between the colloidal/particulate content of the CPP and AL that would reduce or mask the sites available for AL molecules to interact with the SAM. Consequently, the CPP-AL interactions kept the protein-colloidal/particle aggregates suspended and above the PD of the SPR device (Figure 5.7B). This also explains the absence of an observed interaction between the CPP extract and the SAM layer; colloidal/particulate matter present in

the CPP extract would have interacted with the protein-like content in CPP, leaving very limited opportunity for protein-like matter to interact with the SAM layer.

## 5.5. EEMs of Sensor Surface

Surface fluorescence EEMs of the CPP extract, AL and the mixture of CPP and AL on the SAM layer were obtained using a fibre optic probe following the SPR dissociation step (Figure 5.9). The fluorescence peak near Excitation/Emission ~ 380 nm/430 nm was due to radiative recombination of holes in the d-band with electrons in the sp-conduction bands of the gold atoms (Singh *et al.* 2009)underneath the SAM layer and not related to the associated material. The existence of a clear peak-δ for AL and the mixture of CPP/AL signifies that the protein remained attached to the SAM layer subsequent to the dissociation step in both cases (Figure 5.9B & C), which was consistent with the results of SPR analysis. Also, the absence of a clear peak-δ for CPP extract (Figure 5.9A) confirms the SPR results, which indicated no significant protein bound to the SAM layer despite the presence of protein-like matter in the CPP extract. The similarities of the magnitudes of the intensity at δ-peak (~ 7 a.u.) in both Figure 5.9B & C imply that the protein that remained on the SAM layer after the dissociation step was similar for AL and the mixture of CPP/AL. On the other hand, the SPR analysis indicated that the amount of AL that interacted directly with the SAM layer was lower for the CPP and AL mixture as compared to the AL solution alone. The increase in the intensity values in the neighbourhood of the Rayleigh scattering peaks in Figure 5.9 C compared to Figure 5.9A & B (peaks are not visible as only intensities below 14 a.u. are shown) also indicate an increased level of colloidal/particulate matter on the SAM layer for the mixture of CPP/AL. It is reasonable to conclude that part of AL in the mixture of CPP/AL, which did not have direct interaction with the SAM layer, would have interacted with colloidal/particulate matter and remained on the SAM layer after the dissociation step. These observations support the above SPR-based assessment of the interaction between colloidal/particulate and protein-like matter that occurred on the surface of the sensor disk.

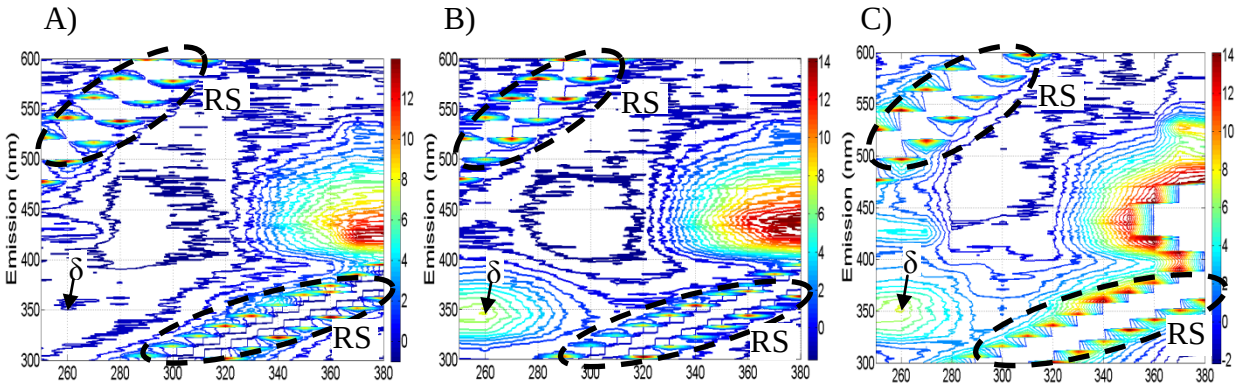


**Figure 5.9 Fluorescence EEMs of the surface of the SPR disk following dissociation.**

**A) CPP, B) AL and C) a mixture of the CPP matter and AL. The EEMs are limited to an intensity of 14 a.u. to allow better resolution of the δ-peak.**

## 5.6. Conclusions

The effect of CPP on AL adsorption to SAM can be seen when both components are mixed together in a 1:5 (wt) CPP to AL ratio. Although the exact mechanism is still unknown, it is hypothesized that the AL protein interacted with CPP particles which remained in the bulk solution away from the SAM layer. The resulting interaction prevented AL from binding non-specifically to the SAM. The ratio between CPP and AL appeared to be an important factor in preventing AL adsorption. In the immobilization experiments, the CPP did not readily adsorb to the immobilized AL, perhaps due to steric hindrance of an AL-CPP binding site, or the density of the AL immobilized on the surface. The multiple injection method was useful as it indicated that the AL would preferentially adhere to the first surface it was exposed to. Fluorescence analysis of the surface confirmed the presence of AL and CPP on the surface, supporting SPR data. It would be useful in future work to optimize the immobilization experiments to determine kinetic constants between CPP to AL. Furthermore, once the constants have been established manipulation of the environmental conditions would be useful for further quantifying the nature of the interactions between the AL and CPP.

# Chapter 6. Modeling β-Lactoglobulin Adsorption to Carboxylic Acid-Terminated Self-Assembled Monolayers

## 6.1. Introduction

Nonspecific adsorption of proteins to solid surfaces is a complicated phenomenon, with the exact mechanism still being debated among researchers. Most proteins are polyampholytic and have numerous tertiary structures which contribute to the large number of interacting forces governing adsorption phenomena (Norde 2008). Once protein has diffused close enough to the surface, previously insignificant forces acting on the protein in the bulk solution become significant and produce changes in the protein's secondary and tertiary structure, which can further new nonspecific interactions between the denatured protein and protein in the bulk solution.

The study of protein nonspecific adsorption benefits many industries, especially those that utilize membrane separation processes such as the food industry. Whey, which is primarily composed of β-lactoglobulin (BLG), is utilized in the food industry as an emulsifier and texturizer. BLG often contributes to fouling of membranes and heat exchange devices during processing (Mulvihill & Donovan 1987). The exact mechanism for BLG-based membrane fouling is not fully understood, but many believe that protein-protein interactions and protein-membrane interactions play an important role in fouling and subsequent flux decline (Mulvihill & Donovan 1987). By studying adsorption to surfaces in a controlled environment, insight into these mechanisms may help predict fouling and in producing new membrane designs to prevent or reduce its occurrence.

There are many mechanisms that are utilized to explain nonspecific adsorption, for example random sequential adsorption of particles (RSA) and protein conformational transitions (P. Schaaf 1989, Rabe *et al.* 2011). A method often utilized to confirm these theories is to compare adsorption kinetics predicted in theory to the experimental data. Surface plasmon resonance (SPR) has been used in a multitude of immunoassays, DNA-protein and protein-protein kinetic studies due to its real time and label free measurements of adsorption events onto the sensor surface (Homola 2008). Since the SPR signal is directly related to the refractive index (RI) on the surface, and the RI is directly proportional to mass accumulation, it is a perfect device for measuring and verifying theoretical models.

Surface Plasmon Resonance (SPR) was utilized to study the real-time adsorption of BLG at pH 6.2 onto carboxylic acid terminated self-assembled monolayers (SAMs). A mechanistic kinetic model was developed to describe the adsorption of BLG.

## 6.2. Theory

Several models were investigated in order to fit the SPR data and determine the adsorption mechanism before the three state monomer model was chosen (see Section 6.2.2). Models that did not generate adequate fits were based on a basic one to one binding model (Oshannessy *et al.* 1993), a fibrillar growth model adapted for surface aggregation (Arnaudov & Vries 2007), and derived surface interaction model, which was expanded from the one to one binding model to include adsorbed protein and bulk protein interactions. Most nonspecific adsorption curves could be fit to a one to one binding model with a conformational surface change. Many researchers also report a positive cooperation effect during the initial stages of adsorption which did not fit with standard exponential type growth kinetics (Minton 2001). The surface induced conformational changes subsequently alter the protein's affinity towards the SAM surface. The current theory suggests that many globular proteins undergo various conformational changes once exposed to a flat planar surface (Rabe *et al.* 2011, Norde 2008).

### 6.2.1. Dimer-Exchange Model

The dimer-exchange model explained BLG adsorption onto methylated silica through a monomer-dimer exchange mechanism (Wahlgren & Elofsson 1997). The fit to the SPR data in this thesis is poor (see Appendix C) and could be attributed to the hydrophobic surface used in Wahlgren & Elofsson's study and the hydrophilic SAM used in this study. The mechanism of adsorption of protein to hydrophobic surfaces is theoretically much different than the mechanism which governs hydrophilic surfaces. This is because hydrophilic surfaces having a much larger dependence on electrostatic interactions (Luey *et al.* 1991, Campiña *et al.* 2010).

Wahlgren & Elofsson utilized BLG's concentration based monomer-dimer equilibrium in their model as the adsorption was conducted at pH 7. At this pH, the BLG monomer is at equilibrium with its dimer (Sakurai & Goto 2002). This equilibrium is governed by the total concentration of BLG in the solution, and thus as the bulk solution concentration changes, so would the

distribution of monomer to dimer. These equations were incorporated into the three-state model discussed in Section 6.2.2.

### 6.2.2. Three Monomer State Model

Rabe *et al.* developed a model to describe BLG adsorption onto hydroxyl covered glass slides under acidic conditions (Rabe *et al.* 2007). The hydrophilic surface is somewhat similar to the hydrophilic SAM used in this study. Under acidic conditions BLG is known to exist as a monomer (Gottschalk *et al.* 2003, Sakurai *et al.* 2001). The authors used citrate buffer in their adsorption experiments and the kinetic data was obtained using supercritical angle fluorescence. This model is based on a large variety of association and dissociation data and explored a fairly large concentration range to justify the three monomer states seen on the surface (Rabe *et al.* 2007).

The model proposes that there are three BLG orientations/conformations that occur as a result of the electrostatic charges present on the SAM/BLG layer: an *initial*, *reversible*, and *irreversible* monomer. The accumulation of a sufficient amount of protein on the surface would cause the electrostatic landscape of the SAM to change, resulting in an altered affinity towards the bulk protein (Rabe *et al.* 2011, Rabe *et al.* 2007, Tie *et al.* 2003). Since BLG contains both positive and negative residues near the isoelectric point (Majhi & Ganta 2006), lateral interactions between adjacent molecules can become too strong once the critical concentration is reached and the proteins must re-orient themselves to reach an energetically favoured state (Daly *et al.* 2003). The model is presented in equations 1-11.

$$\theta_{total} = \theta_{m,1} + \theta_{m,2} + \theta_{m,3} \quad (1)$$

$$\frac{\partial \theta_{m,3}}{\partial t} = k_{m,1-m,3} \cdot \theta_{m,1} + k_{m,2-m,3} \cdot \theta_{m,2} - k_{diss,m,3} \cdot \theta_{m,3} \quad (2)$$

$$\Phi = \frac{\theta_{total}}{\theta_{max}} \quad (3)$$

The following conditions change based on surface coverage:

**if** $\theta_{total} \leq \theta_{crit}$

$$\frac{\partial \theta_{m,1}}{\partial t} = k_m \cdot C_m \cdot \Phi - k_{m,1-m,3} \cdot \theta_{m,1} \quad (4)$$

$$\frac{\partial \theta_{m,2}}{\partial t} = 0 \quad (5)$$

**if** $\theta_{total} > \theta_{crit}$

$$\frac{\partial \theta_{m,1}}{\partial t} = -k_{m,1-m,2} \cdot \theta_{m,1} - k_{m,1-m,3} \cdot \theta_{m,1} \quad (6)$$

$$\frac{\partial \theta_{m,2}}{\partial t} = k_m \cdot C_m \cdot \Phi + k_{m,1-m,2} \cdot \theta_{m,1} - k_{m,2-m,3} \cdot \theta_{m,2} - k_{diss,m,2} \cdot \theta_{m,2} \quad (7)$$

Where $\theta_{m,1}$, $\theta_{m,2}$, and $\theta_{m,3}$ represent the *initial*, *reversible* and *irreversible* BLG monomer surface concentrations, respectively. $\Phi$ represents the ratio between the current amount of protein on the surface $\theta_{total}$ and the theoretical maximum amount of protein on the surface $\theta_{max}$. $k_m$ is the monomer association constant, $k_{m,1-m,3}$ is the exchange from *initial* to *irreversible* state, $k_{m,1-m,2}$ is the exchange from *initial* to *reversible* state, $k_{m,2-m,3}$ is the exchange from the *reversible* to *irreversible* state, $k_{diss,m,2}$ and $k_{diss,m,3}$ are the *reversible* and *irreversible* dissociation constants, $\theta_{crit}$ represents the point at which the surface kinetics "switch." Some of the parameters also have the following dependencies:

$$k_m = k_{m,o} + C_1 \cdot \frac{\theta_{m,1}}{\theta_{max}} \quad (8)$$

$$k_{diss,m,2} = k_{diss,m,2\,o} + C_2 \cdot \frac{\theta_{m,2}}{\theta_{max}} \quad (9)$$

$$k_{m,1-m,2} = C_3 \cdot \frac{\theta_{m,2}}{\theta_{max}} \quad (10)$$

$$k_{m,2-m,3} = C_4 \cdot \frac{\theta_{m,2}}{\theta_{max}} \quad (11)$$

Where $C_1$, $C_2$, $C_3$ and $C_4$ are proportionality constants used to explain co-operativity effects. $k_{m,o}$ and $k_{diss,m,2\,o}$ are the initial association constant and initial dissociation constant, respectively.

This model was adapted to incorporate the monomer concentration dependence from the dimer-exchange model, and shown in equations 12 & 13.

$$C_m = 2 \cdot \left( -\frac{K_d}{8} + \sqrt{\left(\frac{K_d}{8}\right)^2 + \frac{K_d}{4} C_{tot}} \right) \quad (12)$$

$$C_d = C_{tot} - \frac{C_m}{2} \quad (13)$$

$C_{tot}$ represents the total BLG dimer concentration in moles, if there was no equilibrium between BLG monomers and dimers. $C_m$ and $C_d$ represent the concentration of the BLG monomer and dimer at equilibrium in moles, respectively. The only unknown variable in equations 12 and 13 is the dissociation constant ($K_d$). This was taken as $5x10^{-6}$ M, which is the inverse association constant that was determined under approximately the same conditions by Sakurai & Goto (2002) (Sakurai & Goto 2002).

## 6.3. SPR Considerations

### 6.3.1. Initial Rapid Increase in RU due to Changes in Refractive Index

Although SPR is often used at low analyte concentrations to study antigen-antibody interactions, at higher analyte concentrations RI changes occur upon injection of the sample (O'Brien II *et al.* 1999). The concentration of protein in solution is proportional to the overall RI of the bulk solution. The increased RI causes a rapid increase in the SPR signal upon injection. This increase occurs in a very short time frame, which makes it difficult to determine if the protein is adsorbing to the surface or if the change is due to the bulk RI change. Currently, the only way to conduct an accurate analysis is to utilize an SPR device that has two or more SPR channels that allow bulk solution subtraction (O'Brien II *et al.* 1999, Homola 2008). For presentation purposes all SPR data in this chapter are normalised by dividing by 500 (NRU). For the purpose of fitting the SPR data to the models in this study, the initial response unit (RU) increase was removed from the sensorgrams. This was done by zeroing the signal after 1 second after injection and using the subsequent 306 points to fit the sensorgram. This assumption is discussed in Section 6.4.3

### 6.3.2. Conformational Changes and Refractive Index

When protein is adsorbed to a flat planar surface there may be conformational changes in the secondary and tertiary structures of the protein (Norde 2008). Tertiary changes affect the RI of the protein (Sota *et al.* 1998) which generate false positive or negative signals (depending on if

the effective RI is increased or decreased relative to the original state). Previous work based on ethanol-induced BLG conformational changes (Mousavi *et al.* 2008) showed that the deviation from the expected curve fit only amounted to 5 RU, or 2.5% variation over the expected signal (see Section 4.3.6). Such a large conformational change is not expected to occur since BLG is a "hard" globular protein, meaning that it will retain most of its tertiary structure once attached to the surface (Rabe *et al.* 2011). In general, tertiary structure conformational changes only occur at much lower surface concentrations since the protein is no longer sterically hindered by adjacent protein and can effectively spread (Norde 2008). Overall the expected variation in the SPR signal is not thought to be significant enough to warrant a unique "SPR signal to mass" factor, although in future studies this may be worth examining for lower concentration ranges.

## 6.4. Experiments and Data fitting

A typical SPR experiment was performed with an association time of 207 seconds and dissociation time of 100 seconds. Four samples at different BLG concentrations (111, 18.5, 3.29, 0.59 μM) were adsorbed in the first batch study, then a month later new solutions and surfaces were prepared and a second batch of three samples at three additional concentrations (56.0, 7.50, 0.11 μM) were adsorbed. The authors of Rabe *et al* (2007) did not account for the monomer-dimer equilibrium as experiments were conducted at acidic pH, thus the model was adapted to incorporate the monomer-dimer equilibrium effect on the monomer concentration. The data was grouped together and global analysis was used to determine 10 unknown kinetic parameters, see Section 3.5.2. Certain parameters in the model when varied slightly have drastic effects on the association curve, namely $k_m$ and $\theta_{crit}$ (Rabe *et al.* 2007). The parameters were initially estimated when no variation of parameters was allowed in the model (see Appendix C). The results from this data were used as a starting point for another set of optimizations in which the variables were allowed to deviate from the starting points by about 13%. The results for the fit along with kinetic constants are presented in Figure 6.1.

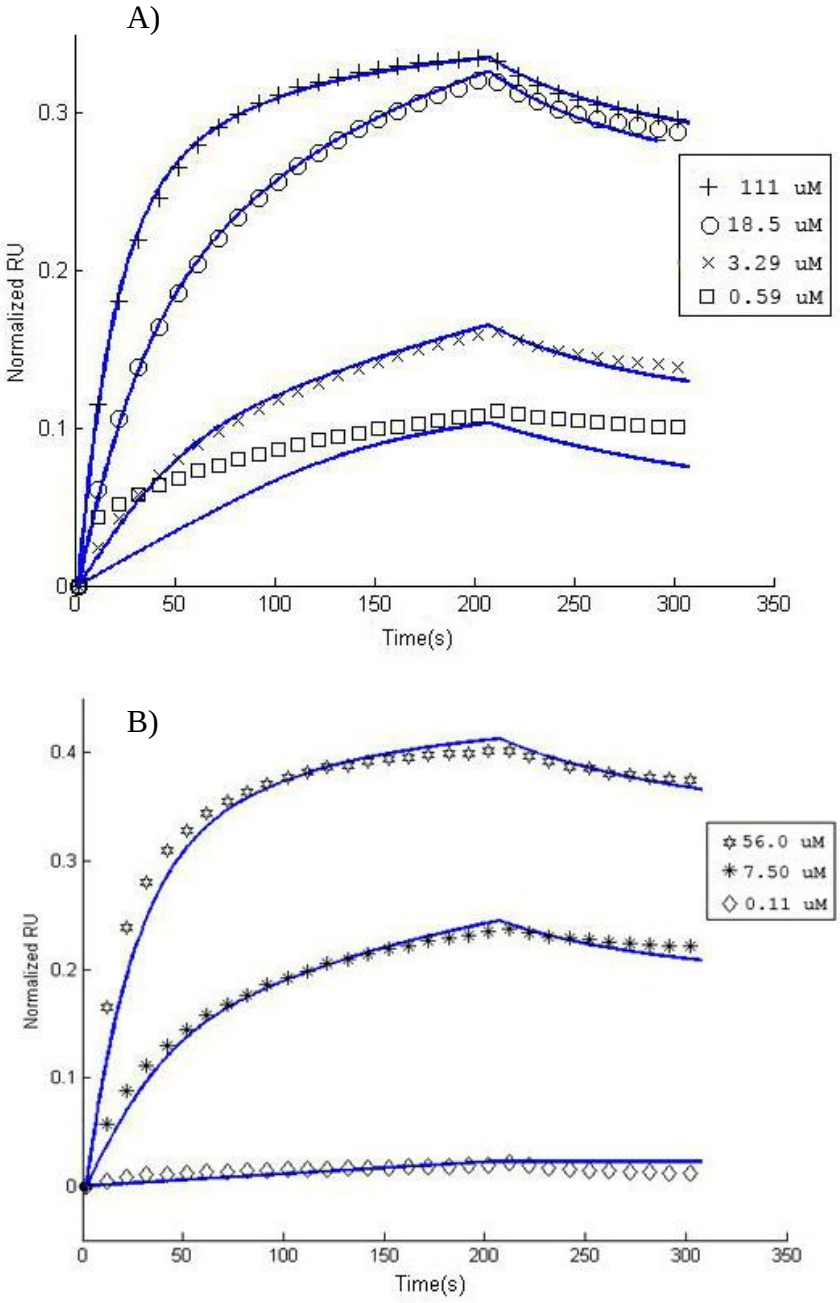


**Figure 6.1: Three state model compared to experimental values.**

**Model fit is represented by the line. Points are experimental values from the SPR analysis. A) First batch of experiments. B) Second batch of experiments. The only difference between batches aside from the concentrations utilized was that batch B was conducted one month after batch A. Batches were utilized together for data analysis. Values were normalised by dividing by 500.**

BLG adsorption to SAMs reached equilibrium faster on SAMs than on the hydrophilic glass slides and methylated silica (Rabe *et al.* 2007, Wahlgren & Elofsson 1997). The increase in

equilibration can be attributed to the charged carboxylic acids which would present a very attractive surface for non-specific adsorption of proteins due to electrostatic forces and hydrogen bonding sites (Patel *et al.* 1997). It should be noted that for this particular model the dimer was not included as an adsorbing species, as will be explained later.

There is a significant improvement in the fit over the dimer exchange model, especially in the lower concentration range, below 50 μM (see Appendix C); also, the shape more accurately reflected the adsorption behaviour. To compare these findings with those of Rabe & Verdes *et al.*(2007), the maximum theoretical association ($\theta_{max}$) was used to normalize the parameters for comparison (see Table 6.1) (Rabe *et al.* 2007).

Most of the values are in the same order of magnitude as those reported by Rabe & Verdes *et al.*(2007) with only $k_{diss,m,2}$ and $C_4$ differing in orders of magnitude (although $C_1$ and $C_2$ differ by about $10^2$, these parameters will be discussed later). The change in parameters translates to a much more transient *reversible*-monomer, not as strong cooperation effect with monomer addition, and a much faster transition from the *reversible* to *irreversible* state.

**Table 6.1: Summary of constants.**

**Global analysis parameters were the initial points used to estimate the individual parameters. NRU represent RU divided by 500 . [1]Values from Rabe *et al.* (2007) were normalized with respect to the maximum surface concentration** (Rabe *et al.* 2007)**.**

| | Concentration (μM) | | | | | | | | | | | Values from Rabe *et al.* (2007)[1] |
|---|---|---|---|---|---|---|---|---|---|---|---|---|
| Parameter | 37 | 222 | 6.58 | 1.17 | 0.21 | 15 | 111 | Average[1] | | | Global Analysis | |
| $k_{m,o}$ [NRU $M^{-1}$ $s^{-1}$] | 717 | 660 | 660 | 848 | 595 | 790 | 890 | 737.13 | ± | 87.13 | 771 | 851 |
| $C_3$ [$10^{-2}$ $s^{-1}$] | 5.97 | 6.26 | 6.55 | 4.89 | 4.89 | 6.45 | 4.41 | 5.63 | ± | 0.70 | 5.43 | 0.07 |
| $k_{diss,m,2}$ [$10^{-2}$ $s^{-1}$] | 0.80 | 0.89 | 0.80 | 0.70 | 0.70 | 0.70 | 0.63 | 0.75 | ± | 0.07 | 0.82 | $1.93 \times 10^{-4}$ |
| $C_4$ [$10^{-2}$ $s^{-1}$] | 3.19 | 2.81 | 3.37 | 3.54 | 3.54 | 3.15 | 2.50 | 3.16 | ± | 0.31 | 2.92 | $4.36 \times 10^{-3}$ |
| $\theta_{max}$ [$10^{-2}$ NRU] | 42.73 | 37.24 | 34.26 | 46.25 | 32.53 | 33.70 | 45.89 | 38.94 | ± | 4.73 | 40.05 | 40.05[1] |
| $\theta_{crit}$ [$10^{-2}$ NRU] | 4.88 | 4.64 | 4.44 | 5.96 | 5.96 | 6.35 | 6.90 | 5.59 | ± | 0.75 | 5.42 | 8.33 |
| $C_2$ [$10^{-2}$ $s^{-1}$] | 0.37 | 0.43 | 0.38 | 0.34 | 0.34 | 0.34 | 0.31 | 0.36 | ± | 0.03 | 0.39 | 4.58 |
| $C_1$ [$10^{-2}$ NRU $s^{-1}$] | 0.04 | 0.04 | 0.04 | 0.05 | 0.04 | 0.04 | 0.05 | 0.04 | ± | 0.00 | 0.04 | $3.27 \times 10^{-3}$ |
| $k_{m,1-m,3}$ [$10^{-7}$ $s^{-1}$] | 2.11 | 2.11 | 2.11 | 2.11 | 2.41 | 2.41 | 2.41 | 2.54 | ± | 0.00 | 2.41 | 23.70 |
| $k_{diss,m,3}$ [$10^{-7}$ $s^{-1}$] | 7.51 | 7.51 | 7.51 | 7.51 | 8.55 | 8.55 | 8.55 | 6.04 | ± | 0.00 | 5.72 | 0.59 |

The 95% confidence interval for the parameters averaged a 11% deviation of the mean. The overall fit was significantly improved as a result of optimizations. It was found that fitting dissociation data was important as this portion of the curve is a direct function of the different monomer conformations on the surface (Rabe *et al.* 2007). In a study where the adsorption of nanoparticles was optimized, it was found that functional group substitutions always had an effect on the dissociation characteristics, whereas the association characteristics may have been unchanged (Tassa *et al.* 2010).

### 6.4.1. Components of the SPR Sensorgram

A plot for the individual components that make up the SPR protein adsorption curve at 56 μM are given in Figure 6.2.

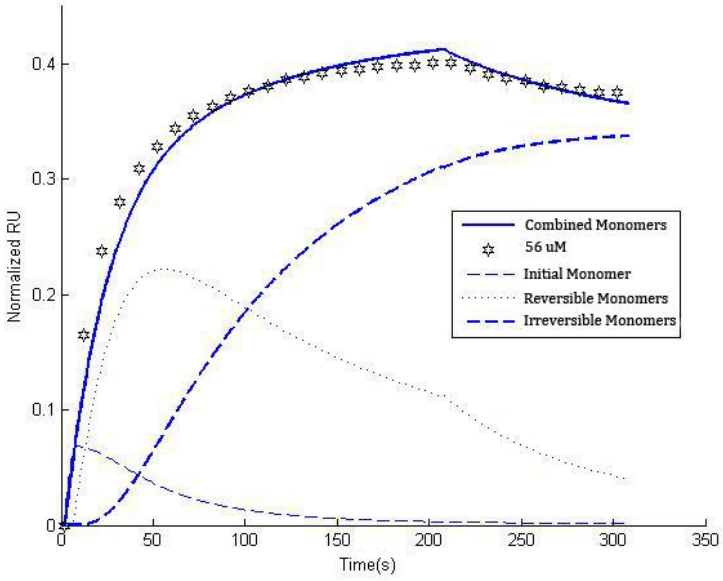


**Figure 6.2: Components vs. time for the three state model at 56 μM.**

**Model fit is represented by the lines. Experimental data points are from SPR analysis. Values were normalised by dividing by 500.**

The *initial*-monomer quickly adheres to the layer until $\theta_{crit}$ is reached. As $\theta_{crit}$ was surpassed at approximately 10 seconds, bulk BLG protein no longer adsorbed as *initial*-monomer, and instead adhered as a *reversible*-monomer. The *initial*-monomer concentration sharply began to decrease, transforming into *reversible*-monomer. A very small amount of *initial*-monomer transformed to *irreversible*-monomer. The *reversible*-monomer surface concentration also began to increase,

shortly followed by the *irreversible*-monomer. As the adsorption continues, the total *reversible*-monomer concentration begins to decrease as total BLG on the surface approaches the maximum surface concentration. The *reversible*-monomer protein transforms to the *irreversible*-monomer, until all the protein is in the *irreversible* state. Once dissociation begins, the *irreversible*-monomer continues to increase, as the remaining *reversible*-monomer was still transitioning to the irreversible state. By this time there was very little of the *initial*-monomer protein on the surface. The *reversible*-monomer also rapidly dissociated from the surface. These findings imply a smaller concentration of *reversible*-monomer on the SAM surface when compared to Rabe & Verdes *et al.*(2007). This can be attributed to the large number of charged carboxylic acid groups on the SAM. The carboxylic acid groups would have a much greater ability to form hydrogen bonds when compared to the hydroxyl groups on the unmodified glass surface (Silin *et al.* 1997), thus increasing adhesion. The electrostatic forces appear to be similar on both surfaces based on the comparable values obtained for the $k_m$ parameter, which represents the ability of BLG to approach the surface from the bulk liquid. This parameter would be based on the net charge difference between BLG and the SAM. This would suggest that once BLG has penetrated to the surface the increased hydrogen bonding results in faster reversible-monomer conformational shifts. This increase in hydrogen bonding would also likely lead to rapid conformational changes to *irreversible*-monomer and keep it tightly bound to the surface.

### 6.4.2. Dimer Adhesion and Monomer-Dimer Equilibrium

The first iteration of the three state monomer model utilized 14 parameters which incorporated the three monomer states as well as dimer adhesion and monomer-dimer exchange. The dimer adhesion was very low in this model, even in the latter stages when the monomer-dimer switching was expected to take place. When the model was programmed to predict the SPR curve for longer association times, the monomer-dimer exchange did not occur; the dimer surface concentration was much lower than the monomer surface concentration. Any dimer on the surface desorbed during the dissociation phase. The lack of adhesion of dimer allowed it to be removed from the model without a significant change in the fit.

The lack of dimer adhesion was predicted by the model possibly because it does not happen on the SAM surface. It is hypothesized that the dimer exchange is only seen at much longer association times. Also, the nonspecific interactions between monomer and SAM may increase

its adhesion to the layer such that the monomer is unable to dissociate from the surface. Current theory suggests that for mixed protein systems, the smaller protein will adhere much more quickly to the surface, followed by the larger protein after sufficient time has passed (LeDuc *et al.* 1995). To test the validity of this hypothesis in the SAM-BLG system, longer adsorption experiments would need to be conducted.

To verify that the monomer-dimer equilibrium was important, a third model was examined in which the three state monomer model was fit without dimer-monomer equilibrium. This model did not have the correct monomer concentration dependence. It did not fit as well as the three state model shown above, since the concentration dependence of the monomer changed the spacing between each adsorption curve, and could not be adequately matched. The model tended to under estimate higher concentrations and overestimate lower concentrations.

### 6.4.3. Discussion of Model Parameters and the Next Steps

The model can be simplified without taking away from the theoretical aspects, that is, still being a mechanistic model rather than empirical. One of the least significant parameters was $C_1$, the linear dependence of $k_m$ with the change in *initial*-monomer on the surface. This parameter was utilized to explain the large change in $k_m$ due to cooperativity effects seen during the initial stages of the adsorption (Rabe *et al.* 2007). The parameter in this experiment is rather low, and when taken out there was no significant change to the model. It could be that this particular parameter was not significant in the concentration regime studied. The parameter can only be accurately resolved at low concentrations and subsequently low association times. Rabe *et al.* (2007) studied low concentrations of the order of $10^{-2}$ μM, which were not studied in this work. In order to obtain an accurate assessment of the cooperative effects represented by $C_1$, a much lower concentration would need to be utilized. The parameter $C_2$, which describes the negative co-operativity in the *reversible*-monomer dissociation constant, was also not as significant in the regime studied. Though removing this parameter did have some effect on the fit at higher concentrations. If dissociation experiments could be conducted at the predicted maximum concentration of *reversible*-monomer (t = 50 seconds, Figure 6.2) , $C_2$ could be resolved. At longer association times, the effects of $C_2$ would diminish due to the greater amount of *irreversible*-monomer present on the surface. Overall the cooperative effects of $C_2$ and $C_1$ were not observed in the association data. The carboxylic acid groups on the SAM present such

strong electrostatic interactions that any gains or reductions that the cooperative effects would have on the kinetic constants appeared to be negligible. This could be further investigated by utilizing SAMs with reduced hydrophilicity such as amine terminated SAMs or mixed SAMs with different ratios of amine and carboxylic acid groups. The reduced hydrophilicty would theoretically have a greater effect on the protein co-operativity parameters $C_1$ and $C_2$.

Although carboxylic acid groups increase electrostatic interactions, the $k_m$ parameter is relatively the same when compared to the experiments of Rabe *et al.* (2007). This finding is inconsistent with theory since $k_m$ represents bulk BLG's affinity towards the SAM due to electrostatic interactions. The $k_m$ parameter may then not be properly resolved, since the initial SPR signal shift during the start of the experiment was eliminated due to RI effects. It is still possible that some of the initial monomer adhesion was removed due to the zeroing after the rapid increase in the RI. This theory should be tested by conducting adsorption experiments at short association times and studying the subsequent dissociation afterwards. This would probe the initial protein regime and may reflect the true composition of BLG on the SAM.

There was little to no transition of the *initial*-monomer to *irreversible*-monomer as represented by the small value of the kinetic constant $k_{m,1-m,3}$. At sufficiently higher concentrations this parameter would be significant as there would be overall a much larger amount of *initial*-monomer on the surface. $\theta_{crit}$ was much lower than reported by Rabe *et al.*, as such, there is only a very brief window during the initial stages of the reaction in which there is more *initial*-monomer than *reversible*-monomer. In the work of Rabe *et al.* the adsorption occurred over a much longer period of time and $\theta_{crit}$ was much higher, thus dissociation constants which resolved the transition between *initial*-monomer to *irreversible*-monomer could be measured. Indeed, there may be some ambiguity in the parameters estimated here unless other dissociation experiments are conducted at smaller association times and lower concentrations.

## 6.5. Conclusions

The three monomer state model was adapted to incorporate the monomer–dimer equilibrium that exists at pH 6.2 for BLG. This changed the monomer concentration dependence on the total BLG concentration from linear to nonlinear. Dimer association with the surface was found to be insignificant and so was not included in the model. The findings help verify the presence of

three different conformations of monomers on the surface. The different conformations are a result of BLG's surface orientation, and minor denaturation of its structure due to interactions with the surface, as described in Chapter 4 and 5. The binding of the initial-monomer to the surface is a very fast process and as such the BLG concentration quickly increases to a point where electrostatic charges and lateral interactions result in a re-orientation of the surface BLG to accommodate a more *reversible*-monomer. As the adsorption continues the *irreversible*-monomer begins to form. Dissociation studies were used to validate the three monomer state model by providing data on the dissociation characteristics of the different conformational states of the monomer. To further verify that the three monomer states exist, dissociation experiments should be conducted at around 50 seconds (the peak amount of *reversible*-monomer), at 3-15 seconds (just before or after $\theta_{crit}$ is reached), and at much longer association times to test the dissociation of the *irreversible*-monomer. Much longer association times would verify the presence of the dimer-monomer exchange reaction.

# Chapter 7. Thesis Conclusions

## 7.1. Conclusions

The following will outline the main conclusions of this thesis and how they relate to the research objectives presented in Chapter 1. Proposed future work is also presented.

- Association and Dissociation Analysis - (Thesis Objective 1)

SPR was demonstrated to be a useful tool for monitoring nonspecific protein aggregation and adsorption in both solution and on surfaces, as reported in Chapters 4 and 5. The association and dissociation analysis utilized in all chapters helped to identify the different components that adsorbed to the sensor surface. These components can be different proteins in multiple orientation/conformations. SPR was also utilized to analyse the relative strength of adsorption for each component. Fluorescence analysis of the surface of the sensor disks using a fibre optic probe (FOP) was developed and confirmed the results from the SPR analysis.

- Hydrophilic SAM - (Thesis Objective 2)

All research reported in this thesis utilized the same hydrophilic SAM based on 11-MUA that was developed to probe protein interactions. The SAM was found to be stable and easily reproduced on new disks. The reproducibility of each protein adsorption experiment was good as long as the surface was properly regenerated prior to the experiment. The best regeneration was found to be by electrochemical cleaning.

- BLG adsorption - (Thesis Objective 3)

BLG was a practical model protein system allowing for reproducible SPR experiments. The wealth of information available in the literature on BLG was also useful for providing sufficient background for interpretation of the results.

- BLG and PA structure stabilization - (Thesis Objective 3 & 4)

Chapter 4 was an investigation of the effects of association of BLG with PA. The analysis of association data alone was difficult, but when the dissociation data was analysed it provided sufficient data to identify different BLG conformational changes on the SAM surface. The addition of PA into solution stabilized BLG's structure, slowing its conformational changes due

to buffer and surface denaturation. The conformational changes prevented BLG from dissociating from the surface. Intrinsic fluorescence data were also utilized to confirm the presence of BLG conformations as revealed by analysing differences in the fluorescence EEM.

- AL and CPP interactions through changes in SPR adsorption - (Thesis Objectives 1 & 5)

Chapter 5 examined the change in surface adsorption of AL due to association with CPP. The standard SPR method of analysis, in which AL was immobilized onto the SPR surface, did not produce a sufficient signal to be effectively utilized. Other methods were developed to solve this problem, such as multiple injection and mixed injection. The multiple injection method involved subsequent association experiments of either AL or CPP matter on the same sensor surface without regeneration. The results showed that AL adhered much more strongly to the first surface it was exposed to, regardless of CPP or SAM. This knowledge was used to design the mixed injection method, which showed that when AL and CPP were mixed in solution before adsorption, the subsequent interaction hindered association between AL and SAM. Fluorescence surface scans confirmed that different components adsorbed to the surface. The verification of the physical interaction between CPP and validated the results of principle component analysis (PCA) conducted in other work, which theoretically predicted interactions between these two components.

- BLG adsorption described by Three-state model - (Thesis Objective 3 & 6)

A mechanistic model was developed based on information from the literature that suitably described the nonspecific BLG–SAM adsorption SPR data. The model predicted three monomer conformations/orientations of BLG on the surface. An important addition to the model was the monomer-dimer equilibrium of BLG in solution, as it provided the correct relationship between total bulk concentration and monomer bulk concentrations. Interestingly, the dimer did not bind at all to the surface. It was suspected this was due to the short association times investigated in this study.

## 7.2. Future Work

FOP surface scans can be utilized to observe the changes in protein secondary structure, particularly as BLG changes between β-sheet and α- helical structures on the surface of the SPR

sensor disks. Unfortunately, the signal attenuation of the FOP scans is too large and reproducibility low in order to completely deduce these changes. The small amount of protein on the surface means that highly reproducible measurements are required to determine structural changes. An investment in FOP – gold surface scan methodology would improve the sensitivity of the sensor for measuring different protein conformational states. A SPR instrument could be enhanced with a fluorescent FOP, which would perform fluorescent scans of the surface during acquisition of the SPR signal. The real time-change SPR signal could then be correlated to specific conformational changes through fluorescence data.

To improve the study of PA and BLG interactions presented in Chapter 4, removal of PA from the BLG-PA solution and utilizing the resulting BLG for SPR adsorption experiments would help isolate wither the PA in solution or the PA attached to BLG is causing the change in adsorption. In Chapter 5 the interactions between AL and CPP were examined. This could be further investigated if the immobilization of AL could be optimized. Changes in environmental conditions such as pH and temperature and their effect on AL and CPP interactions could be studied. The model developed in Chapter 6 could be improved by conducting dissociation experiments at predicted times when the different monomer conformations/orientations are at their maximum. This would help in verifying the predicted model parameters in relation to the dynamics in the kinetic behaviour. Further experiments at longer association times would also help validate the lack of dimer-monomer exchange and dimer binding.

## References


Aguilar, M. & Small, D. 2005, "Surface plasmon resonance for the analysis of beta-amyloid interactions and fibril formation in alzheimer's disease research", *Neurotoxicity Research*, vol. 7, no. 1, pp. 17-27; 27.

Almeida, A.J. & Souto, E. 2007, "Solid lipid nanoparticles as a drug delivery system for peptides and proteins", *Advanced Drug Delivery Reviews*, vol. 59, no. 6, pp. 478-490.

Amy, G. 2008, "Fundamental understanding of organic matter fouling of membranes, ", *Desalination*, vol. 231, no. (1-3), pp. 44-51.

Arnaudov , L.N. & Vries, R. 2007, "Theoretical modeling of the kinetics of fibrilar aggregation of bovine *β*-lactoglobulin at *p*H 2", *Journal of Chemical Physics*, vol. 126, no. 14.

Autolab 2006, *Autolab ESPRIT/SPRINGLE User manual: Surface Plasmon Resonance*, Eco Chemie B.V., Kanaalweg, Netherlands.

Aymard, P., Durand, D. & Nicolai, T. 1996, "The effect of temperature and ionic strength on the dimerisation of β-lactoglobulin", *International journal of biological macromolecules*, vol. 19, no. 3, pp. 213-221.

Barbana, C., Pérez, M.D., Sánchez, L., Dalgalarrondo, M., Chobert, J.M., Haertlé, T. & Calvo, M. 2006, "Interaction of bovine α-lactalbumin with fatty acids as determined by partition equilibrium and fluorescence spectroscopy", *International Dairy Journal*, vol. 16, no. 1, pp. 18-25.

Barnes, W.L. 1998, "Fluorescence near interfaces: The role of photonic mode density", *Journal of Modern Optics*, vol. 45, no. 4, pp. 661-699.

Barnes, W.L., Dereux, A. & Ebbesen, T.W. 2003, "Surface plasmon subwavelength optics", *Nature*, vol. 424, no. 6950, pp. 824-830.

Beccati, D., Halkes, K.M., Batema, G.D., Guillena, G., Carvalho de Souza, A., van Koten, G. & Kamerling, J.P. 2005, "SPR Studies of Carbohydrate–Protein Interactions: Signal Enhancement of Low-Molecular-Mass Analytes by Organoplatinum(II)-Labeling", *ChemBioChem*, vol. 6, no. 7, pp. 1196-1203.

Bee, J.S., Davis, M., Freund, E., Carpenter, J.F. & Randolph, T.W. 2010, "Aggregation of a monoclonal antibody induced by adsorption to stainless steel", *Biotechnology and bioengineering*, vol. 105, no. 1, pp. 121-129.

Bhattacharjee, S., Bhattacharjee, C. & Datta, S. 2006, "Studies on the fractionation of β-lactoglobulin from casein whey using ultrafiltration and ion-exchange membrane chromatography", *Journal of Membrane Science*, vol. 275, no. 1-2, pp. 141-150.

Bonanno, L.M. & DeLouise, L.A. 2007, "Steric Crowding Effects on Target Detection in an Affinity Biosensor", *Langmuir*, vol. 23, no. 10, pp. 5817-5823.

Box, G., Hunter, W., Hunter, S. & Hunter, W. 1978, *Statistics for Experimenters: An Introduction to Design, Data Analysis, and Model Building*, John Wiley & Sons.

Branco, M.C., Pochan, D.J., Wagner, N.J. & Schneider, J.P. 2010, "The effect of protein structure on their controlled release from an injectable peptide hydrogel", *Biomaterials*, vol. 31, no. 36, pp. 9527-9534.

Bucher, J., Santesson, L. & Kern, K. 1994, "Thermal Healing of Self-Assembled Organic Monolayers: Hexane- and Octadecanethiol on Au(111) and Ag(111)", *Langmuir*, vol. 10, no. 4, pp. 979-983.

Busti, P., Gatti, C.A. & Delorenzi, N.J. 1998, "Some aspects of [beta]-lactoglobulin structural properties in solution studied by fluorescence quenching", *International journal of biological macromolecules,* vol. 23, no. 2, pp. 143-148.

Campiña, J.M., Souza, H.K.S., Borges, J., Martins, A., Gonçalves, M.P. & Silva, F. 2010, "Studies on the interactions between bovine β-lactoglobulin and chitosan at the solid–liquid interface", *Electrochimica Acta,* vol. 55, no. 28, pp. 8779-8790.

Canaria, C.A., So, J., Maloney, J.R., Yu, C.J., Smith, J.O., Roukes, M.L., Fraser, S.E. & Lansford, R. 2006, "Formation and removal of alkylthiolate self-assembled monolayers on gold in aqueous solutions", *Lab on a Chip,* vol. 6, no. 2, pp. 289-295.

Capron, I., Nicolai, T. & Durand, D. 1999, "Heat induced aggregation and gelation of [beta]-lactoglobulin in the presence of [kappa]-carrageenan", *Food Hydrocolloids,* vol. 13, no. 1, pp. 1-5.

Chan, R. & Chen, V. 2004, "Characterization of protein fouling on membranes: opportunities and challenges", *Journal of Membrane Science,* vol. 242, no. 1-2, pp. 169-188.

Chapman, R.G., Ostuni, E., Takayama, S., Holmlin, R.E., Yan, L. & Whitesides, G.M. 2000, "Surveying for Surfaces that Resist the Adsorption of Proteins", *Journal of the American Chemical Society,* vol. 122, no. 34, pp. 8303-8304.

Choi, S., Yang, Y. & Chae, J. 2008, "Surface plasmon resonance protein sensor using Vroman effect", *Biosensors and Bioelectronics,* vol. 24, no. 4, pp. 893-899.

Clark, S.R., Billsten, P. & Elwing, H. 1994, "A fluorescence technique for investigating protein adsorption phenomena at a colloidal silica surface", *Colloids and Surfaces B: Biointerfaces,* vol. 2, no. 5, pp. 457-461.

Cooper, M.A. 2002, "Optical biosensors in drug discovery", *Nat Rev Drug Discov,* vol. 1, no. 7, pp. 515-528.

Cornec, M. & Narsimhan, G. 1998, "Effect of Contaminant on Adsorption of Whey Proteins at the Airâ^'Water Interface", *Journal of Agricultural and Food Chemistry,* vol. 46, no. 7, pp. 2490-2498.

Creamer, L.K. 1995, "Effect of Sodium Dodecyl Sulfate and Palmitic Acid on the Equilibrium Unfolding of Bovine .beta.-Lactoglobulin", *Biochemistry,* vol. 34, no. 21, pp. 7170-7176.

Cuypers, P.A., Weillems, G.M., Hemker, H.C. & Hermens, W.T. 1987, "Adsorption Kinetics of Protein Mixtures A Tentative Explanation of the Vroman Effect", *Annals of the New York Academy of Sciences,* vol. 516, no. 1, pp. 244-252.

Dall'Acqua, W., Goldman, E.R., Eisenstein, E. & Mariuzza, R.A. 1996, "A Mutational Analysis of the Binding of Two Different Proteins to the Same Antibody", *Biochemistry,* vol. 35, no. 30, pp. 9667-9676.

Daly, S.M., Przybycien, T.M. & Tilton, R.D. 2003, "Coverage-Dependent Orientation of Lysozyme Adsorbed on Silica", *Langmuir,* vol. 19, no. 9, pp. 3848-3857.

Day, Y.S. & Myszka, D.G. 2003, "Characterizing a drug's primary binding site on albumin", *Journal of pharmaceutical sciences,* vol. 92, no. 2, pp. 333-343.

de Bruijn, H.E., Altenburg, B.S.F., Kooyman, R.P.H. & Greve, J. 1991, "Determination of thickness and dielectric constant of thin transparent dielectric layers using surface plasmon resonance", *Optics Communications,* vol. 82, no. 5-6, pp. 425-432.

Dickinson, E. & Galazka, V.B. 1991, "Emulsion stabilization by ionic and covalent complexes of [beta]-lactoglobulin with polysaccharides", *Food Hydrocolloids,* vol. 5, no. 3, pp. 281-296.

Dijksma, M., Kamp, B., Hoogvliet, J.C. & Van Bennekom, W.P. 2000, "Formation and electrochemical characterization of self-assembled monolayers of thioctic acid on

polycrystalline gold electrodes in phosphate buffer pH 7.4", *Langmuir*, vol. 16, no. 8, pp. 3852-3857.

Dixon, M.C. 2008, "Quartz crystal microbalance with dissipation monitoring: enabling real-time characterization of biological materials and their interactions", *Journal of biomolecular techniques*, vol. 19, no. 3, pp. 151.

Dufour, E. & Haertlé, T. 1990, "Alcohol-induced changes of β-lactoglobulin - retinol-binding stoichiometry", *Protein engineering*, vol. 4, no. 2, pp. 185-190.

Elshereef, R., Budman, H., Moresoli, C. & Legge, R.L. 2010, "Probing protein colloidal behavior in membrane-based separation processes using spectrofluorometric Rayleigh scattering data", *Biotechnology progress*, .

Elshereef, R., Budman, H., Moresoli, C. & Legge, R.L. 2006, "Fluorescence spectroscopy as a tool for monitoring solubility and aggregation behavior of beta-lactoglobulin after heat treatment", *Biotechnology and bioengineering*, vol. 95, no. 5, pp. 863-874.

Eustis, S. & El-Sayed, M. 2006, "Why gold nanoparticles are more precious than pretty gold: Noble metal surface plasmon resonance and its enhancement of the radiative and nonradiative properties of nanocrystals of different shapes", *Chemical Society Reviews*, vol. 35, no. 3, pp. 209-217.

Euston, S.R., Finnigan, S.R. & Hirst, R.L. 2000, "Aggregation kinetics of heated whey protein-stabilized emulsions", *Food Hydrocolloids*, vol. 14, no. 2, pp. 155-161.

Fernández, C. & Minton, A.P. 2009, *Static Light Scattering From Concentrated Protein Solutions II: Experimental Test of Theory for Protein Mixtures and Weakly Self-Associating Proteins*, Cell Press.

Fiksdal, L. & Leiknes, T. 2006, "The effect of coagulation with MF/UF membrane filtration for the removal of virus in drinking water", *Journal of Membrane Science*, vol. 279, no. 1-2, pp. 364-371.

Floris, R., Bodnár, I., Weinbreck, F. & Alting, A.C. 2008, "Dynamic rearrangement of disulfide bridges influences solubility of whey protein coatings", *International Dairy Journal*, vol. 18, no. 5, pp. 566-573.

Frapin, D., Dufour, E. & Haertle, T. 1993, "Probing the fatty acid binding site of beta-lactoglobulins", *Journal of protein chemistry*, vol. 12, no. 4, pp. 443-449.

Frederix, F., Bonroy, K., Reekmans, G., Laureyn, W., Campitelli, A., Abramov, M.A., Dehaen, W. & Maes, G. 2004, "Reduced nonspecific adsorption on covalently immobilized protein surfaces using poly(ethylene oxide) containing blocking agents", *Journal of Biochemical and Biophysical Methods*, vol. 58, no. 1, pp. 67-74.

Ganesh, V., Pal, S.K., Kumar, S. & Lakshminarayanan, V. 2006, "Self-assembled monolayers (SAMs) of alkoxycyanobiphenyl thiols on gold--A study of electron transfer reaction using cyclic voltammetry and electrochemical impedance spectroscopy", *Journal of colloid and interface science*, vol. 296, no. 1, pp. 195-203.

Gezimati, J., Creamer, L.K. & Singh, H. 1997, "Heat-Induced Interactions and Gelation of Mixtures of beta-Lactoglobulin and alpha-Lactalbumin", *Journal of Agricultural and Food Chemistry*, vol. 45, no. 4, pp. 1130-1136.

Ghirlando, R. 2011, "The analysis of macromolecular interactions by sedimentation equilibrium", *Methods*, vol. 54, no. 1, pp. 145-156.

Gottschalk, M., Nilsson, H., Roos, H. & Halle, B. 2003, "Protein self-association in solution: The bovine beta-lactoglobulin dimer and octamer", *Protein Science*, vol. 12, no. 11, pp. 2404-2411.

Guo, L., Facci, J.S., McLendon, G. & Mosher, R. 1994, "Effect of Gold Topography and Surface Pretreatment on the Self-Assembly of Alkanethiol Monolayers", *Langmuir*, vol. 10, no. 12, pp. 4588-4593.

Hamada, D. & Dobson, C.M. 2002, "A kinetic study of beta-lactoglobulin amyloid fibril formation promoted by urea", *Protein Science*, vol. 11, no. 10, pp. 2417-2426.

Hambling, S.G., McAlpine, A.S. & Sawyer, L. 1992, "Advanced Dairy Chemistry: Proteins" in , ed. P. F. Fox, Elsevier Applied Science, London.

Hanemaaijer, J.H., Robbertsen, T., van, d.B. & Gunnink, J.W. 1989, "Fouling of ultrafiltration membranes. The role of protein adsorption and salt precipitation", *Journal of Membrane Science*, vol. 40, no. 2, pp. 199-217.

Hanlon, A.D., Larkin, M.I. & Reddick, R.M. 2010, "Free-Solution, Label-Free Protein-Protein Interactions Characterized by Dynamic Light Scattering", *Biophysical journal*, vol. 98, no. 2, pp. 297-304.

Hartvig, R.A., an de Weert, M., Østergaard, J., Jorgensen, L. & Jensen, H. 2011, "Protein Adsorption at Charged Surfaces: The Role of Electrostatic Interactions and Interfacial Charge Regulation", *Langmuir*, vol. 27, no. 6, pp. 2634-2643.

Heise, H. 2008, "Solid-State NMR Spectroscopy of Amyloid Proteins", *ChemBioChem*, vol. 9, no. 2, pp. 179-189.

Hodneland, C.D., Lee, Y., Min, D. & Mrksich, M. 2002, "Selective immobilization of proteins to self-assembled monolayers presenting active site-directed capture ligands", *Proceedings of the National Academy of Sciences*, vol. 99, no. 8, pp. 5048-5052.

Homola, J. 2008, "Surface Plasmon Resonance Sensors for Detection of Chemical and Biological Species", *Chemical reviews*, vol. 108, no. 2, pp. 462-493.

Ishida, T., Tsuneda, S., Nishida, N., Hara, M., Sasabe, H. & Knoll, W. 1997, "Surface-Conditioning Effect of Gold Substrates on Octadecanethiol Self-Assembled Monolayer Growth", *Langmuir*, vol. 13, no. 17, pp. 4638-4643.

Jacquemart, R., Chavane, N., Durocher, Y., Hoemann, C., De Crescenzo, G. & Jolicoeur, M. 2008, "At-line monitoring of bioreactor protein production by surface plasmon resonance", *Biotechnology and bioengineering*, vol. 100, no. 1, pp. 184-188.

Jermann, D., Pronk, W., Kägi, R., Halbeisen, M. & Boller, M. 2008, " Influence of interactions between NOM and particles on UF fouling mechanisms", *Water Research*, vol. 42, no. 14, pp. 3870-3878.

Jermann, D., Pronk, W., Meylan, S. & Boller, M. 2007, "Interplay of different NOM fouling mechanisms during ultrafiltration for drinking water production", *Water research*, vol. 41, no. 8, pp. 1713-1722.

Johnsson, L., Baxter, G.A., Crooks, S.R.H., Brandon, D.L. & Elliott, C.T. 2002, "Reduction of Sample Matrix Effects - The Analysis of Benzimidazole Residues in Serum by Immunobiosensor", *Food and Agricultural Immunology*, vol. 14, no. 3, pp. 209-216.

Kausaite-Minkstimiene, A., Ramanaviciene, A., Kirlyte, J. & Ramanavicius, A. 2010, "Comparative Study of Random and Oriented Antibody Immobilization Techniques on the Binding Capacity of Immunosensor", *Analytical Chemistry*, vol. 82, no. 15, pp. 6401-6408.

Kontopidis, G., Holt, C. & Sawyer, L. 2004, "Invited Review: {beta}-Lactoglobulin: Binding Properties, Structure, and Function", *Journal of dairy science*, vol. 87, no. 4, pp. 785-796.

Konuma, T., Sakurai, K. & Goto, Y. 2007, "Promiscuous Binding of Ligands by β-Lactoglobulin Involves Hydrophobic Interactions and Plasticity", *Journal of Molecular Biology*, vol. 368, no. 1, pp. 209-218.

Köβlinger, C., Uttenthaler, E., Drost, S., Aberl, F., Wolf, H., Brink, G., Stanglmaier, A. & Sackmann, E. 1995, "Comparison of the QCM and the SPR method for surface studies and immunological applications", *Sensors and Actuators B: Chemical,* vol. 24, no. 1-3, pp. 107-112.

Kretschmann, E. & Raether, H. 1968, "Radiative decay of non radiative surface plasmons excited by light (Surface plasma waves excitation by light and decay into photons applied to nonradiative modes) ", vol. 23A, pp. 2135.

Lalande, M. & Tissier, J. 1985, "Fouling of Heat Transfer Surfaces Related to beta-Lactoglobulin Denaturation During Heat Processing of Milk", *Biotechnology progress,* vol. 1, no. 2, pp. 131-139.

LeDuc, C.A., Vroman, L. & Leonard, E.F. 1995, "A Mathematical Model for the Vroman Effect", *Industrial & Engineering Chemistry Research,* vol. 34, no. 10, pp. 3488-3495.

Lee, B., Hong, D., Lee, S. & Kuboi, R. 2004, "Analysis of protein back-extraction processes in alcohol- and carboxylic acid-mediated AOT reverse micellar systems based on structural changes of proteins and reverse micelles", *Biochemical engineering journal,* vol. 22, no. 1, pp. 71-79.

Lee, B., Shimanouchi, T., Umakoshi, H. & Kuboi, R. 2006, "Evaluation of carboxylic acid-induced conformational transitions of [beta]-lactoglobulin: Comparison of the alcohol effects on [beta]-lactoglobulin", *Biochemical engineering journal,* vol. 28, no. 1, pp. 79-86.

Lee, D.N. & Merson, R.L. 1975, "Examination of Cottage Cheese Whey Proteins by Scanning Electron Microscopy: Relationship to Membrane Fouling during Ultrafiltration", *Journal of dairy science,* vol. 58, no. 10, pp. 1423-1432.

Lee, N., Amy, G. & Croué, J. 2006, "Low-pressure membrane (MF/UF) fouling associated with allochthonous versus autochthonous natural organic matter", *Water research,* vol. 40, no. 12, pp. 2357-2368.

Liu, G., Wu, Z. & Craig, V.S.J. 2008, "Cleaning of Protein-Coated Surfaces Using Nanobubbles: An Investigation Using a Quartz Crystal Microbalance", *The Journal of Physical Chemistry C,* vol. 112, no. 43, pp. 16748-16753.

Luey, J., McGuire, J. & Sproull, R.D. 1991, "The effect of pH and NaCl concentration on adsorption of β-lactoglobulin at hydrophilic and hydrophobic silicon surfaces", *Journal of colloid and interface science,* vol. 143, no. 2, pp. 489-500.

Mackie, A.R., Husband, F.A., Holt, C. & Wilde, P.J. 1999, "Adsorption of beta-Lactoglobulin variants A and B to the air-water interface", *International Journal of Food Science & Technology,* vol. 34, no. 5-6, pp. 509-516.

Majhi, P.R. & Ganta, R.R. 2006, "Electrostatically Driven Protein Aggregation: β-Lactoglobulin at Low Ionic Strength", *Langmuir,* vol. 22, no. 22, pp. 9150-9159.

Majhi, P.R., Ganta, R.R., Vanam, R.P., Seyrek, E., Giger, K. & Dubin, P.L. 2006, "Electrostatically Driven Protein Aggregation: β-Lactoglobulin at Low Ionic Strength", *Langmuir,* vol. 22, no. 22, pp. 9150-9159.

Marshall, A.D., Munro, P.A. & Tragardh, G. 1997, "Influence of permeate flux on fouling during the microfiltration of [beta]-lactoglobulin solutions under cross-flow conditions", *Journal of Membrane Science,* vol. 130, no. 1-2, pp. 23-30.

Masson, J., Battaglia, T.M., Cramer, J., Beaudoin, S., Sierks, M. & Booksh, K.S. 2006, "Reduction of nonspecific protein binding on surface plasmon resonance biosensors", *Analytical and Bioanalytical Chemistry,* vol. 386, no. 7-8, pp. 1951-1959.

Mateo, C., Fernández-Lorente, G., Abian, O., Fernández-Lafuente, R. & Guisán, J.M. 2000, "Multifunctional Epoxy Supports: A New Tool To Improve the Covalent Immobilization of Proteins. The Promotion of Physical Adsorptions of Proteins on the Supports before Their Covalent Linkage", *Biomacromolecules,* vol. 1, no. 4, pp. 739-745.

Matsubara, K., Kawata, S. & Minami, S. 1988, "A Compact Surface Plasmon Resonance Sensor for Measurement of Water in Process", *Applied Spectroscopy,* vol. 42, no. 8, pp. 1375-1379.

Mauriz, E., Calle, A., Manclús, J.J., Montoya, A., Hildebrandt, A., Barceló, D. & Lechuga, L.M. 2007, "Optical immunosensor for fast and sensitive detection of DDT and related compounds in river water samples", *Biosensors and Bioelectronics,* vol. 22, no. 7, pp. 1410-1418.

McWhirter, A., Wahlstrom, L., de Mol, N.J. & Fischer, M. 2008, *Handbook of Surface Plasmon Resonance,* The Royal Society of Chemistry.

Meléndez, J., Carr, R., Bartholomew, D., Taneja, H., Yee, S., Jung, C. & Furlong, C. 1997, "Development of a surface plasmon resonance sensor for commercial applications", *Sensors and Actuators, B: Chemical,* vol. 39, no. 1-3, pp. 375-379.

Melendez, J., Carr, R., Bartholomew, D.U., Kukanskis, K., Elkind, J., Yee, S., Furlong, C. & Woodbury, R. 1996, "A commercial solution for surface plasmon sensing", *Sensors and Actuators, B: Chemical,* vol. 35, no. 1-3, pp. 212-216.

Meynier, A., Rampon, V., Dalgalarrondo, M. & Genot, C. 2004, "Hexanal and t-2-hexenal form covalent bonds with whey proteins and sodium caseinate in aqueous solution", *International Dairy Journal,* vol. 14, no. 8, pp. 681-690.

Mills, O.E. & Creamer, L.K. 1975, "A conformational change in bovine β-lactoglobulin at low pH", *Biochimica et Biophysica Acta (BBA) - Protein Structure,* vol. 379, no. 2, pp. 618-626.

Minton, A.P. 2001, "Effects of Excluded Surface Area and Adsorbate Clustering on Surface Adsorption of Proteins. II. Kinetic Models", *Biophysical journal,* vol. 80, no. 4, pp. 1641-1648.

Mousavi, S.H., Chobert, J., Bordbar, A. & Haertle • aertleHaer & Haer& Haer & Haer. & Haer & Haer II. Kinetic Models", Models", on Surface Adsor*Journal of Agricultural and Food Chemistry,* vol. 56, no. 18, pp. 8680-8684.

Mulvihill, D.M. & Donovan, M. 1987, "Whey Proteins and Their Thermal Denaturation - A Review", *Irish Journal of Food Science and Technology,* vol. 11, no. 1, pp. 43-75.

Muresan, S., van der Bent, A. & de Wolf, F.A. 2001, "Interaction of [beta]-Lactoglobulin with Small Hydrophobic Ligands As Monitored by Fluorometry and Equilibrium Dialysis: Nonlinear Quenching Effects Related to Protein-Protein Association", *Journal of Agricultural and Food Chemistry,* vol. 49, no. 5, pp. 2609-2618.

Murray, B.S. & Cros, L. 1998, "Adsorption of [beta]-lactoglobulin and [beta]-casein to metal surfaces and their removal by a non-ionic surfactant, as monitored via a quartz crystal microbalance", *Colloids and Surfaces B: Biointerfaces,* vol. 10, no. 4, pp. 227-241.

Myszka, D.G. & Rich, R.L. 2000, "Implementing surface plasmon resonance biosensors in drug discovery", *Pharmaceutical science & technology today,* vol. 3, no. 9, pp. 310-317.

Nakatani, K., Kobori, A., Kumasawa, H., Goto, Y. & Saito, I. 2004, "The binding of guanine–guanine mismatched DNA to naphthyridine dimer immobilized sensor surfaces: kinetic aspects", *Bioorganic & medicinal chemistry,* vol. 12, no. 12, pp. 3117-3123.

Narayan, M. & Berliner, L. 1998, "Mapping fatty acid binding to beta-lactoglobulin: Ligand binding is restricted by modification of Cys 121", *Protein Sci,* vol. 7, no. 1, pp. 150-157.

Naujok, R.R., Duevel, R.V. & Corn, R.M. 1993, "Fluorescence and Fourier Transform surface-enhanced Raman scattering measurements of methylene blue adsorbed onto a sulfur-modified gold electrode", *Langmuir,* vol. 9, no. 7, pp. 1771-1774.

Norde, W. 2008, "My voyage of discovery to proteins in flatland …and beyond", *Colloids and Surfaces B: Biointerfaces,* vol. 61, no. 1, pp. 1-9.

O'Brien II, M.J., Brueck, S.R.J., Perez-Luna, V.H., Tender, L.M. & Lopez, G.P. 1999, "SPR biosensors: simultaneously removing thermal and bulk-composition effects", *Biosensors and Bioelectronics,* vol. 14, no. 2, pp. 145-154.

O'Neill, T.E. & Kinsella, J.E. 1987, "Binding of alkanone flavors to .beta.-lactoglobulin: effects of conformational and chemical modification", *Journal of Agricultural and Food Chemistry,* vol. 35, no. 5, pp. 770-774.

Oshannessy, D.J., Brighamburke, M., Soneson, K.K., Hensley, P. & Brooks, I. 1993, "Determination of Rate and Equilibrium Binding Constants for Macromolecular Interactions Using Surface Plasmon Resonance: Use of Nonlinear Least Squares Analysis Methods", *Analytical Biochemistry,* vol. 212, no. 2, pp. 457-468.

O'Sullivan, C.K. & Guilbault, G.G. 1999, "Commercial quartz crystal microbalances - theory and applications", *Biosensors and Bioelectronics,* vol. 14, no. 8-9, pp. 663-670.

P. Schaaf, J.T. 1989, "Surface Exclusion Effects in adsorption Processes", *The Journal of chemical physics,* vol. 91, no. 7.

Palecek, S.P. & Zydney, A.L. 1994, "Intermolecular electrostatic interactions and their effect on flux and protein deposition during protein filtration", *Biotechnology progress,* vol. 10, no. 2, pp. 207-213.

Patel, N., Davies, M.C., Hartshorne, M., Heaton, R.J., Roberts, C.J., Tendler, S.J.B. & Williams, P.M. 1997, "Immobilization of Protein Molecules onto Homogeneous and Mixed Carboxylate-Terminated Self-Assembled Monolayers", *Langmuir,* vol. 13, no. 24, pp. 6485-6490.

Peiris, B.R.H., Halle, C., Haberkamp, J., Legge, R.L., Peldszus, S., Moresoli, C., Budman, H., Amy, G., Jekel, M. & Huck, P.M. 2008, "Assessing nanofiltration fouling in drinking water treatment using fluorescence fingerprinting and LC-OCD analyses", *Water science and technology: water supply,* vol. 8, pp. 459-465.

Peiris, R.H., Budman, H., Moresoli, C. & Legge, R.L. 2011, "Development of a species specific fouling index using principal component analysis of fluorescence excitation-emission matrices for the ultrafiltration of natural water and drinking water production", *Journal of Membrane Science,* vol. 378, no. 1-2, pp. 257-264.

Peiris, R.H., Budman, H., Moresoli, C. & Legge, R.L. 2010a, "Understanding fouling behaviour of ultrafiltration membrane processes and natural water using principal component analysis of fluorescence excitation-emission matrices", *Journal of Membrane Science,* vol. 357, no. 1-2, pp. 62-72.

Peiris, R.H., Budman, H., Moresoli, C. & Legge, R.L. 2009, "Acquiring reproducible fluorescence spectra of dissolved organic matter at very low concentration", *Water science and technology,* vol. 60, pp. 1385-1392.

Peiris, R.H., Hallé, C., Budman, H., Moresoli, C., Peldszus, S., Huck, P.M. & Legge, R.L. 2010b, "Identifying fouling events in a membrane-based drinking water treatment process using principal component analysis of fluorescence excitation-emission matrices", *Water research,* vol. 44, no. 1, pp. 185-194.

Persson, B., Stenhag, K., Nilsson, P., Larsson, A., Uhlén, M. & Nygren, P.-. 1997, "Analysis of oligonucleotide probe affinities using surface plasmon resonance: A means for mutational scanning", *Analytical Biochemistry,* vol. 246, no. 1, pp. 34-44.

Phillips, S.K. & Cheng, J.Q. 2008, "Surface Plasmon Resonance" in *Molecular Biomethods handbook*, eds. J.M. Walker & R.R. Rapley, 2nd Edition edn, Humana Press, Totowa, NJ, pp. 809.

Phizicky, E.M. & Fields, S. 1995, "Protein-protein interactions: methods for detection and analysis", *Microbiology and Molecular Biology Reviews,* vol. 59, no. 1, pp. 94-123.

Qi , X.L., Holt, C., McNulty, D., Clarke, D.T., Brownlow, S. & Jones, G.R. 1997, "Effect of temperature on the secondary structure of beta-lactoglobulin at pH 6.7, as determined by CD and IR spectroscopy: a test of the molten globule hypothesis.", *Biochemical Journal,* vol. 324, no. 1, pp. 341-346.

Rabe, M., Verdes, D., Rankl, M., Artus, G.R.J. & Seeger, S. 2007, "A Comprehensive Study of Concepts and Phenomena of the Nonspecific Adsorption of [beta]-Lactoglobulin", *ChemPhysChem,* vol. 8, no. 6, pp. 862-872.

Rabe, M., Verdes, D. & Seeger, S. 2011, "Understanding protein adsorption phenomena at solid surfaces", *Advances in Colloid and Interface Science,* vol. 162, no. 1-2, pp. 87-106.

Ragona, L., Fogolari, F., Zetta, L., Pérez, D.M., Puyol, P., De, K.,Kees, LÖhr, F., RÜterjans, H. & Molinari, H. 2000, "Bovine [beta]-lactoglobulin: Interaction studies with palmitic acid", *PRS,* vol. 9, no. 07, pp. 1347-1356.

Raiber, K., Terfort, A., Benndorf, C., Krings, N. & Strehblow, H. 2005, "Removal of self-assembled monolayers of alkanethiolates on gold by plasma cleaning", *Surface Science,* vol. 595, no. 1-3, pp. 56-63.

Reddy, T.T., Lavenant, L., Lefebvre, J. & Renard, D. 2006, "Swelling Behavior and Controlled Release of Theophylline and Sulfamethoxazole Drugs in beta-Lactoglobulin Protein Gels Obtained by Phase Separation in Water/Ethanol Mixture", *Biomacromolecules,* vol. 7, no. 1, pp. 323-330.

Rippner Blomqvist, B., Ridout, M.J., Mackie, A.R., Wärnheim, T., Claesson, P.M. & Wilde, P. 2004, "Disruption of Viscoelastic beta-Lactoglobulin Surface Layers at the Air-'Water Interface by Nonionic Polymeric Surfactants", *Langmuir,* vol. 20, no. 23, pp. 10150-10158.

Roach, P., Farrar, D. & Perry, C.C. 2005, "Interpretation of Protein Adsorption:Surface-Induced Conformational Changes", *Journal of the American Chemical Society,* vol. 127, no. 22, pp. 8168-8173.

Ron, H., Matlis, S. & Rubinstein, I. 1998, "Self-Assembled Monolayers on Oxidized Metals. 2. Gold Surface Oxidative Pretreatment, Monolayer Properties, and Depression Formation", *Langmuir,* vol. 14, no. 5, pp. 1116-1121.

Sakurai, K. & Goto, Y. 2002, "Manipulating Monomer-Dimer Equilibrium of Bovine beta-Lactoglobulin by Amino Acid Substitution", *Journal of Biological Chemistry,* vol. 277, no. 28, pp. 25735-25740.

Sakurai, K., Oobatake, M. & Goto, Y. 2001, "Salt-dependent monomer-dimer equilibrium of bovine beta-lactoglobulin at pH 3", *Protein Science,* vol. 10, no. 11, pp. 2325-2335.

Samanta, D. & Sarkar, A. 2011, "Immobilization of bio-macromolecules on self-assembled monolayers: methods and sensor applications", *Chemical Society Reviews,* vol. 40, no. 5, pp. 2567-2592.

Saravia, F., Zwiener, C. & Frimmel, F.H. 2006, "Interactions between membrane surface, dissolved organic substances and ions in submerged membrane filtration", *Desalination,* vol. 192, no. 1-3, pp. 280-287.

Schoenfisch, M.H. & Pemberton, J.E. 1998, "Air Stability of Alkanethiol Self-Assembled Monolayers on Silver and Gold Surfaces", *Journal of the American Chemical Society,* vol. 120, no. 18, pp. 4502-4513.

Schokker, E.P., Singh, H., Pinder, D.N., Norris, G.E. & Creamer, L.K. 1999, "Characterization of intermediates formed during heat-induced aggregation of [beta]-lactoglobulin AB at neutral pH", *International Dairy Journal,* vol. 9, no. 11, pp. 791-800.

Schreiber, F. 2004, "Self-assembled monolayers: from 'simple' model systems to biofunctionalized interfaces", *Journal of Physics: Condensed Matter,* vol. 16, no. 28, pp. R881.

Schreiber, F. 2000, "Structure and growth of self-assembling monolayers", *Progress in Surface Science,* vol. 65, no. 5-8, pp. 151-257.

Schurr, M. & Bloomfield, V. 1977, "Dynamic Light Scattering Of Biopolymers And Biocolloid", *Critical reviews in biochemistry and molecular biology,* vol. 4, no. 4, pp. 371-431.

Shan, X., Patel, U., Wang, S., Iglesias, R. & Tao, N. 2010, "Imaging Local Electrochemical Current via Surface Plasmon Resonance", *Science,* vol. 327, no. 5971, pp. 1363-1366.

Shen, C. & Lin, J. 2011, "Improving the Surface Biocompatibility with the Use of Mixed Zwitterionic Self-Assembled Monolayers Prepared by a Proper Solvent", *Langmuir,* vol. 27, no. 11, pp. 7091-7098.

Shimomura, M., Nomura, Y., Zhang, W., Sakino, M., Lee, K.-., Ikebukuro, K. & Karube, I. 2001, "Simple and rapid detection method using surface plasmon resonance for dioxins, polychlorinated biphenylx and atrazine", *Analytica Chimica Acta,* vol. 434, no. 2, pp. 223-230.

Sigal, G.B., Mrksich, M. & Whitesides, G.M. 1997, "Using Surface Plasmon Resonance Spectroscopy To Measure the Association of Detergents with Self-Assembled Monolayers of Hexadecanethiolate on Gold", *Langmuir,* vol. 13, no. 10, pp. 2749-2755.

Silin, V., Weetall, H. & Vanderah, D.J. 1997, "SPR Studies of the Nonspecific Adsorption Kinetics of Human IgG and BSA on Gold Surfaces Modified by Self-Assembled Monolayers (SAMs)", *Journal of colloid and interface science,* vol. 185, no. 1, pp. 94-103.

Silva, R.A., UrzuÌ • a, M.D., Petri, D.F.S. & Dubin, P.L. 2010, "Protein Adsorption onto Polyelectrolyte Layers: Effects of Protein Hydrophobicity and Charge Anisotropy", *Langmuir,* vol. 26, no. 17, pp. 14032-14038.

Singh, A.K., Rai, A.K. & Bicanic, D. 2009, "Controlled Synthesis and Optical Properties of Pure Gold Nanoparticles", *Instrumentation Science & Technology,* vol. 37, no. 1, pp. 50-60.

Snopok, B.A. & Kostyukevich, E.V. 2006, "Kinetic studies of protein–surface interactions: A two-stage model of surface-induced protein transitions in adsorbed biofilms", *Analytical Biochemistry,* vol. 348, no. 2, pp. 222-231.

Sota, H., Hasegawa, Y. & Iwakura, M. 1998, "Detection of Conformational Changes in an Immobilized Protein Using Surface Plasmon Resonance", *Analytical Chemistry,* vol. 70, no. 10, pp. 2019-2024.

Stenberg, E., Persson, B., Roos, H. & Urbaniczky, C. 1991, "Quantitative determination of surface concentration of protein with surface plasmon resonance using radiolabeled proteins", *Journal of colloid and interface science,* vol. 143, no. 2, pp. 513-526.

Stevens, R.C., Soelberg, S.D., Near, S. & Furlong, C.E. 2008, "Detection of cortisol in saliva with a flow-filtered, portable surface plasmon resonance biosensor system", *Analytical Chemistry*, vol. 80, no. 17, pp. 6747-6751.

Susanto, H., Arafat, H., Janssen, E.M.L. & Ulbricht, M. 2008, "Ultrafiltration of polysaccharide-protein mixtures: Elucidation of fouling mechanisms and fouling control by membrane surface modification", *Separation and Purification Technology*, vol. 63, no. 3, pp. 558-565.

Takeuchi, K. & Wagner, G. 2006, "NMR studies of protein interactions", *Current opinion in structural biology*, vol. 16, no. 1, pp. 109-117.

Tassa, C., Duffner, J.L., Lewis, T.A., Weissleder, R., Schreiber, S.L., Koehler, A.N. & Shaw, S.Y. 2010, "Binding Affinity and Kinetic Analysis of Targeted Small Molecule-Modified Nanoparticles", *Bioconjugate chemistry*, vol. 21, no. 1, pp. 14-19.

Tie, Y., Calonder, C. & Van Tassel, P.R. 2003, "Protein adsorption: Kinetics and history dependence", *Journal of colloid and interface science*, vol. 268, no. 1, pp. 1-11.

Timasheff, S.N. & Townend, R. 1961, "Molecular Interactions in beta-Lactoglobulin. V. the Association of the Genetic Species of beta-Lactoglobulin below the Isoelectric Point2", *Journal of the American Chemical Society*, vol. 83, no. 2, pp. 464-469.

Townend, R. & Timasheff, S.N. 1960, "Molecular Interactions in beta-Lactoglobulin. III. Light Scattering Investigation of the Stoichiometry of the Association between pH 3.7 and 5.22", *Journal of the American Chemical Society*, vol. 82, no. 12, pp. 3168-3174.

Ulman, A. 1996, "Formation and Structure of Self-Assembled Monolayers", *Chemical reviews*, vol. 96, no. 4, pp. 1533-1554.

Vetri, V. & Militello, V. 2005, "Thermal induced conformational changes involved in the aggregation pathways of beta-lactoglobulin", *Biophysical chemistry*, vol. 113, no. 1, pp. 83-91.

Wahlgren, M. & Elofsson, U. 1997, "Simple Models for Adsorption Kinetics and Their Correlation to the Adsorption of β-Lactoglobulin A and B", *Journal of colloid and interface science*, vol. 188, no. 1, pp. 121-129.

Wang, Q. & Swaisgood, H.E. 1993, "Characteristics of {beta}-Lactoglobulin Binding to the All-Trans-Retinal Moiety Covalently Immobilized on CeliteTM", *Journal of dairy science*, vol. 76, no. 7, pp. 1895-1901.

Willey, T.M., Vance, A.L., van Buuren, T., Bostedt, C., Terminello, L.J. & Fadley, C.S. 2005, "Rapid degradation of alkanethiol-based self-assembled monolayers on gold in ambient laboratory conditions", *Surface Science*, vol. 576, no. 1-3, pp. 188-196.

Wu, S., Pérez, M.D., Puyol, P. & Sawyer, L. 1999, "β-Lactoglobulin Binds Palmitate within Its Central Cavity", *Journal of Biological Chemistry*, vol. 274, no. 1, pp. 170-174.

Zhang, S. 2003, "Fabrication of novel biomaterials through molecular self-assembly", *Nat Biotech*, vol. 21, no. 10, pp. 1171-1178.

Zhang, X., Ge, N. & Keiderling, T.A. 2007, "Electrostatic and Hydrophobic Interactions Governing the Interaction and Binding of β-Lactoglobulin to Membranes", *Biochemistry*, vol. 46, no. 17, pp. 5252-5260.

Zimmerman, J.K., Barlow, G.H. & Klotz, I.M. 1970, "Dissociation of [beta]-lactoglobulin near neutral pH", *Archives of Biochemistry and Biophysics*, vol. 138, no. 1, pp. 101-109.

Zydney, A.L. 1998, "Protein Separations Using Membrane Filtration: New Opportunities for Whey Fractionation", *International Dairy Journal*, vol. 8, no. 3, pp. 243-250.

# Appendix A. Chapter 4: Statistics

The dissociation experiments were conducted as describe (see Chapter 3 & 4). A summary of the results analysed using Yates method (Box *et al.* 1978) is presented in Table B.1. The error was estimated from averaging of the variances of the replicates. The response value utilized was the final value after 120 seconds of dissociation normalized by the maximum association of the previous association run.

**Table A.1: Results from ANOVA analysis.**
**Estimated error of $1x10^{-4}$ (16 df) and $F_{crit,\ (1\ ,16,0.01)}$=6.36. Insignificant (F less than $F_{crit}$) are highlighted with a (*).**

| Factors | Effect | SS | df | MS | F |
|---|---|---|---|---|---|
| **A** | 0.006539 | 0.000342102 | 1 | 0.000342102 | 1.069931 |
| **B** | -0.03233 | 0.008360986 | 1 | 0.008360986 | 26.14917 |
| **C*** | -0.01461 | 0.001707846 | 1 | 0.001707846 | 5.341327 |
| **D** | -0.03741 | 0.011196535 | 1 | 0.011196535 | 35.01742 |
| | | | | | |
| **AB*** | 0.028572 | 0.006530799 | 1 | 0.006530799 | 20.42522 |
| **AC*** | 0.027724 | 0.006148803 | 1 | 0.006148803 | 19.23052 |
| **AD*** | -0.00548 | 0.000240282 | 1 | 0.000240282 | 0.751488 |
| **BC** | 0.025047 | 0.005018932 | 1 | 0.005018932 | 15.69682 |
| **BD** | 0.016855 | 0.002272595 | 1 | 0.002272595 | 7.107594 |
| **CD*** | 0.001907 | 2.90975E-05 | 1 | 2.90975E-05 | 0.091003 |
| **ABC*** | -0.02663 | 0.005672287 | 1 | 0.005672287 | 17.74021 |
| **ABD** | 0.037366 | 0.011169748 | 1 | 0.011169748 | 34.93364 |
| **ACD** | -0.00548 | 0.000240282 | 1 | 0.000240282 | 0.751488 |
| **BCD** | -0.02021 | 0.003268023 | 1 | 0.003268023 | 10.22082 |
| **ABCD*** | -0.01443 | 0.001665115 | 1 | 0.001665115 | 5.207686 |

Table B.1 was utilized to fit a linear model given by Equation 1B which provided predictions of the concentrations on the SAM after a dissociation event.

$$Y = AVG + Ax_1 + Bx_2 + Dx_4 + BCx_2x_3 + BDx_2x_4 + ABD\ x_1\ x_2\ x_4 + ACD\ x_1x_3x_4 + BCDx_2x_3x_4 \quad (1B)$$

Where Y was the predicted normalized dissociation; AVG was the average between all replicates; A, B, D, BD, ABD, ACD, BCD correspond to half the effect seen in Table 5.1; and

$x_1$, $x_2$, $x_3$, $x_4$ represent either a -1 or +1 and correspond to factors A, B, C, and D as presented in Table 4.1.

It was noted that factor C which relates to PA, was insignificant if analysed alone. Factor C appeared in several significant terms (BC, ACD, and BCD) and as a consequence, became significant when analysed with other factors. As discussed in Chapter 4, the effect of PA was considerable.

Only one three-order interaction was ruled out (ABC), demonstrating the complications involved when trying to analyse and predict protein adsorption phenomena in what might be considered a relatively simple system. In the recent literature, protein adsorption is considered to be a complicated process, especially when nonspecific adsorption is occurring (Rabe *et al.* 2011) which justifies a factorial approach to resolve significant factors and interactions.

# Appendix B. Chapter 5: Calculations

## C1. Monolayer Coverage Calculations

Utilizing the hydrodynamic radius of 2.48 nm for AL and assuming a circular footprint the surface area coverage was calculated using $A = \pi r^2$ (Branco *et al.* 2010). This assumption is fair given that when AL is sufficiently loaded on a surface there is no significant spreading (Norde 2008). The surface area covered by an individual protein is then 19.32 $nm^2$ . The approximate area being probed by the SPR interface is about 2 $mm^2$ which translates into approximately 1.03 x $10^{11}$ molecules of AL. Using Avogadro's number; this is equivalent to $1.7x10^{-13}$ moles of AL on the sensor surface. The molecular weight of AL is 14.2 kD or 14200 g $mol^{-1}$ (Barbana *et al.* 2006), or 2.42 ng of AL. Dividing this number by the SPR interface gives an approximate surface concentration of 1.21 ng $mm^{-2}$. According to the SPR manual (Autolab 2006), 1 ng $mm^{-2}$ results in 120 RU so the expected response for a monolayer of AL on the sensor surface is 145 RU.

## C2. Percentage Colloidal Calculations

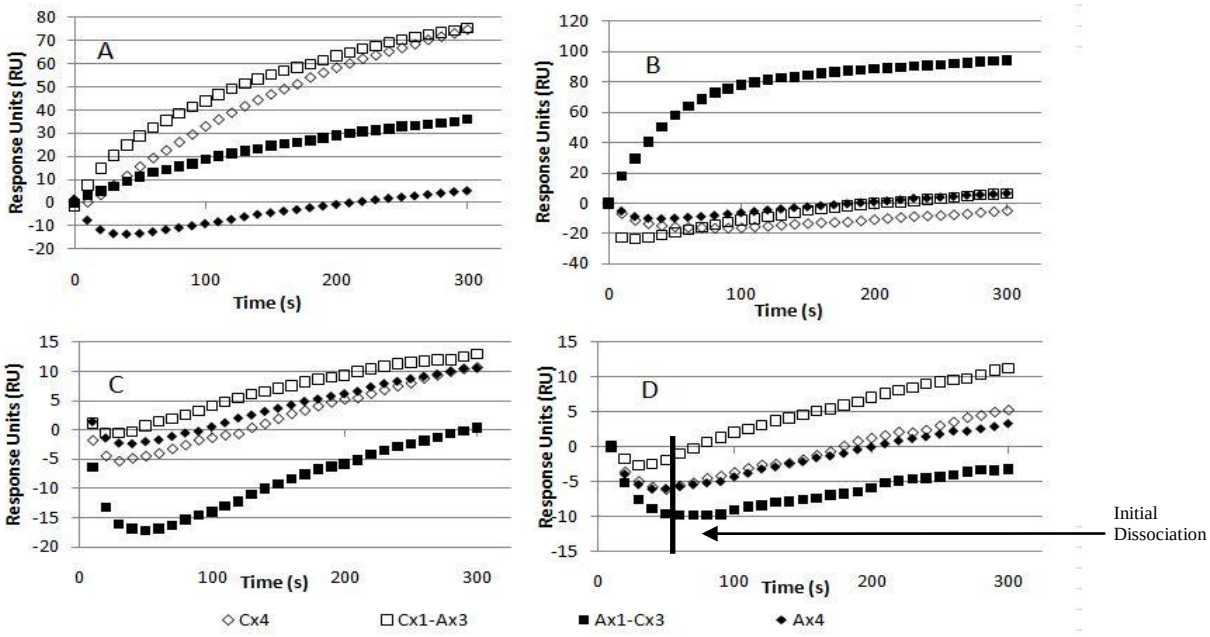


**Figure B.1 Results of the multiple injection experiments re-zeroed at the injection time.**

**This is opposed to the single baseline zero as presented in Fig. 5. The line in D shows an example of the initial dissociation discussed in the text.**

A downward trend or dissociation occurred during the first few seconds of association for many of the sensorgrams. This initial dissociation became much more apparent for later injections in the sequence (Figure C.1D). These changes are not attributed to temperature shifts, since the dips appeared during the latter stages of the experiment once there has been significant AL/CPP accumulation on the surface. The exact nature of these binding events is not clear, since there are multiple reasons that can cause these types of phenomena (Rabe *et al.* 2007, Rabe *et al.* 2011). Some may be due to protein re-arrangement on the surface, leading to altered kinetics, or some signals may be caused by matrix effects which occurred as more analytes accumulated on the surface. The matrix effects can contribute to false positives and false negatives on the sensorgram (Johnsson *et al.* 2002). The effects themselves are minor, but make quantitative analysis of the curves difficult.

To determine maximum loading, the difference between the final point of association and the baseline in Figure 5.5D was taken. Similarly, to determine "After Buffer Wash" the difference was taken between the final point of dissociation and the baseline in Figure 5.5E. To determine "Approximate % Colloidal" the difference was taken between the final point of association and the initial point of association for each run in Figure C.1A & D , and added together based on the component that was being injected. If any initial dissociation (see example in Figure C.1D) was present, the minimum of the initial dissociation was taken instead of the point at t = 0. Although this disregarded what occurred before the start of the minimum of the initial dissociation, it is difficult to precisely estimate the mass without having a dual channel machine. Equation 1C was used to calculate the "Percent Dissociation" column. The "Percent Dissociation" is due to protein desorbing from the surface as a result of the beginning of an actual dissociation phase, not to be confused with the ambiguous initial dissociation discussed earlier in this appendix.

$$Percent\ Dissociation = \frac{After\ Dissociatioon}{Maximum\ Association} \times 100\% \qquad (1C)$$

# Appendix C. Chapter 6: Initial Models and Parameter Estimations

## C1. Dimer Exchange Model

The dimer-exchange model was developed to be simple and reasonably describe the adsorption phenomenon (Wahlgren & Elofsson 1997). The main component of this model is the exchange of monomer and dimers on the surface as a result of the Vroman effect. The Vroman effect occurs in multi-component protein mixtures in which the surface first loads with the smallest molecular weight proteins which are eventually displaced by the larger proteins in the mixture (Cuypers *et al.* 1987). This effect has been studied in a multitude of protein systems (Choi *et al.* 2008).

The dimer exchange model and the associated fitting curves are presented below.

$$\frac{\partial \theta_{m,1}}{\partial t} = k_m^{on} \cdot C_m \cdot \Phi - k_{m,1-d} \cdot \theta_{m,1} \cdot C_d - k_{m,1-m,2} \cdot \theta_{m,1} \cdot C_d \quad (1D)$$

$$\frac{\partial \theta_{m,2}}{\partial t} = k_{m,1-m,2} \cdot \theta_{m,1} \cdot C_d - k_{m,2-d} \cdot \theta_{m,2} \cdot C_d - k_m^{off} \cdot \theta_{m,2} \quad (2D)$$

$$\frac{\partial \theta_d}{\partial t} = k_d^{on} \cdot C_d \cdot \Phi + k_{m,1-d} \cdot \theta_{m,1} \cdot C_d + k_{m,2-d} \cdot \theta_{m,2} \cdot C_d - k_d^{off} \cdot \theta_d \quad (3D)$$

$$\Phi = 1 - \frac{\theta_{total}}{\theta_{max}} \quad (4D)$$

$$\theta_{total} = \theta_d + \theta_{m,2} + \theta_{m,1} \quad (5D)$$

Where $\theta_{m,1}$ and $\theta_{m,2}$ are the surface concentration of two types of monomers, $\theta_d$ the dimer surface concentration, $\theta_{max}$ is the theoretical maximum surface concentration, $k_m^{on}$ is the monomer association parameter, $k_d^{on}$ is the dimer association constant, $k_{m,1-d}$ is monomer one to dimer exchange constant, $k_{m,2-d}$ is monomer two to dimer exchange constant, $k_{m,1-m,2}$ is the constant for the transition from *m*,1-monomer to *m*,2-monomer, $k_m^{off}$ is the monomer dissociation constant and $k_d^{off}$ is the dimer dissociation constant. $C_m$ and $C_d$ are the bulk solution monomer and dimer concentrations and do not change with time. To calculate $C_m$ and $C_d$, the monomer-dimer equilibrium constants were utilized (Wahlgren & Elofsson 1997).

$$C_m = 2 \cdot \left( -\frac{K_d}{8} + \sqrt{\left(\frac{K_d}{8}\right)^2 + \frac{K_d}{4} C_{tot}} \right) \quad (6D)$$

$$C_d = C_{tot} - \frac{C_m}{2} \quad (7D)$$

These authors also studied two BLG genetic variants separately and found that the kinetic constants differed by a factor of 7.9 (Wahlgren & Elofsson 1997). In this study, the BLG provided most probably contained the two genetic variants (Hambling *et al.* 1992) and were not separated or analysed individually.

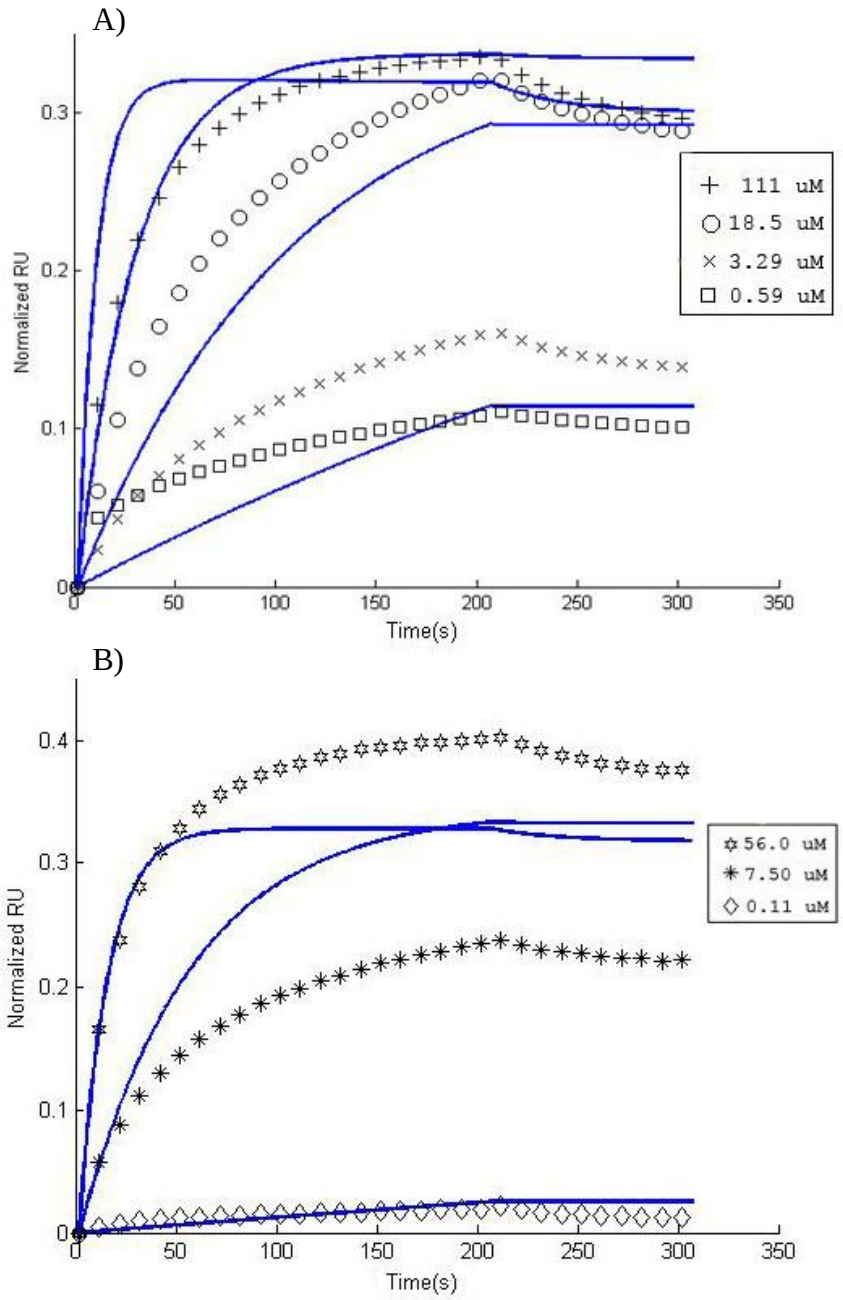


**Figure C.1 Dimer exchange model (lines) compared to experimental values (points).**

**A) First batch of experiments. B) Second batch of experiments. Values were normalised by dividing by 500.**

The dimer exchange model shows a fairly poor fit for both association and dissociation curves. Examining the model parameters presented in Table D.1, it appears that the second monomer was more tightly bound to the layer than the first, suggesting a conformational change once absorbed. This second monomer did not dissociate as readily as the dimer did once on the

surface. It appears that overall the dimer has a much lower affinity for the surface than the monomer, as expected (Wahlgren & Elofsson 1997).

**Table C.1: Constants for dimer-exchange model**

| Constants | Value | Units |
|---|---|---|
| $k_m^{on}$ | 469.3 | $M^{-1}s^{-1}$ |
| $k_{m,1-d}$ | 9.99 | $M^{-1}s^{-1}$ |
| $k_{m,1-m,2}$ | 16.18 | $M^{-1}s^{-1}$ |
| $k_{m,2-d}$ | 1.00 | $M^{-1}s^{-1}$ |
| $k_d^{on}$ | 26.97 | $M^{-1}s^{-1}$ |
| $k_m^{off}$ | $2.08 \times 10^{-7}$ | $s^{-1}$ |
| $k_d^{off}$ | 0.02327 | $s^{-1}$ |
| $\theta_{max}$ | 0.3667 | |

## C2. Parameters for Initial State Model

The following curves were fit using the three monomer state model presented in Section 6.2.2.

No variation in the parameters was allowed, and all curves were fit at the same time.

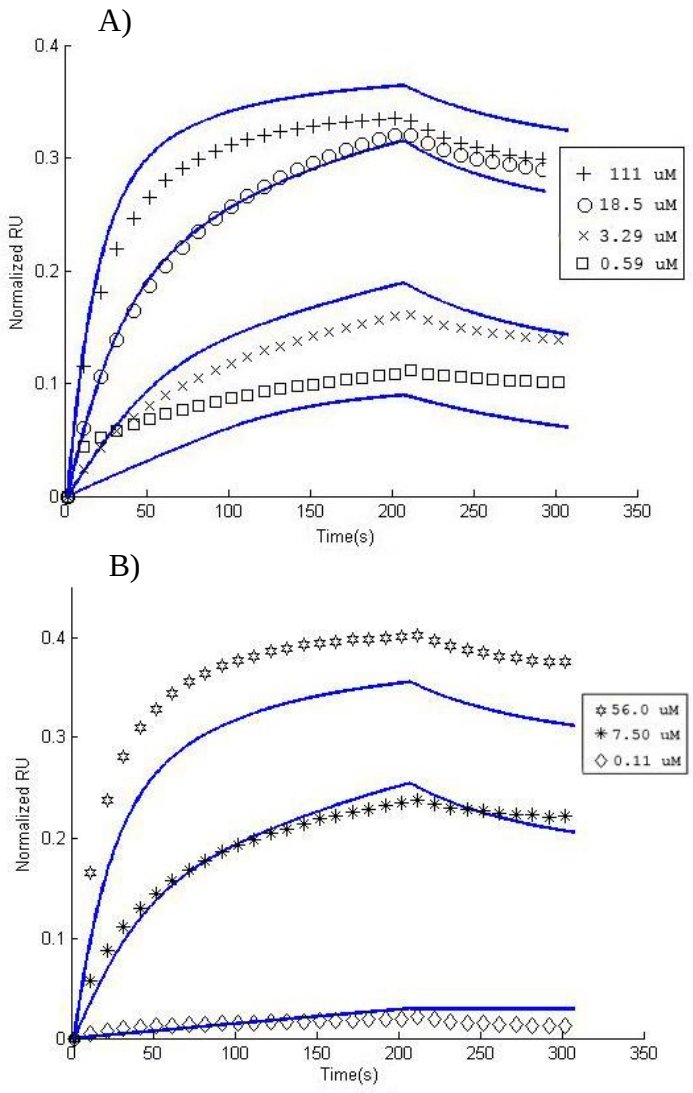


**Figure C.2 Three state model (lines) compared to experimental values (points).**

**A) First batch of experiments. B) Second batch of experiments. Values were normalised by dividing by 500.**